Dynamic Downscaling for Future Climate Scenario and Hydrologic Simulation using WRF and VIC models

Thesis Submitted to Andhra University, Visakhapatnam
in partial fulfillment of the requirement for the award of
Master of Technology in Remote Sensing and GIS

ANDHRA UNIVERSITY

Submitted By

ANUPRIYA GOYAL

Supervised By

Dr. S. P. Aggarwal
Scientist 'SF', Head,
Water Resources Department,
IIRS, Dehradun

Dr. Praveen Thakur
Scientist 'SE',
Water Resources Department,
IIRS, Dehradun

Water Resources Department
Indian Institute of Remote Sensing
Indian Space Research Organization, Dept. of Space, Government of India,
4, Kalidas Road, Dehradun – 248001, India

August, 2013

DECLARATION

This document describes work undertaken as part of a programme of study at the Water Resources Department of Indian Institute of Remote Sensing. All views and opinions expressed therein remain the sole responsibility of the author, and do not necessarily represent those of the Institute. The document comprises only my original work and due acknowledgement has been made in the text to all other material used.

Date: *08.07.2013* ***ANUPRIYA GOYAL***

CERTIFICATE

This is to certify that thesis entitled "**Dynamic Downscaling for Future Climate Scenario and Hydrologic Simulation using WRF and VIC models**" submitted by **Ms Anupriya Goyal** in partial fulfillment of the requirement for the award of degree of Master of Technology in Remote Sensing and GIS to Andhra University, Visakhapatnam is a record of the candidate's own work carried out by her under the supervision of Dr. S.P. Aggarwal and Dr. Praveen Thakur in Water Resources Department at Indian Institute of Remote Sensing, Dehradun, Uttarakhand, India. The matter embodied in this thesis is original and has not been submitted for the award of any other degree.

Dr. S. P. Aggarwal
Scientist 'SF',
Head, Water Resources Department,
IIRS, Dehradun

Dr. Praveen Thakur
Scientist 'SE',
Water Resources Department,
IIRS, Dehradun

Dr. Y. V. N. Krishnamurthy
Director,
IIRS, Dehradun

Dr. S. K. Saha
Dean (Academics),
IIRS, Dehradun

ACKNOWLEDGEMENT

I thank God for His abundant blessings throughout my stay here in IIRS.

I thank the Indian Institute of Remote Sensing for the giving me the opportunity to join the M.Tech. programme and providing a healthy and secure environment to study.
I extend my thanks to Andhra University for providing us the opportunity to pursue this course.

I would like to thank Dr. Y. V. N. Khrishnamurthy, Director, IIRS for providing all the facilities needed to complete my M.Tech in Remote Sensing & GIS.
I also extend my gratitude to Dr. S. K. Saha, Group Director, Earth Resources and System Studies Group and Dean (Academics), IIRS and Dr. Shefali Agrawal, Course Director for their support during the programme.

I gratefully acknowledge my supervisors Dr. S. P. Aggarwal, Head, Water Resources Department and Dr. Praveen Kumar Thakur, Scientist 'SE', WRD for patiently guiding me this past year ensuring my research meets the objectives and is up to the standard. Their advice and suggestions has helped me immensely in my research and is highly appreciated.

My sincere thanks are reserved to Dr. Bhaskar Nikam Scientist 'SD', Dr. Vaibhav Garg, Scientist 'SD', Dr. Arpit Chouksey, Scientist 'SC' and Prasun K. Gupta, Scientist 'SC' for their insightful suggestions.

I acknowledge Dr. Richard Jones and Dr. Wilfran Moufouma-Okia from the UK Met Office Hadley Centre for Climate Change for providing the HadCM3 forcing data for the WRF simulation. I also acknowledge Dr. Francina Dominguez and Dr. Om P. Tripathi from University of Arizona for their roles in making available the GCM data set.

I thank Mansi, Anudeep, Suman, Rajtantra, Tarul, Kirthiga and all my batchmates for their immense cooperation. I also extend my thanks to Sanjukta Saha, Surajit Ghosh, Suruchi Aggarwal, Pratik Dash and Kritika Kothari for their necessary support.

My thanks also go to other faculty members and staff of the department who had directly or indirectly helped me in course of time.

I am equally thankful to all the staff at IIRS who have contributed in making my life comfortable during my stay at IIRS.

During my project work I have been greatly supported by my friends to whom I am grateful for always being there for me and encouraging me all the way.

I am also grateful to Mr. Rajeev Kumar Chauhan for his constant motivation and encouragement.
I wish to give special thanks to my parents, Mr. Anil Kumar Goyal and Mrs. Sunita Goyal, who brought me up to this position inspiring and supporting my pursuits and are always my guides to step ahead. I also thank my siblings Dr. Anupama and Ashish for being the source of my inspiration.

I would like to thank everybody who was important to the successful realization of my thesis, as well as expressing my apology that I could not mention them individually.

ANUPRIYA GOYAL

ABSTRACT

Changes in temperature and precipitation alter the climatic conditions and subsequently hydrological and watershed processes in the long run. The effects of changes due to climatic variability on hydrological responses have been extensively carried out at watershed and river basin scales. Future climate scenario is best demonstrated by Global Climatic Models (GCM). GCM better estimates future climate variables. The resolution of GCM is still too coarse to capture regional and local climate scenario to simulate hydrological processes at basin scale.

Dynamical downscaling approach is employed in the present study to provide adequate spatial and temporal resolution to represent regional heterogeneity in atmospheric fields. Dynamic Downscaling of six hourly meteorological data from HadCM3 at 2.5° X 3.75° grids to generate three hourly model outputs at 25 X 25 km grids for the Ganga basin was successfully done using Weather Research and Forecasting (WRF) model with Advanced Research WRF (ARW) core. The choice of the domain, in terms of spatial extent and resolution, is one the vital factors affecting the realism of the phenomenon of downscaling. Computer resources and system architecture also play an important role to achieve efficient computational cost.

A physically based semi distributed Variable Infiltration Capacity (VIC) hydrological model was forced using downscaled atmospheric fields to simulate the hydrology of the Ganga river basin and analysis were carried out of the impact of climatic variability on hydrological regime. The simulated average rainfall for 2020 is in compliance with the average annual rainfall over the Ganga basin with an overall decrease of 4%. The estimated runoff of 257mm for the year 2020 is found to be lesser than that of 2006 when averaged over the entire basin. The present study shows that the year 2020 experiences an early onset of monsoon season and receives heavy rainfall in the month of June while the number of rainy days in a monsoon season decreases and per day intensity of rainfall increases. Subsequently, the runoff intensity per day increases with an overall decrease in total runoff in the year 2020.

Keywords: Future climate change scenario, dynamic downscaling, WRF-ARW, hydrologic simulation, VIC hydrological model.

TABLE OF CONTENTS

LIST OF FIGURES

LIST OF TABLES

1. INTRODUCTION

1.1 Background and Motivation

In the Fourth Assessment Report (AR4) Synthesis Report of Intergovernmental Panel on Climate Change (IPCC), 2007, it has been stated that South Asia is the most sensitive to the climate change impacts. The Ganga basin being one of the largest river systems located in South Asia owing to its varied topography experiences spatial and temporal variability in distribution of precipitation over the entire basin. According to various experiments conducted it has been observed that atmosphere is getting warmer over a period of time and an evident subsequent increase in extreme precipitation events is triggering an amplification of the global hydrologic cycle for regions that fall under extratropical zones (Huntington, 2006, Groisman, 2005). Figure 1.1 shows the geographical distribution of the extremes in regional zones. The disproportionate changes in heavy and very heavy precipitation during the past decades were documented as either an increase (+) or decrease (-) compared to the change in the annual and/or seasonal precipitation (Groisman *et al*, 2005, Trenberth *et al*., 2007).

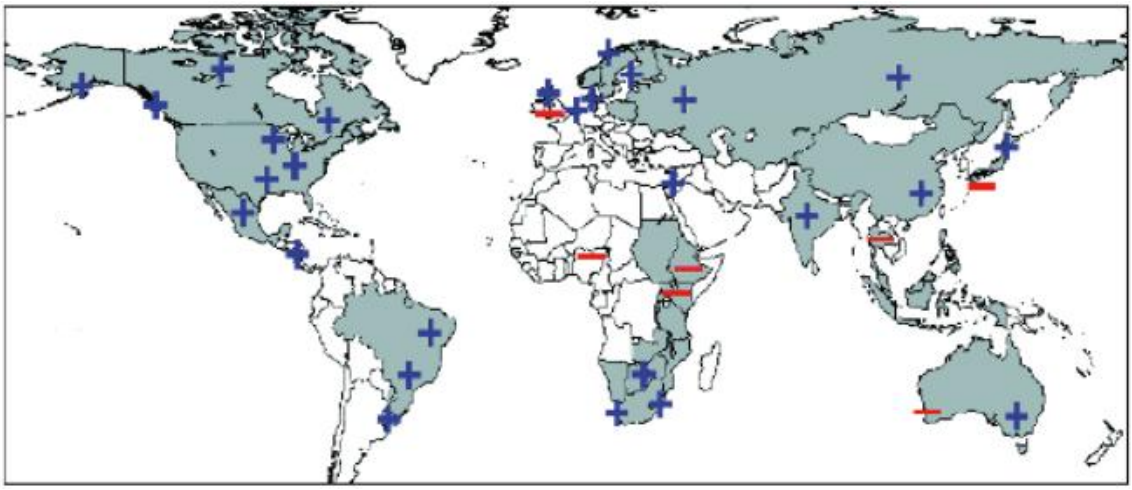

Figure 1.1 *Geographical distributions of the extremes*

(Groisman et al, 2005, Trenberth et al., 2007)

The intensification of the hydrologic regime due to impacts induced upon hydrologic and meteorological parameters by climate change in future implies that there is need to develop future climate change scenarios and study its implication on future hydrologic characteristics of the region of interest. The study will be a useful tool to analyze the future risks and prepare for their control to protect life and property.

The preparedness for the future scenario will definitely lead to efficient natural resources management and will be a foundation for an advanced and developed nation.

1.2 Importance of Hydrologic Cycle

Water is essence of all forms of life on the Earth. Indisputably, it is the presence of this blissful element that marks the flow of life and energy throughout the planet. The existence of water in three phases of solid, liquid and gas circulates both water and heat in atmosphere (Asrar and Dozier, 1994). The following figure is a pictorial representation of hydrologic cycle and its constituent processes.

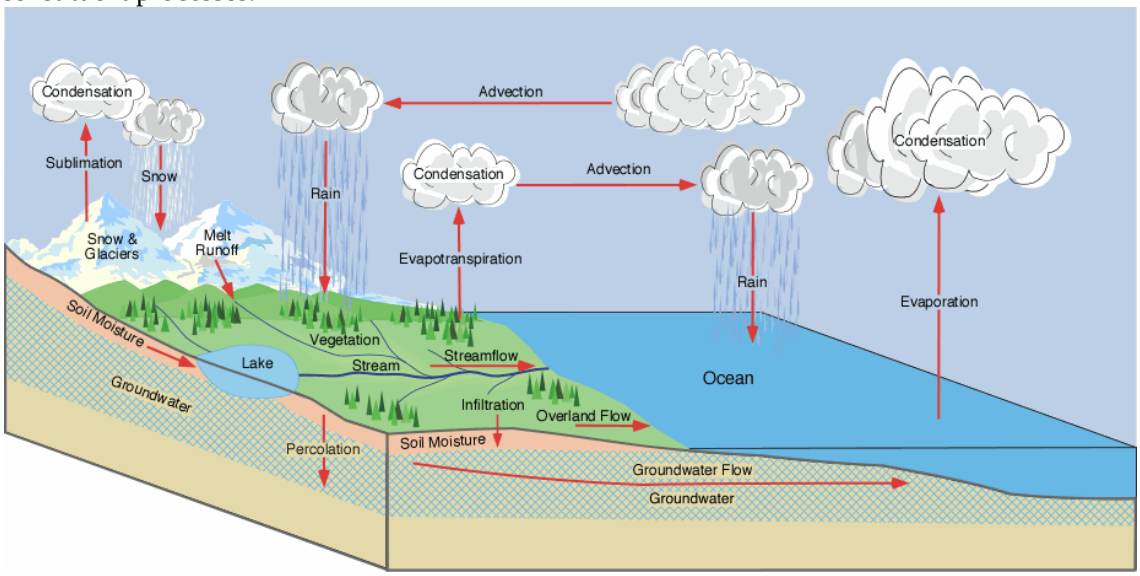

Figure 1.2 *The Hydrologic Cycle (Pidwirn M., 2006)*

The exchange of water between various geo-spheres of the Earth involves flow of energy and fluxes of water, also including, several other chemical elements. The climatic change implications exert huge impact on the hydrologic cycle. The hydrology of an area is a representation of not only its physical, chemical and biological processes but also its distinguished relation with the rest of the world in terms of its tradition, means of living, basic occupation etc. Thus, studying the hydrology of a catchment and analyzing the hydrologic components becomes a quantifying tool in quantifying, managing and preserving the resources of the region efficiently. The important hydrologic components of the catchment are precipitation, infiltration, evapotranspiration, soil moisture, soil depth, storage water, baseflow and runoff. The watershed at the regional scale is generally considered to be the most logical geographical unit of streamflow analysis and water resources management as it is efficient to monitor the hydrologic simulation at regional level. Water budget is a means of accounting for all the water that flows in and out of a watershed. Water balance equation is the scientific method for measuring the amount of water entering, stored within and leaving a watershed. It is represented mathematically as:

$$Q = P - \Delta S - ET \quad (1.1)$$

Where,
P is precipitation,
Q is surface runoff,
ET is evapotranspiration, and
S is storage in the control volume.

Runoff characterizing the response of a catchment to precipitation includes the integrated effects of the topography, soil type and land use classification of the area. Hence, the knowledge of streamflow pattern is an important key to understand the climatic conditions of the area and to study the impact of changes in climate on basin hydrology.

1.3 Hydrologic Simulation

Hydrological modelling is one of the efficient ways for consistently analyzing the long term hydrologic pattern of the basin and carrying out various behavioural studies. The hydrologic components as discussed above are modelled by mathematical representations known as hydrological models. Hydrologic models can be distinguished into deterministic and stochastic models, lumped and distributed models. Traditional water balance approach is lumped. However, all hydrological models are imperfect representations of reality and have their own merits and limitations. Many parameters are observable (e.g. basin area, slope, elevation, vegetation type) although some parameters are unobservable. AVSWAT (Arc View Soil and Water Assessment Tool), HEC-RAS (Hydrologic Engineering Centre- River Analysis System), MIKE-SHE, Variable infiltration Capacity model, HEC-HMS (Hydrologic Engineering Centre-Hydrologic Modelling System) are some of the physically based distributed hydrologic models. In the present study the Variable Infiltration Capacity (VIC) land surface hydrologic model has been used for modeling water balance and river flow regime.

Hydrological models serve a range of purposes but they are used primarily to estimate runoff from sequences of rainfall and the meteorological information needed to estimate potential evaporation. They can be used to estimate river flows at ungauged sites, fill gaps in broken records or extend flow records with respect to longer records of rainfall and to evaluate the impacts of external influences (such as climate change) (Mishra, 2008). There are many simulation models in use; the skill is in selecting the right model for the job and balancing data requirements against the cost of model implementation. Hydrologic model value lies in its ability, when correctly chosen and adjusted to extract the maximum amount of information from the available data in order to provide reliable information for managing water resources in a sustained manner.

1.4 Future Climate Scenario

Intergovernmental Panel on Climate Change (IPCC) Fourth Assessment Report (AR4) in continuation of the Third Assessment Report (TAR) provides an overview of the recent and past changes in climate scenarios as reproduced by the climate models. It is to be noted that the climate models are based on fundamental principles of physics and follow the well established laws of physics, for instance, Thermodynamics law, Newton's Law of motion, Equation of continuity and momentum etc. The well established, physical based Global Circulation Models in strong collaboration with the remote sensing based Earth Observation Systems attempt to estimate and resolve the climate induced impacts in past, present and future on large-scale climate systems.

Atmosphere-Ocean General Circulation Models (AOGCMs) are believed to efficiently assess and estimate the physical parameters of the future climate system at continent or global scales.

Global circulation model gives prediction of future climate variables on global scale. The data of GCM is average representation of conditions so regional climate model is required for

increasing the prediction accuracy of model. A regional climate model (RCM) is a downscaling tool that adds fine scale (high resolution) information to the large-scale projections of a global general circulation model (GCM).

1.4.1 IPCC SRES Scenarios

The Special Report on Emissions Scenarios (SRES) establish different future world development possibilities in the 21st century, taking into consideration the possible changes in various factors in future including economic development, technological development, energy intensities, energy demand, and structure of energy use, resources availability, population change, and land-use change. The possibilities of changes in future developments are categorized mainly in the form of four major storylines quantified as four scenarios families namely A1, A2, B1 and B2. There are total of 40 different scenarios constructed across these four major scenario families. As per the belief of the authors of the SRES scenarios all the developed scenario families along with all the constructed emission scenarios have equal potential to be plausible and hence, are not prioritized or assigned any probabilities to them.
The dataset of SRES A2 scenario used in this study was commissioned by the IPCC and discussed in detail by Nakicenvoic *et al*. (2000)**.** The A2 story line is marked by its highly heterogeneous world. This particular scenario is characterized by continuous increase in population (Lutz, 1996). Population reaches over 10 billion by 2050. Medium economic growth with up to 2.3 GDP is expected by mid of 21st century with emphasis on regionally oriented economy. Per capita income is also considered to be in a medium range as compared to the other story lines. Also, the A2 scenario family is marked with high use of primary energy with slow developments in technology. The governance is self-reliant with preservation of local identities.

The study is designed such that it collects the relevant findings on the Global Climatic Models from numerous experiments conducted and documented in the existing literature. The conclusions are drawn by highlighting the sensitivity and adaptability of these models to climate change induced impacts. The Global Climatic Model that exists in concordance with the dynamics of climate is considered the most suitable for the study.

1.5 Integrated Modeling

The impact of projected 21st century climate conditions on stream flow is estimated using a weather research and forecasting model wherein the dynamically downscaled outputs of future climate scenarios from global climate models are used to drive a macro scale hydrology model. In this study, boundary conditions from a general circulation model are used to produce dynamically downscaled precipitation and temperature data. The GCM used in the study not only used to provide lateral boundary conditions but is also used to force the interior of the model which is then subjected to appropriate physical approximations embedded in the Regional Climate model (RCM) that helps maintaining the appropriate variability in model parameters at large scales and upper levels. These data are used to force a hydrology model which simulates run off during a reference period and a future period for a given future climate scenario. Here the high resolution weather data is generated from Weather Research and Forecasting (WRF) model (http://www.mmm.ucar.edu/wrf/users) that serves as input to

Variable Infiltration Capacity Model (VIC) a hydrological simulation model for predicting the future hydrology scenario of Ganga Basin. Forcing of hydrological model with downscaled parameters is an active area of research world over.

1.6 Downscaling

Downscaling, or translation across scales, is set of techniques that relate local and regional-scale climate variables to the larger scale atmospheric forcing (Hewitson and Crane, 1996). The downscaling approach was developed specifically to address present needs in global environmental change research, and the need for more detailed temporal and spatial information from Global Climate Models (GCM). Two general categories exist for downscaling techniques: process based techniques focused on nested models, and empirical techniques using one form or another of transfer function between scales (Hewitson and Crane, 1996). The downscaling techniques: Statistical and dynamical downscaling techniques allow scientists to use global climate model outputs as inputs into weather models (Lenart, 2008).

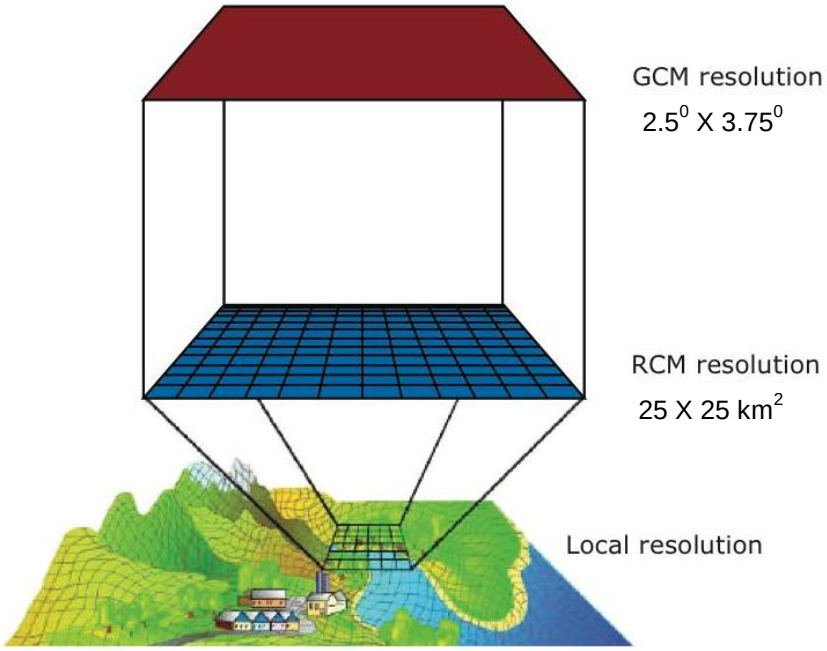

Figure 1.3 *Dynamic Downscaling. Adapted from CRU*

Approvingly, the figure above depicts graphically the downscaling process where the GCM with a coarse resolution of 2.5^o X 3.75^o is downscaled to the 25 km basin scale. The high resolution topography, landcover, soil type covering the local domain from satellite data as static inputs and meteorological data such as temperature, wind speed, specific humidity etc. for lateral boundary conditions and initial condition from GCM are used to drive the RCM.

1.6.1 Significance

Analyzing the impact of future climate change on hydrological regimes is hampered by the disparity of scales between general circulation model output and the spatial resolution required by catchment-scale hydrological simulation models. The GCM better simulates global conditions with spatial scales of more than hundreds of kilometers while to simulate the hydrology of a basin we need to observe an area at spatial scale of 0-50 km. Also, GCM skillfully represents the mean annual and seasonal temporal scales but the temporal scales of mean daily observations are better handled by downscaling the GCM data to regional scale. Hence, on the basis of limitations of GCM at a local or basin scale as a main requirement of the present study it may be safe to state that as the accuracy of GCM decreases at finer resolution, we need to downscale the GCM data for impact studies needing higher resolution inputs. In order to overcome this, the projections of precipitation and the air temperature changes will be downscaled from the GCM (DDC, IPCC) to the Ganga Basin.
The regional climate model used for dynamical downscaling in the present study is Weather Research and Forecasting (WRF) Model, which uses modeling principles proven in Numerical weather Prediction (NWP) and regional climate applications that minimize the generation of small-scale noise and, thus, is robust and computationally efficient (Janjic, 2011)

1.7 Role of Remote Sensing and GIS

Remote sensing has shown great promise for providing an abundance of data and information that were lacking with the in-situ observations. It has also been a valuable tool in many hydrologic modeling applications due to its capability of providing unrestricted collection of information with wide spatial coverage and temporal repeat. Remote sensing data like DEM, Land use/Land cover map and Soil map and other hydrometeorological data generated from remote sensing satellite images will be used to improve the forecast of land surface hydrological processes. The raw data acquired from satellites when processed using various image processing procedures provide useful and viable information for successfully estimating various hydrometeorological and land surface parameters such as incident radiation, surface temperature, precipitation, albedo, land use and land cover, leaf area index etc. A number of other variables relevant to the derivation of energy and moisture fluxes at the land surface can be obtained from remote sensing applications (Entekhabi *et al*., 1999). The application of remotely sensed data is most advantageous in the those hydrological analysis exercises where the data is inadequate due to either the area lies in an inaccessible region or the existing techniques do not provide sufficient or satisfactory information.
Spatially distributed Hydrological models such as VIC model takes into consideration the heterogeneity over a vast catchment area for which they require huge amount of high resolution geographical and temporal data to simulate the water balance of the area effectively. The use of remote sensing and GIS equip hydrologists with state of the art and cost efficient technology to work efficiently with spatially and temporally varying complex hydrological processes.
Remote sensing could contribute to hydrologic information provided the matter is handled by hydrologists experienced in qualitative hydrological reasoning based on knowledge of the field conditions of a particular catchment (Shelton and Estes, 1981).

Models for simulating water budget for a catchment take into account detailed physical and hydraulic relationships with respect to data availability, knowledge, computer capacity and time available. In the past the spatial reference of the time series data has been modeled in a simplified way by reference algorithms and statistical interpolation methods (Wolf-Schumann and Vallant, 1996). The recent advancement in the field of time varying aspect of GIS data has been proved to be of huge importance to the hydrologists who aim to simulate the movement of water in a catchment with large volumes of data.

One of the widely employed application of remote sensing and GIS techniques is processing of a digital elevation model (DEM) to analyze the morphometric characteristics of a watershed and extract hydrologic catchment properties such as elevation, slope, aspect, delineation of basin boundary, flow direction matrix, flow accumulation matrix, stream order, stream length, drainage map etc.

A geographic information system is a system for turning large volumes of spatial data into useful information (Tomlinson, 1972).

Remote sensing has held a great deal of promise for hydrology, mainly because of the potential to observe areas and entire river basins rather than merely points (Dadhwal, 2010).

1.8 GAP AREAS

1. Fewer studies on dynamic downscaling in the context of Indian region.
2. Still research is in progress to predict the future hydrological scenario using dynamically downscaled GCM data as input.
3. Statistical downscaling conducted in India lacks physical basis

1.9 RESEARCH QUESTIONS

1. How dynamic downscaling of GCM based hydro meteorological input can be done in WRF model?
2. What will be the effect of downscaled future climate change scenario on hydrological regime?

1.10 RESEARCH OBJECTIVES

1. Downscaling the GCM based hydro-meteorological outputs using WRF model for land surface hydrological modeling.
2. Hydrological simulation using VIC model for future climate change scenario as downscaled by WRF model.

1.11 Structure of the Thesis

Chapter 1 Introduction
The chapter provides a brief introduction to the changing climate scenario in the World especially in Ganga Basin, with emphasis on downscaling approach of deaggration of GCM outputs to match the needs for impact studies on regional scale including the importance of hydrologic cycle and role of Remote sensing and GIS, followed by the challenges faced, the objectives and the research.

Chapter 2 Literature Review
The chapter covers the various researches carried out in the field of analyzing climatic variability evoked due to future climate change scenarios and its impact on future hydrology. This chapter discusses in detail the Hydrological cycle, its importance, hydrological modelling, types of hydrological models and role of Remote sensing/GIS in modelling hydrology An overview of various techniques used and applied for downscaling is also provided. Previous works on methods and applications of Hydrologic and downscaling models have been reviewed extensively.

Chapter 3 Model Overview
This section explores the structure of the models and their architecture used for the study. The chapter provides description of various constituent processes involved in

Chapter 4 Study Area
This chapter gives a brief overview of the geographic environment of the Ganga basin describing its location and extent, climate experienced, hydrology of climate, physiographic details, soils, agriculture and land use land cover. The demographic aspects of the basin are also presented.

Chapter 5 Materials/Data Used
The chapter provides brief descriptions of various remotely sensed satellite data, ground observations at different station locations, hydrometeorological datasets and other ancillary data used to carry out processing of the study. It also points out various software, instruments and other computer languages employed to process the datasets.

Chapter 6 Methodology
This chapter describes the overall research design and explains the methodology deployed in the study. This section addresses the procedures for generating various input parameters for simulation, calibration and validation of the models.

Chapter 7 Results and Discussions
Results of the simulations of forecasting and hydrological models analysis are evinced in this chapter; thereby, the outcomes are statistically analysed and their accuracy are assessed and discussed.

Chapter 8 Conclusions and Recommendations
This chapter is arranged to make conclusions based on an overall review of the results. Further the scope of future improvement has been provided.

2. LITERATURE REVIEW

2.1 Impact of Future Climate Scenario on Hydrology

As per the IPCC reports, many countries, face severe challenges due to change in climate resulting in increase in temperature, thus, amplification of extreme weather events—floods, storms, droughts. It is expected that the global climate change will have significant impacts on the regime of hydrologic extremes. As a consequence, the design and management of water resource systems will have to adapt to the changing hydrologic extremes further affecting the socio-economic developments. Main objectives of climate and weather prediction are to improve the accuracy of weather predictions with the most detailed spatial resolution feasible and to substantially improve the capability for seasonal forecasting at regional scales (Cihlar *et al*., 2000). This study is carried out to analyze the future impacts of climate change on the hydrology of the Ganga Basin. In recent years, numerous studies have investigated the impact of climate change on hydrology and water resources in many regions (Arnell and Reynard, 1996, Bergstrom *et al*., 2001, Middelkoop *et al*., 2001, Gao *et al.*, 2002, Menzel and Burger, 2002, Pilling and Jones, 2002, Arnell *et al.*, 2003 and Christensen *et al*., 2004).

Surface processes control the depth of the simulated atmospheric boundary layer in meteorological models, and the simulated surface and subsurface transport of water in hydrological models (Peters-Lidard, McHenry *et al.*, 1999). Improved hydrologic condition estimates are useful for agriculture, ecology, civil engineering, water resources management, rainfall-runoff prediction, atmospheric process studies, climate and weather/climate prediction, and disaster management (Rodell and Houser, 2004).

One of the major problems in distributed modeling is parameter identifiability, owing to a mismatch between model complexity and the level of data which is available to parameterize, initialize, and calibrate such models (Troch *et al.*, 2003).

The relationship of land surface processes with climate variables (e.g. precipitation and air temperature) and associated extreme events is well known (Huntington, 2006). Many global and regional studies have examined the impact of projected future climatic change on hydrologic variables (Barnett *et al*., 2005, Christensen *et al*., 2004, Milly *et al*., 2005, Sheffield and Wood, 2008, Wuebbles and Hayhoe, 2004), however, most of these have focused on changes to floods and drought frequencies and not on changes to daily stream flow variability.

Fewer studies have been conducted on dynamic downscaling in the context of Indian regime. Still researches are in progress to predict the future hydrological scenario using dynamically downscaled GCM data as input.

2.2 Hydrological Cycle and Water Balance

Hydrology is the scientific discipline that deals with water cycle. The study of origin, movement, distribution, and of water on earth and its atmosphere is known as hydrology (Subramnya, 2008). The processes involved in circulation water from land and water bodies to the atmosphere and back again different states such as gas, liquid, or solid (Maidment, 1992) is known as hydrologic cycle. Water cycle or Hydrologic cycle can be constitutes of certain physical processes which form a continuum of water movement on globe. Important components are evapotranspiration, precipitation, interception, infiltration, percolation, and runoff. Evapotranspiration accounts for water evaporating from the ground, seas and lakes, snow, even raindrops combined with transpiration by plants. Condensation is the process of water changing from a vapor to a liquid. Precipitation is water being released from clouds as rain, sleet, snow or hail and reaching the ground. Interception is the volume of water caught by vegetation. Infiltration occurs when a portion of the precipitation that reaches the Earth's surface seeps into the ground. The soil moisture is the volume fraction of water held in various layers of soil. Percolation is the downward movement of water through soil and rock. Percolation is the movement of water through soil layers by gravitational pull or capillary action. Runoff is precipitation that reaches the surface of the Earth but does not infiltrate the soil. Runoff can also come from melted snow and ice. As soon as it enters a channel, runoff becomes streamflow.

Water budget of an area accounts for all the water that flows in and out of that area. The area of land draining into a stream or a water course at a given outlet point is said to be a catchment or a drainage basin (Subramanya, 2008). The water budget equation for an area in its simplest form can be written as,

$$\textit{Mass inflow - mass outflow = change in water storage} \qquad (2.1)$$

For a given catchment, the mathematical statement of hydrological cycle within a given time frame incorporating principles of mass and energy continuity for water in its various phases is termed as the water budget or water balance. In its simplest form it is expressed as,

$$P - Q - ET - G = \Delta S \qquad (2.2)$$

Where,
P is precipitation,
Q is surface runoff,
G is subsurface runoff,
ET is evapotranspiration,
And ΔS is change in storage.

Table 2.1 *Estimated Global Water Cycle (NWRFC, NOAA)*

Type Of Water	Location	Volume		Percent Of Total Volume
		millions of cu. miles	millions of cu kilometer	
Salt Water				97.00
	Oceans	314.2	1308.0	(96.4%)
	Saline Bodies	2.1	8.7	(0.6%)
Fresh Water				2.90
	Ice & Snow	6.9	28.7	(2.1%)
	Lakes	0.5	2.1	(0.15%)
	Rivers	0.01	0.04	(0.003%)
	Accessible Groundwater	1.0	4.2	(0.31%)
Atmospheric				0.10
	Sea Evaporation	0.1	0.42	(0.03%)
	Land Evaporation	0.05	0.21	(0.015%)
	Precipitation Over Sea	0.09	0.37	(0.03%)
	Precipitation Over Land	0.03	0.12	(0.01%)
	Water Vapor	0.005	0.02	(0.002%)
Rounded Total		326.00	1357.00	100.0

The average annual precipitation received in India is 4,000 km^3, out of which 700 km^3 is immediately lost to the atmosphere, 2,150 km^3 soaks into the ground and 1,150 km^3 flows as surface runoff. The total water resources in the country have been estimated as 1,953 km^3. The annual water availability in terms of utilizable water resources in India is 1,122 km^3. Besides this, the quantity of 123 km^3 to 169 km^3 additional return flow will also be available from increased use from irrigation, domestic and industrial purposes by the year 2050. The per capita availability of utilizable water, which was about 3,000 m^3 in the year 1951, has been reduced to 1,100 m^3 in 1998 and is expected to be 687 m^3 by the year 2050.

Table 2.2 *Per Capita Availability of Water in India (Water Budget, NIH)*

Year	1951	1991	2010	2025	2050
Population (10^6)	361	846.3	1,157	1,333	1,581
Average Water Resources (m^3/person/year)	3,008	128.3	938	814	687

The equation for hydrologic water balance of the country for average annual conditions can be written as:

$$P + I = Q_s + E_T + Q_g + \Delta S + \varepsilon \quad (2.3)$$

Where,
P is the total precipitation,
E_T is total evapotranspiration,
I is the total inflow water,
Q_s is the outflow as surface water to oceans and other countries,
Q_g is the ground outflow,
and ΔS represents the change in soil moisture storage.

Table 2.3 *Hydrologic Water Balance of India (All components in million ha-m per year) (Water Budget, NIH)*

Inflow		Outflow	
Term	Value	Term	Value
P	400	E_T	278
I_s	20	Q_s	126
I_g	4	Q_g	20
Total	424	Total	424

2.3 Hydrological modeling and types of hydrological models

"Prior to the advent of the unit hydrograph by Sherman (1932), hydrologic modelling was mostly empirical and based on limited data." (Singh, 1996, Fiorentino, 1996). Since the advent of the hydrograph, hydrologic modelling has developed into data intensive, computer software driven science. Today, there are models covering every facet of water's interaction with the environment. This sub-section is meant to provide some background to hydrologic modelling, focusing on physically-based watershed modelling.

In Figure 2.1, the first level of separation between the watershed models depends on whether or not the model includes randomness in its calculations. Providing a particular input into a deterministic model always produces the same output. Stochastic models usually do the statistical analysis to depict the nature of hydrology. Distributed models represent the spatial distribution of the variables taking into consider the heterogeneity of the terrain. Lumped models, however, produce the results by spatially averaging the variables. The third level of separation considers the handling of temporal variation within a model. Variations in flow with change in time are adequately simulated using deterministic watershed models while the output is always different when working with the stochastic model. In the field of deterministic modelling, recent efforts are focused towards developing physically-based models, which try to represent natural processes as closely as possible (Mishra, 2008).

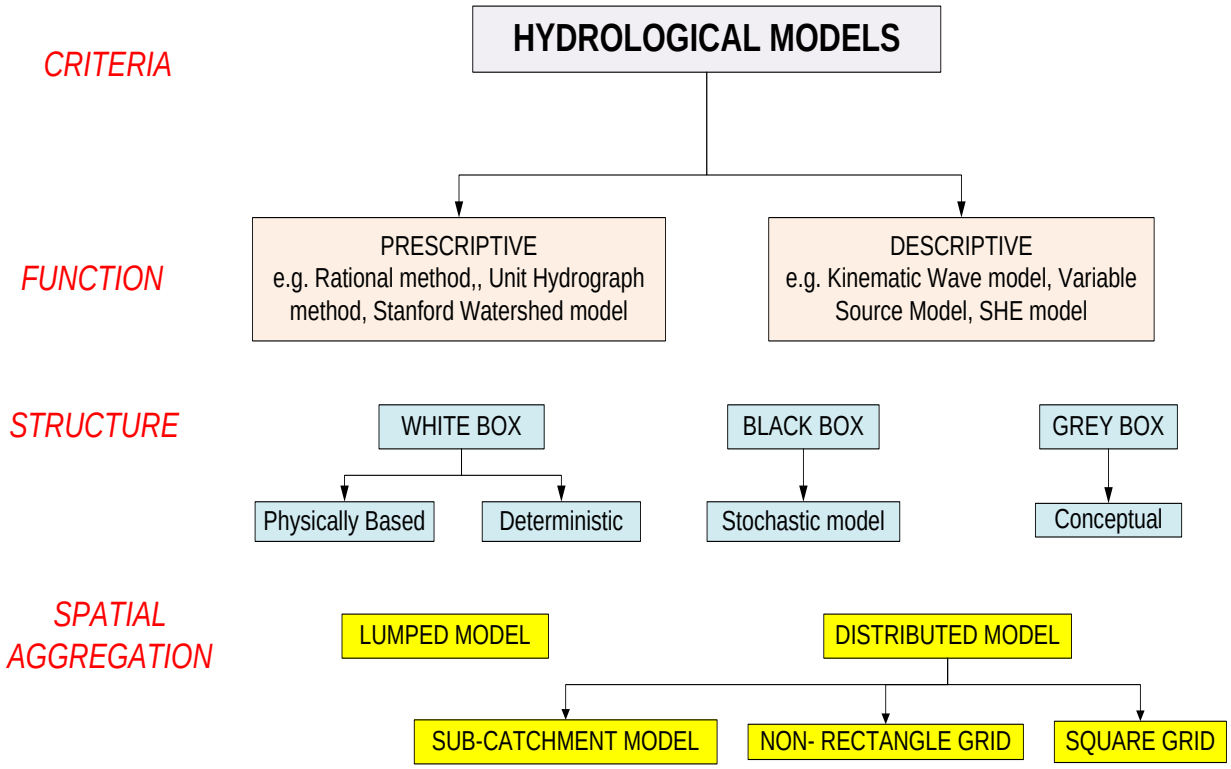

Figure 2.1 *Classification of Watershed Hydrologic Models (Schulze, 2002)*

2.3.1 Lumped Models

These models describe the watershed as a single entity with a single rainfall input (mean rainfall). The discharge at the watershed outlet is described based on a global dynamic of the system. There are numerous lumped hydrologic models. These models are usually based on the concept of the unit hydrograph, UH. Lumped hydrologic models are those models that commonly ignore spatial variations of precipitation, water flow, and other related processes, focusing instead on spatially averaged inputs, outputs, and parameter values. Lumped models are limited in their ability to achieve the physically-based goal because of this spatial averaging necessary for the variables. They are unable to account for the complexities of hydrologic processes and systems. Lumped models therefore are usually limited to those catchments where spatial variability does not dictate the outcome of an event (Muszik, 1996).

2.3.2 Distributed Models

"A truly distributed model of a process is possible only if the process can be described by an equation having an analytical solution" (Muszik, 1996). These types of models are physically based; meaning they are based on observed parameters rather than estimations. While the majority of distributed models require some degree of lumping, their objective is to account for spatial variations of hydrologic processes and parameters. Previously, limitations of distributed models came from computing the vast amount of data required to run the model. However, due to advancements in computers and modelling software, the current limitation for distributed modelling is the lack of available distributed hydrologic data (Muszik, 1996). In most of the distributed hydrologic models, HRU's (Hydrologic Response Units) are delineated by combining topography, soil properties, land use and other pertinent properties. Distributed models are especially useful, for example, when impacts of land use change are to be studied or for analyzing spatially varying flood responses.

2.4 Coupling VIC with GCM

The Variable Infiltration Capacity Model (VIC) is a macro scale hydrologic model for water and energy balance, developed over the last 10 years at the University of Washington and Princeton University. The first version of the VIC model is described in detail by Liang *et al*. (1994) and Liang *et al*. (1996a). To explore and examine the sensitivity of GCM to climate change, the VIC model was incorporated into GFDL's R15 model and implemented in the GFDL and Max-Planck-Institute (MPI) GCMs (Stamm *et al*., 1994).

Xu Liang *et al.* (1994) in their study dealing with investigation of VIC model for incorporating land surface water and energy fluxes in GCM. A land surface hydrological model that is a generalization of the variable infiltration capacity (VIC) model was described suitable for application in GCM. VIC model which incorporates a two-layer description of the soil column is formulated for a fully coupled application within a GCM. The upper layer is characterized by the typical VIC spatially distributed scheme of soil moisture capacities, and the layer below is spatially aggregated, and uses the Arno (Francini and Pacciani, 1991) drainage term. The model partitions the area of interest (e.g., grid cell) into N+I land surface cover types; for each land cover type the fraction of roots in the upper and lower zone is specified. Evaporation and transpiration are parameterized by a Penman-Monteith technique, applied separately to bare soil and vegetation classes. Evaporation from water intercepted by the vegetation is also represented. In addition, the model contains an energy-based snow accumulation and ablation parameterization.

There have been several studies that aim towards coupling VIC with GCM models to predict climate change impact. In one such study in China in the Hanjiang basin by Guo *et al.* (2009), a Smooth Support Vector Machine (SSVM) was employed for statistical downscaling of GCM parameters to simulate the runoff using VIC model. Daily precipitation and temperature output of GCM from two different SRES scenarios, A2 and B2, were used to observe the climate

change induced changes in the hydrology of the basin. The Variable Infiltration Capacity (VIC) distributed hydrological model with a 9 ×9 sq. km. grid resolution was established and calibrated in the Hanjiang basin of China. Validation results gave a clear indication that the VIC model could simulate the runoff hydrograph with high model efficiency and low relative error with respect to observed precipitation and temperature data.

The VIC model was developed with an aim to represent horizontal resolution and subgrid heterogeneity in a simple way for incorporation in GCMs. Employing the infiltration and surface runoff scheme in Xianjiang model (Zhao, 1980). Besides the above improvements to the water budget and energy balance processes in the VIC model, efforts have been made to provide better meteorological forcings through the data preprocessor. Using algorithms by Kimball *et al*. (1997), Thornton and Running (1999), and Bras (1990), a full suite of hydrologic variables is constructed from limited observed driving data (precipitation, maximum and minimum air temperature, and wind speed) (Nijssen *et al*., 2001). The overall VIC model framework has been described in detail in literature (Liang *et al*. 1994; Liang *et al*., 1996a; Nijssen *et al*., 1997).

The key characteristics of the grid-based VIC are the representation of vegetation heterogeneity, multiple soil layers with variable infiltration, and non-linear base flow.

As compared to other land surface models, VIC's distinguishing hydrologic features are:

(a) Its representation of subgrid variability in soil moisture storage capacity as a spatial probability distribution, to which surface runoff is related (Zhao *et al*., 1980)

(b) Its parameterization of base flow, which occurs from a lower soil moisture zone as a nonlinear recession (Dumenil and Todini, 1992).

As discussed by Lohmann *et al*. (1998) the representation of soil hydrology (soil water storage, surface runoff generation and sub-surface drainage) has a critical influence on the predicted long-term water and energy balances. Hydrologic simulation using a distributed model, resulted in a decreasing trend for the 2020s and 2050s, and an overall increasing trend for the 2080s.

2.5 IPCC SRES: A2 Family Scenario

A Special Report on Emission Scenario (SRES) establish different future world development possibilities in the 21st century, taking into consideration the possible changes in various factors in future including economic development, technological development, energy intensities, energy demand, and structure of energy use, resources availability, population change, and land-use change. The possibilities of changes in future developments are categorized mainly in the form of four major storylines quantified as four scenarios families namely A1, A2, B1 and B2.

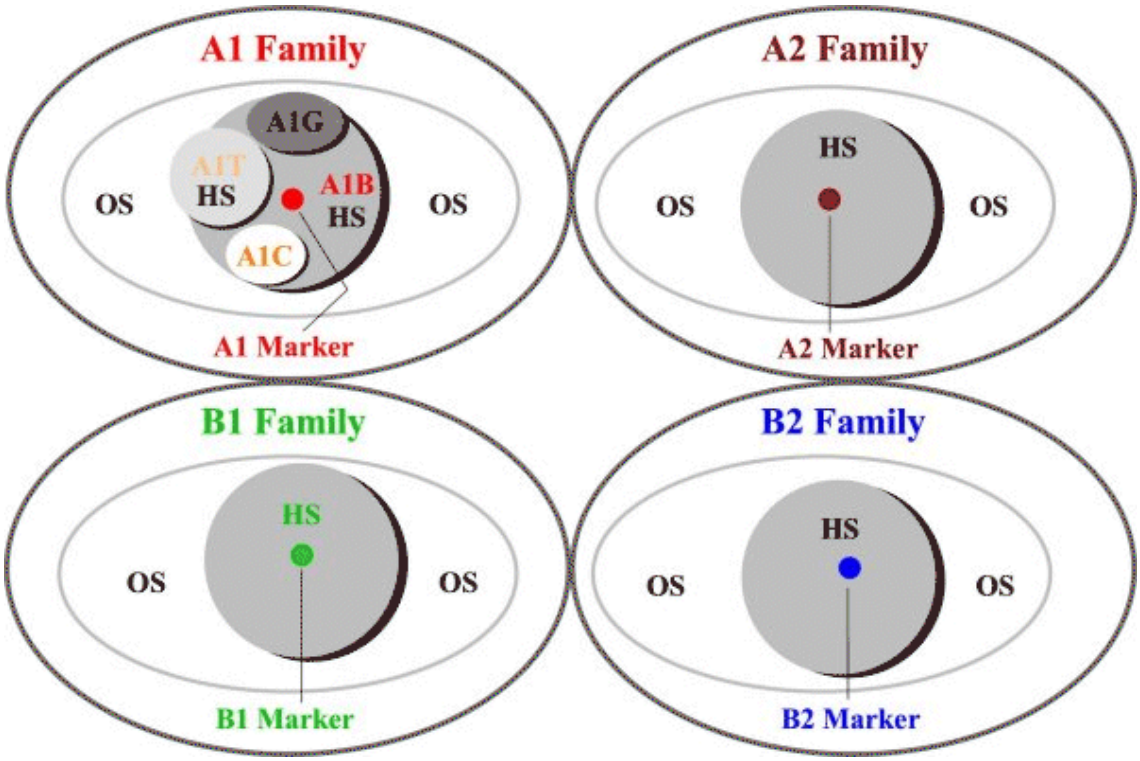

Figure 2.2 *Classification of SRES scenarios in a multidimensional space (Nakicenovic et al., 2000); HS: Harmonized scenario, OS: Other Scenarios*

Nebojsa Nakicenovic and Rob Swart (2000) have discussed in the report on emission scenarios about four major scenario families (A1, A2, B1, and B2), each of which consists of a number of scenarios. There are total of 40 different scenarios constructed across these four major scenario families. Some of these have "harmonized" inputs - they share similar pre-specified global population and GDP trajectories. They are marked as "HS" for (globally) harmonized scenarios. All other scenarios of the same family based on the quantification of the storyline chosen by the modeling team are marked as "OS." The A1 family is divided into four scenario groups that explore alternative developments in the future energy sector. Finally, one of the harmonized scenarios is designated as the characteristic representative of each family and is the marker scenario.

The following table adapted from Special Report on Emission Scenarios gives an overview of main driving forces for the four SRES marker scenarios for 2100 if not indicated otherwise. Numbers in brackets show the range across all other scenarios from the same scenario family as the marker. (IND regions include industrialized countries and DEV region includes developing countries).

Table 2.4 *Main driving forces for the four major SRES scenarios for 2100. (Nebojsa Nakicenovic and Rob Swart, 2000)*

	Population In Billion	**Economic Growth, GDP_{mex}[a]**	**Per Capita Income, GDP_{mex}/capita**	**Primary Energy Use**	**Hydrocarbon Resource Use[b]**	**Land- Use Change[c]**
A1	Lutz (1996) Low ~7 billion 1.4 IND 5.6 DEV	Very high 1990- 2020: 3.3 (2.8- 3.6) 1990- 2050: 3.6 (2.9- 3.7) 1990- 2100: 2.9 (2.5- 3.0)	Very high in IND: US$ 107,300 (60,300- 113,500) in DEV: US$ 66,500 (41,400- 69,800)	Very high 2.226 (1,002- 2,683) EJ Low energy intensity of 4.2 MJ/ US$ (1.9- 5.1)	Varied in four scenario groups: Oil: Low to very high 20.8 (11.5- 50.8) ZJ Gas: High to very high 42.2 (19.7- 54.9) ZJ Coal: Medium to very high 15.9 (4.4- 68.3) ZJ	Low. 1990- 2100: 3% cropland, 6% grasslands 2% forests
A2	Lutz (1996) High ~15 billion 2.2 IND 12.9 DEV	Medium 1990- 2020: 2.2 (2.0- 2.6) 1990- 2050: 2.3 (1.7- 2.8) 1990- 2100: 2.3 (2.0- 2.3)	Low in DEV Medium in IND in IND: US$ 46,200 (37,100- 64,500) in DEV: US$ 11,000 (10,300- 13,700)	High 1,717 (1,304- 2.040) EJ High energy intensity of 7.1 MJ/ US$ (5.2- 8.9)	Scenario dependent: Oil: Very low to medium 17.3 (11.0- 22.5) ZJ Gas: Low to high 24.6 (18.4- 35.5) ZJ Coal:Medium to Very high 46.8 (20.1- 47.7) ZJ	Medium n.a. from ASF

B1	Lutz (1996) Low ~7 billion 1.4 IND 5.7 DEV	High 1990- 2020: 3.1 (2.9- 3.3) 1990- 2050: 3.1 (2.9- 3.5) 1990- 2100: 2.5 (2.5- 2.6)	High in IND: US$ 72,800 (65,300- 77,700) In DEV: US$ 40,200 (40,200- 45,200)	Low. 514 (514- 1,157) EJ Very low energy intensity of 1.6 EJ/ US$ (1.6- 3.4)	Scenario dependent: Oil: Very low to high 19.6 (15.7- 19.6) ZJ Gas: Medium to high 14.7 (14.7- 31.8) ZJ Coal: Very low to high 13.2 (3.3- 27.2) ZJ	High 1990- 2100: -28% cropland -45% grassland +30% forests
B2	UN (1998) Median ~10 billion 1.3 IND 9.1 DEV	Medium 1990- 2020: 3.0 (2.2- 3.1) 1990- 2050: 2.8 (2.1- 2.9) 1990- 2100: 2.2 (2.0- 2.3)	Medium in IND: US$ 54,400 (42,400- 61,100) In DEV: US$ 18,000 (14,200- 21,500)	Medium 1,357 (846- 1,625) EJ Medium energy intensity of 5.8 MJ/ US$ (4.3- 6.5)	Oil: Low to medium 19.5 (11.2- 22.7) ZJ Gas: Low to medium 26.9 (17.9- 26.9) ZJ Coal: Low to very high 12.6 (12.6- 44.4) ZJ	Medium 1990- 2100: +22% cropland +9% grasslands +5% forests[d]

(A. Exponential growth rates after World Bank (1999) method (given on pages 371 to 372) is calculated using the different base years from the models.
B. Resource availability is generally combined with scenario specific rates of technological change.
C. Residual and other land- use categories are not shown in the Table.
D. Land- use data for B2 marker taken from AIM land- use B2 scenario run.)

The dataset of SRES A2 scenario used in this study was commissioned by the IPCC and discussed in detail by Nakicenvoic *et al*. (2000)**.** The A2 story line is marked by its highly heterogeneous world. This particular scenario is characterized by continuous increase in population (Lutz, 1996). Population reaches over 10 billion by 2050. Medium economic growth with up to 2.3 GDP is expected by mid of 21st century with emphasis on regionally oriented economy. Per capita income is also considered to be in a medium range as compared to the other story lines. Also, the A2 scenario family is marked with high use of primary energy with

slow developments in technology. The governance is self-reliant with preservation of local identities. Economic development is regionally oriented and economic and technological development is relatively slow, compared to the other story lines. From these major factors, and using Integrated Assessment Models (IAMs), emissions of the major greenhouse gases were developed for the 21st century. Cumulative CO_2 emissions by the middle and end of the 21st century are projected to be about 600 and 1850 GtC respectively, and expected CO_2 concentrations (in parts per million, ppm) for the middle and end of the 21st century in this scenario are about 575 and 870 ppm, respectively. The current concentration of CO_2 is about 380 ppm. Methane and nitrous oxide increases grow rapidly in the 21st century. Sulfur dioxide increases to a maximum value just before 2050 (105 MtS/yr) and then decreases in the second half of the century (60 MtS/yr by 2100) (Nakicenvoic 2000).

2.6 GCM v/s RCM

With reference to prior discussion in the introduction chapter, it has been observed that GCM better simulates global conditions with typically greater than 100 km spatial scales, mean annual and seasonal temporal scales and high vertical scales. The major working variables include wind, temperature and pressure. While to resolve regional physical phenomenon of an area occurring at a mesoscale or microscale there is a need to produce well distributed regional details. For instance, to simulate hydrology of a region we need to observe 0-50 km of spatial scales, mean daily temporal values and near surface data with evapotranspiration, runoff, and soil moisture as principle working variables. The advantage of an RCM lies in compensating for the decreasing accuracy of GCM at higher resolution scale for impact studies. RCM can resolve more accurately many surface features, such as complex mountain topographies and coastlines.

Landman W., in his presentation, Downscaling; An introduction, exclusively pointed out that there are important differences between the real world and the world as represented by GCMs. The model representation of small-scale effects (such as topography) important to local climate could be poorly represented in the GCM, however it is plausible to produce detailed simulations for selected regions by nesting a Regional Climate Model (RCM; or LAM) into a global GCM. For driving the initial and time-dependent lateral boundary conditions of GCM, large-scale fields are used. The RCM is coupled to a global model which regularly provides boundary conditions to the RCM during the model integration. RCM produces better regional detail of temperature and precipitation distribution. The study concluded that RCM is apt to simulate regional structures better represents orographic precipitation. In the vertical, the model-level data have to be interpolated on pressure levels. In the horizontal, the model grid data are transferred to a latitude-longitude or to a polar stereographic grid; in the case of spectral models, the spectral coefficients have to be transformed into grid points.
(http://www.wmo.int/pages/prog/wcp/wcasp/clips/modules/module_forecasts.html)

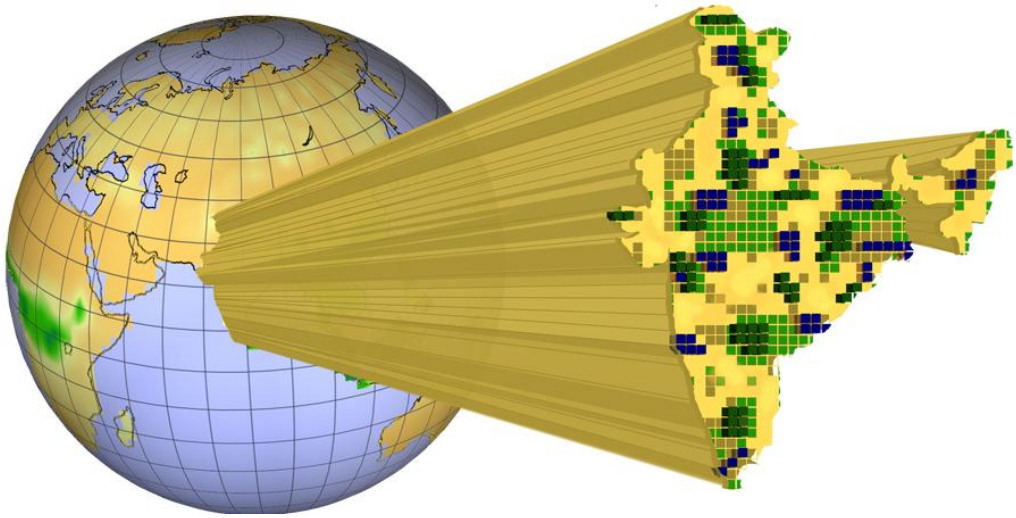

Figure 2.4 *Downscaling of Global grid to Regional scale (design credit: Geneva Hill)*

2.7 Projected future climate forcing data

UKMO-HadCM3, 1997 is a GCM Sponsored by Hadley Centre for Climate Prediction and Research/Met office, UK. The atmosphere top resolution of the model is 2.5° x 3.75° encompassing the top pressure upto 5 hPa with 19 vertical levels (Pope *et al*., 2000). The Ocean Resolution 1.25° x 1.25° with 20 vertical levels (Gordon *et al*., 2000). The model has no adjustments for flux (Gordon et. al., 2000). Majority of GCM do not use flux adjustments any longer (Manabe and Stouffer, 1988; Sausen *et al*., 1988) to decrease the effect of climate drift.
Burke *et al*. (2006) in their study showed that the HadCM3 model, on a global basis and at decadal time scales, 'reproduces the observed drying trend' as defined by the PDSI if the anthropogenic forcing is included, although the model does not always simulate correctly the regional distributions of wet and dry areas (source: Ch.8 IPCC, TAR)

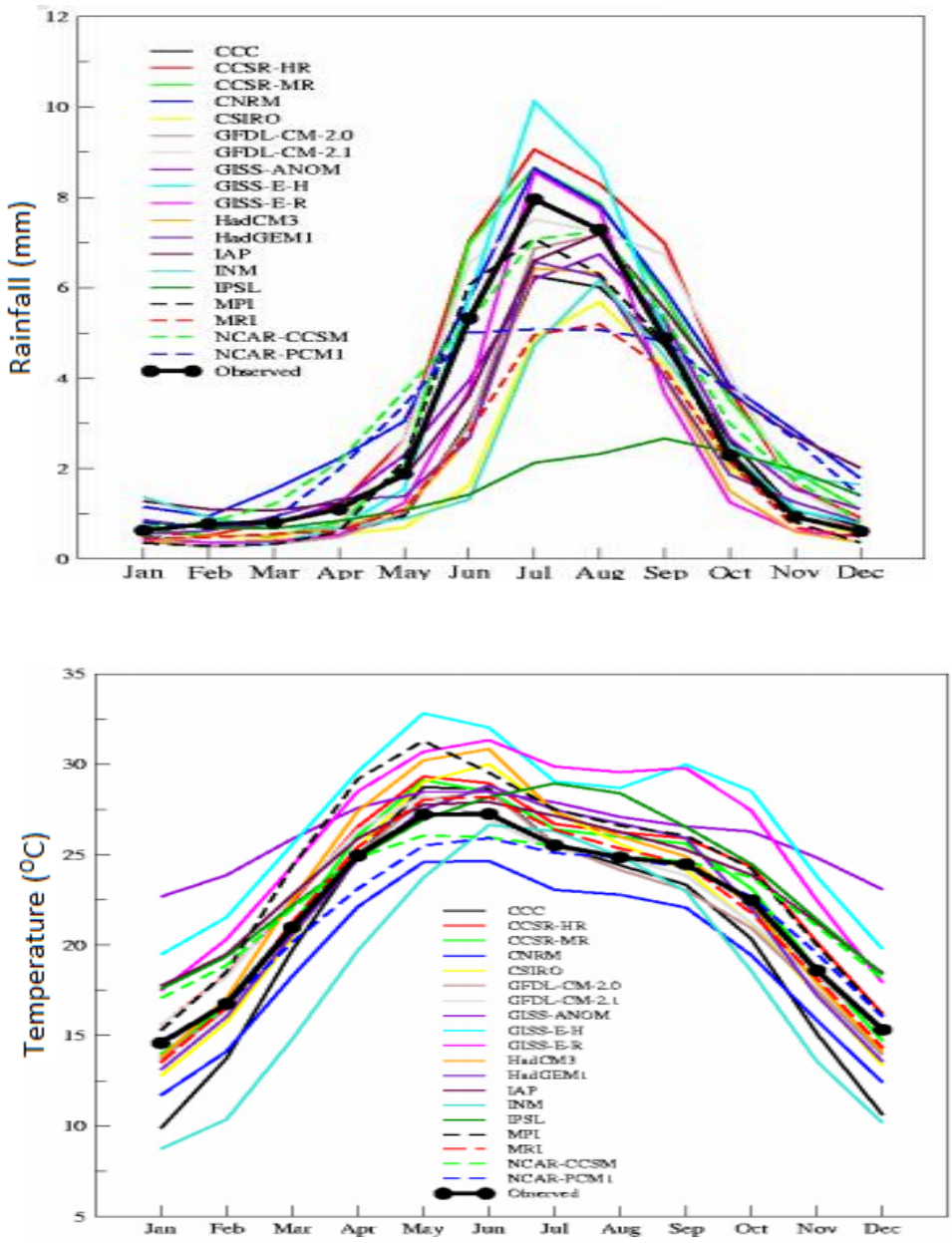

Figure 2.5 *Annual cycles of rainfall and temperature in the 20th century as simulated by various GCMs (IPCC AR4)*

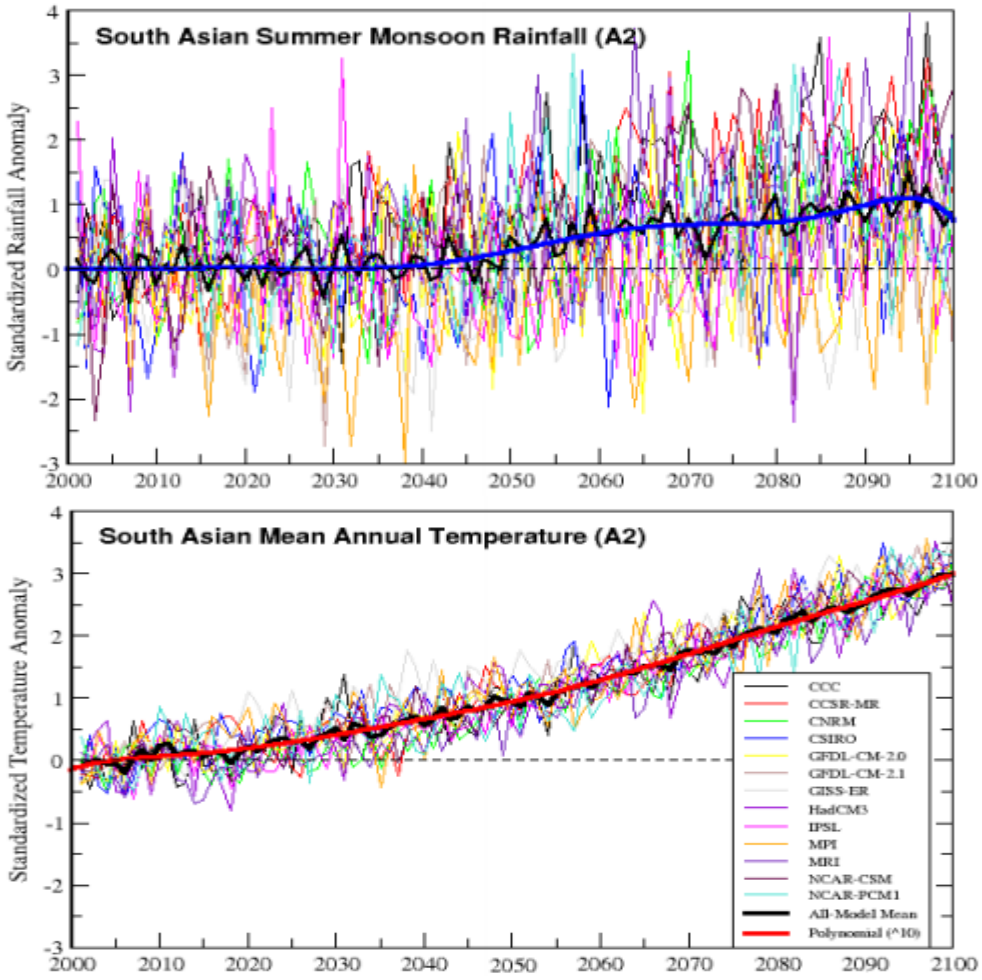

Figure 2.6 *Future scenarios for summer monsoon rainfall over South Asia under A2 scenario as simulated by AOGCMs (IPCC AR4)*

Turner & Slingo (2008) studied uncertainty in predicted changes to intensification of the most extreme events over monsoon regions in the Indian region using the HadCM3 model.

Moors *et al.* (2011) in their study dealing with the issue of adaptation to changing water resources in the Ganges basin**,** runs an ensemble of regional climate model (RCM) to project future air temperatures and precipitation on a 25 km grid for the Ganges basin in northern India, with an aim to assessing impact of climate change on water resources and determining what multi-sector adaptation measures and policies might be adopted at different spatial scales. Results showed that there is an increase in mean annual temperature over the period from 2000 to 2050, averaged over the Ganges basin, in the range 1–4 °C. Projections of simulated precipitation show that due to dominating effect of natural variability on the climate change signal, there is a considerable uncertainty concerning change in regional annual mean

precipitation by 2050. The results of RCMs do suggest an increase in annual mean precipitation in this region to 2050, but lack significant trend.

2.8. Downscaling

Downscaling methods are developed to obtain local-scale surface weather from regional-scale atmospheric variables that are provided by GCMs. With downscaling, a low resolution image is enhanced to a finer resolution using another higher resolution data product and a certain regression procedure. Two main forms of downscaling technique exist:

1. **Statistical downscaling**, where a statistical relationship is established from observations between large scale variables, like atmospheric surface pressure, and a local variable, like the wind speed at a particular site. The relationship is then subsequently used on the GCM data to obtain the local variables from the GCM output.
2. **Dynamical downscaling**, where output from the GCM is used to drive a regional, numerical model in higher spatial resolution, which therefore is able to simulate local conditions in greater detail.

Figure 2.7 *Local Sub Grid Variability (dept. of Washington.edu)*

2.8.1 Statistical Downscaling

Also called empirical downscaling, is a tool for downscaling climate information from coarse spatial scales to finer scales. It is less technically demanding than regional modeling. It is thus possible to downscale from several GCMs and several different emissions scenarios relatively quickly and inexpensively for many decades or even centuries, rather than the brief "time slices" of the dynamical downscaling approach. It is even possible to tailor scenarios for specific localities, scales, and problems. The spatial resolution applied in regional climate modeling is still too coarse for many impact studies, and some variables are either not available or not realistically reproduced by regional models. However, the major weakness of statistical downscaling is the assumption that observed links between large-scale predictors and local predictands will persist in a changed climate. A problem when applying statistical downscaling

techniques to daily values is that the observed autocorrelation between the weather at consecutive time steps is not necessarily reproduced also, Statistical downscaling does not necessarily reproduce a physically sound relationship between different climate elements (Lenart, 2008)

2.8.2 Dynamical Downscaling

With dynamic downscaling, a low resolution image is enhanced to a finer resolution using output from another higher resolution data product and a certain numerical procedure to drive a mesoscale regional, numerical model, which therefore is able to simulate local conditions in higher spatial and temporal resolution (Kim *et.al*., 1984 and Lenart, 2008).
It fits output from GCMs into regional meteorological models. Rather than using equations to bring global-scale projections down to a regional level, dynamic downscaling involves using numerical meteorological modeling to reflect how global patterns affect local weather conditions. The level of detail involved strains computer capabilities, so computations can only tackle individual GCM outputs and brief time slices. Yet climatologists generally consider three decades about the minimum for deducing climatic conditions from the vagaries of weather. (Kattsov and Vladimir, 2010, Lenart, 2008, Bader *et al*., 2008, Maurer and Hidalgo, 2007).
All the atmospheric processes as we can put are governed by certain laws of physics which can be expressed mathematically in the form of various differential equations. These set of equations are put together to constitute a numerical model. Hence, a numerical model is a mathematical representative of a physical system and falls under the category of dynamic downscaling. Downscaling of extreme events at a larger resolution in numeric and physical based future regional climate model simulations will provide sufficient information at the spatial scale necessary for climate change decision making and adaptation (Castro *et al*., 2011)

Some refined form of dynamic downscaling simulation use a grid nesting. The model-level data needs to be interpolated on vertical pressure levels. The model grid data are projected to a horizontal latitude-longitude or to a polar stereographic grid; in the case of spectral models, the spectral coefficients have to be transformed into grid points. Both empirical and dynamical downscaling techniques have the potential to improve on large-scale forecasts of GCMs. Empirical techniques are easy to use and do not require lots of computational resources; climate might be unstable. Dynamical techniques are relatively complex and consume a lot of computational resources; skill limited by parameterization schemes, etc. To justify its operational use, dynamical techniques should outperform empirical techniques (Landman).

In a study by Gupta *et al*. (2011), SCS model was used to estimate runoff at National scale and results were analyzed at 10 km spatial and monthly temporal scales during normal climatic (1951-1950) and projected climatic scenario (2080 projections from HADCM3). . Runoff is one of the key parameters used as an indicator of hydrological process. This study was taken up to analyse the climate change impact on the runoff of river basins of India. The Global Circulation Model (GCM) output of Hadley centre (HADCM3) projected climate change data was used.

Scenario for 2080 (A2 scenario indicating more industrial growth) was selected. The runoff was modeled using the Curve Number (CN) method in spatial domain using satellite derived current Landuse/cover map. The derived runoff was compared with the runoff using normal climatic data (1951-1980). The results showed that there is a decline in the future climatic runoff in most of the river basins of India compared to normal climatic runoff. The findings of the study showed that in Ganga river basin reported runoff in the year 1975 was 55.0 Mha-m. The estimated normal runoff in the years 1951 to 1980 was 37.6 Mha-m while the estimated projected runoff for 2080; A2 scenario was 29.60 Mha-m. Major reductions in total annual runoff of Ganga were of 8.7 Mha.

2.9 WRF Model: Physics parameterizations

Shekhar *et al*. (2012) in a study of numerically simulating the high precipitation event over Leh region on 05August, 2010 used two cloud microphysics parameterization schemes namely WSM3 and WSM6 for the sensitivity experiments and analyzed the results to examine the performance of both the schemes in capturing such extreme localized heavy rainfall events. Results showed that the WSM6 microphysics was able to simulate the precipitation near to the observation. It was also found that precipitation simulated in WSM6 scheme (70 mm) was in good agreement with the TRMM observed precipitation (90 mm). Cloud microphysical process plays an important role through direct influences on the cold pool strength (due to rainfall evaporation) and latent heating (due to condensation) (Rajeevan *et al*., 2010). Sensitivity of cloud microphysics in predicting extreme heavy rainfall events was done by many researchers (Deb *et al*.2008; Kumar *et al*.2008) and analyzed the heavy rainfall events by using different microphysics and cumulus parame-terization schemes in WRF mesoscale model. Litta *et al*. (2007) has done the same studies with MM5 mesoscale model. Two experiments were conducted by using two different cloud microphysics (WSM3 and WSM6), and inter-comparison of important parameters such as wind at different levels, precipitation, longitude–height cross-section of meridional and vertical winds had been studied. WRF single moment 6 Class graupel scheme (Hong *et al*. 2004) consists of ice, snow, and graupel processes suitable for high resolution simulations, and the other is WRF single moment 3 class scheme (Hong *et al*.2004) which is a simple efficient scheme that has ice, snow, and graupel processes including the ice sedimentation and other new ice phase parameterizations suitable for mesoscale grid resolutions. The computational procedure was described by Hong and Lim (2006). In WSM6, the freezing/melting processes are computed during the fall-term sub-steps to increase accuracy in the vertical heating profile of these processes. The order of the processes was also optimized to decrease the sensitivity of the scheme to the time step of the model.

2.10 Climate Change Impact on Global Hydrology

Changes in land surface hydrology due to changing climate have potentially far reaching implications both for human populations and for regional-scale physical and ecological processes. Nijssen *et al*. (2001c) targeted nine large river basins to analyze the regional hydrological consequences of climate predictions in a global context using VIC land surface model. Climate scenarios from eight GCMs were obtained from the Intergovernmental Panel on Climate Change Data Distribution Center (IPCC-DDC). The daily data were used to drive the VIC model to calculate a set of derived components (evapotranspiration, runoff, snow water equivalent, and soil moisture) and to study the water balance of each of the continents. For each 2° × 2° model grid cell land surface characteristics such as elevation, soil, and vegetation were specified. Vegetation types were extracted from the 1 km, global land classification of Hansen *et al*. (2000). Vegetation parameters such as height and minimum stomatal resistance were assigned to each individual vegetation class. Soil textural information and soil bulk densities were derived from the 5 minute FAO-UNESCO digital soil map of the world (FAO, 1995). The remaining soil characteristics, such as porosity, saturated hydraulic conductivity, and the exponent for the unsaturated hydraulic conductivity equation were based on Cosby *et al*. (1984).

In a study in China in the Hanjiang basin by Guo *et al*. (2009) a Smooth Support Vector Machine (SSVM) was employed for statistical downscaling of GCM parameters to simulate the runoff using VIC model. Daily precipitation and temperature output of GCM from two different SRES scenarios, A2 and B2, were used to observe the climate change induced changes in the hydrology of the basin. The Variable Infiltration Capacity (VIC) distributed hydrological model with a 9 ×9 sq. km. grid resolution was established and calibrated in the Hanjiang basin of China. Validation results gave a clear indication that the VIC model could simulate the runoff hydrograph with high model efficiency and low relative error with respect to observed precipitation and temperature data. The trends of precipitation and temperature projected under the A2 and B2 scenarios will decrease in the 2020s and increase in the 2080s. However, in the 2050s, the precipitation will decrease under the A2 scenario and there will be no significant changes under the B2 scenario, but the temperature will be not obviously change under either scenario. Under both scenarios, the impact analysis of runoff made with the downscaled precipitation and temperature time series as input to the VIC model.

Dušan Trninić (2010) discussed the impact of climatic variability on the watershed and channel hydrology. They suggested that over the coming years, climatic variability will have an impact on food and water security in significant and highly uncertain ways. Developing countries will bear the brunt of the adverse consequences, particularly from climate change. This is largely because the rural populations of developing countries for whom agricultural production is the primary source of direct and indirect employment and income will be most affected due agriculture's vulnerability to climatic variability processes. The agricultural sector is the largest consumer of water resources, and variability in water supply has a major influence on health

and welfare in poor areas. With water scarcity and extreme weather events expected to increase under climate change, water security could decline significantly in rural areas.

Changes in temperature and precipitation alter the climatic conditions and subsequently hydrological and watershed processes in the long run. The effects of changes due to climatic variability on catchment hydrological responses have been extensively carried out at watershed and river basin scales. Studies concluded that precipitation strongly affects runoff, evapotranspiration, base flow relative to other climatic variables (Bosch and Hewlett, 1982). There has been a growing need to study, understand and quantify the impact of climatic variability on hydrologic regime, both water quantity and quality. This is necessary for satisfying and managing water resources requirements of increasing population. Additionally, changes in climatic variables such as precipitation alter the rate at which water runs off the land surface and infiltrates the soil column and how groundwater conditions are changing with respect to time. Overall water balance is being affected by climatic variability.

Studies are carried out at national scale in U.S. (Adams, 2000) have shown that some significant changes in the timing and amount of runoff will result from plausible changes in climatic variables. Furthermore it indicates that U.S. watersheds with a substantial snowpack in winter will experience major changes in the timing and intensity of runoff as average temperatures rise. Reductions in spring and summer runoff, increases in winter runoff, and earlier peak runoff are all common responses to rising temperatures. Large changes in the reliability of water yields from reservoirs could result from small changes in inflows.

Alexandrov and Genev (2003) studied the impact of climatic variability and change impact on water resources in Bulgaria. They studied the variability in temperature, precipitation and river runoff during the 20^{th} century. Possible scenario for temperature and precipitation were prepared by assuming current trends. In 20^{th} century annual runoff is expected to decrease up to 14% in 50 years and by 20% at the end of century in Bulgaria. Also for future scenario from GCMs has been used for simulating 21^{st} century scenario by assuming other parameters as same. They found out decreasing trend of water resources in Bulgaria.

Gosain *et.al*. (2006) studied Climate change impact assessment on hydrology of Indian river basins. A distributed hydrological model namely SWAT (Soil and Water Assessment Tool) has been used. Simulation over entire river basins of the country has been made using 40 years (20 years belonging to control or present and 20 years for GHG (Green House Gas) or future climate scenario) of simulated weather data. The initial analysis has revealed that under the GHG scenario, severity of droughts and intensity of floods in various parts of the country may get deteriorated. Thus, climate change impacts are going to be most severe in the developing world, because of their poor capacity to adapt to climate variability. India also comes under this category. The NATCOM study was the first attempt to quantify the impact of the climate change on the water resources of the country. The Ganga river has been selected as the one which has been predicted to have maximum impact on account of the water resources in northern India. The study reveals that this river basin is expected to receive comparatively higher level of precipitation in future and a corresponding increase in evapotranspiration and water yield is also predicted.

3. MODEL OVERVIEW

3.1 Weather Research and Forecasting (WRF) Model v3.4.1

WRF: *Weather Research and Forecasting Model* is a product of collaborative partnership, principally among NCAR, NOAA, NCEP, FSL, AFWA, FAA) It is flexible, state-of-the-art atmospheric and weather simulation system, portable and efficient on available parallel computing platforms, suitable for use in a broad range of applications across scales ranging from meters to thousands of kilo-meters and includes real-time NWP, forecast research, parameterization research, coupled-model applications and teaching (www.wrf-model.org).

3.1.1 Components of WRF model:

- WRF Pre-processing System (WPS)
- WRF-ARW solver n codes
- WRF Postprocessor (WPP)
- RIP (Read, Interpolate, Plot)
- Model Evaluation Tools (MET)

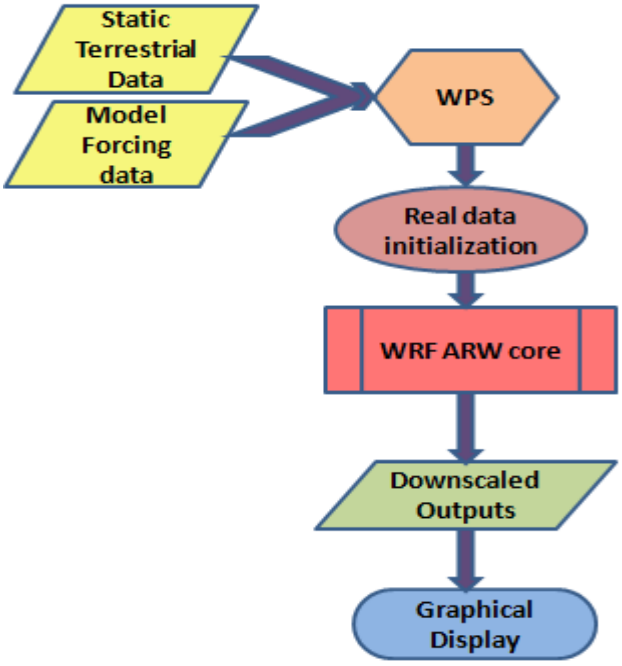

Figure 3.1 *Major Components of WRF model*

3.1.2 WRF Pre-processing System (WPS)

WPS is used to interpolate terrestrial data and meteorological data for real data simulation. Following utilities are exploited in WPS for the preparation of inputs for the dynamic core of the model:

a) Geogrid: Defines simulation domain and ARW nested domains. It interpolates the static geographic data to the grids of the model domain. Some of the time Invariant terrestrial fields interpolated by geogrid are:
   - Topography heightLand use categories
   - Soil type (top layer & bottom layer)
   - Annual mean soil temperature
   - Monthly vegetation fraction
   - Monthly surface albedo

b) Ungrib: It degribs or extracts the Grib format meteorological fields into intermediate format.

c) Metgrid: It interpolates the time varying meteorologic data from another model extracted by ungrib to the domain defined by geogrid horizontally.

The various interpolation options available are:

- 4-point bilinear
- 16-point overlapping parabolic
- 4-point average (simple or weighted)
- 16-point average (simple or weighted)
- Grid cell average
- Nearest neighbor
- Breadth-first search

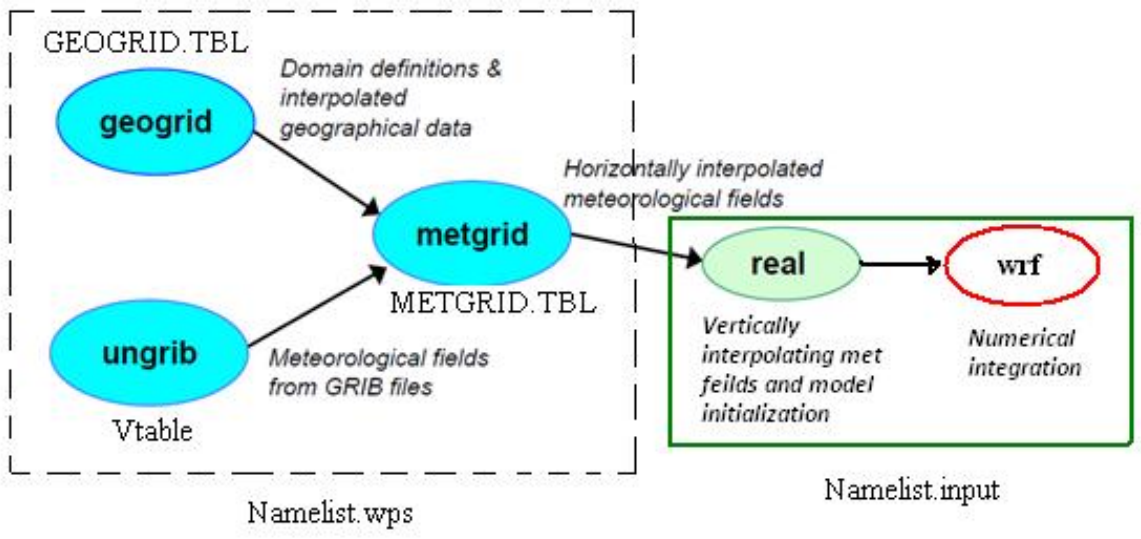

Figure 3.2 *Summary of WRF Process Flow (Duda, 2010)*

3.1.3 WRF-ARW solver

It contains an initialization program and numerical integration program that performs the dynamic downscaling of GCM.

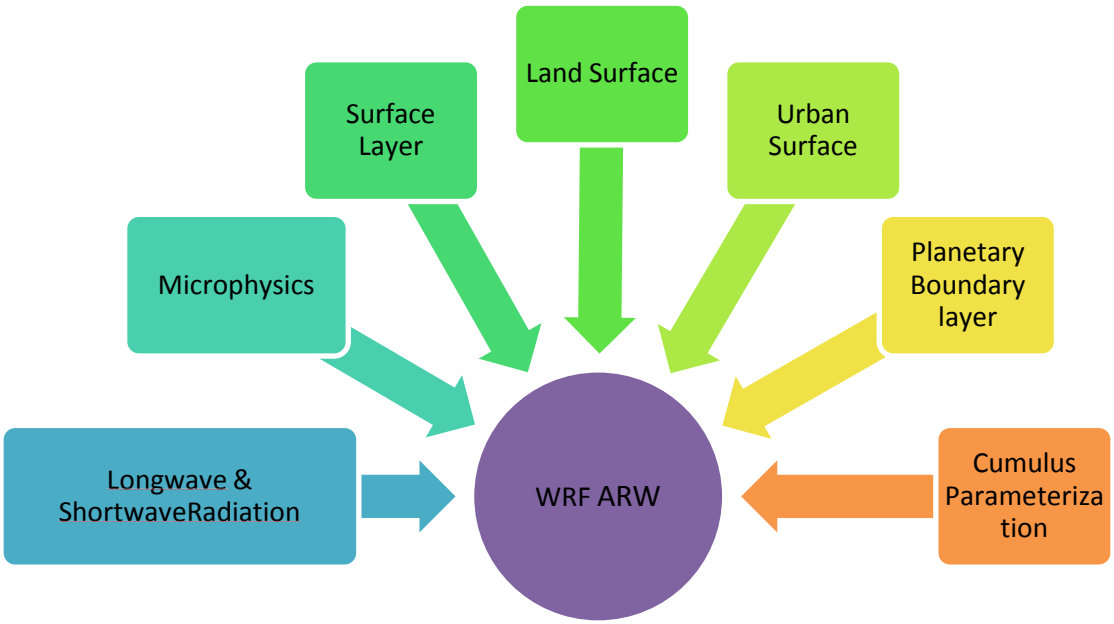

Figure 3.3 *Physics Parameters of WRF ARW Solver*

3.1.4 Model Equations

Equation of Physics used by the model core (Prashant, 2012)

(i) II Law of Newton's Theory

$$\frac{\partial u}{\partial t} = -u\frac{\partial u}{\partial x} - v\frac{\partial u}{\partial v} - w\frac{\partial u}{\partial z} + fv - \frac{1}{\rho}\frac{\partial p}{\partial x} + F_x \quad (3.1)$$

$$\frac{\partial v}{\partial t} = -u\frac{\partial v}{\partial x} - v\frac{\partial v}{\partial v} - w\frac{\partial v}{\partial z} - fu - \frac{1}{\rho}\frac{\partial p}{\partial y} + F_y \quad (3.2)$$

$$\frac{\partial w}{\partial t} = -u\frac{\partial w}{\partial x} - v\frac{\partial w}{\partial v} - w\frac{\partial w}{\partial z} - \frac{1}{\rho}\frac{\partial p}{\partial x} - g \quad (3.3)$$

(ii) *Continuity Equation*

$$\frac{\partial \rho}{\partial t} = -\rho\left(\frac{\partial u}{\partial x} + \frac{\partial v}{\partial y} + \frac{\partial w}{\partial z}\right) \qquad where, \qquad \frac{\partial u}{\partial x} + \frac{\partial v}{\partial y} + \frac{\partial w}{\partial z} = 0 \quad (3.4)$$

(iii) I Law of Thermodynamics

$$Q = C_P\frac{dT}{dt} - \frac{1}{\rho}\frac{dp}{dt} \quad (3.5)$$

(iv) Humidity Conservation

$$\frac{\partial q}{\partial t} = -u\frac{\partial q}{\partial x} - v\frac{\partial q}{\partial v} - w\frac{\partial q}{\partial z} + E - P \quad (3.6)$$

3.1.5 WRF Post Processor

It is used for postprocessing the WRF outputs. In the present study an alternative UPP was used.

3.1.6 Unified Post Processor (UPP)

It reads the WRF outputs and invokes the graphical routines for the purpose of visualization of model outputs using Grid Analysis and Display System (GRADS).

3.1.7 Model Evaluation Tool (MET)

It compares gridded model output with point based or gridded observations.

3.2 WRF Domain Wizard

WRF Domain Wizard is a Graphical User Interface (GUI) tool written in java language for running various processes of WPS. It enables user to create gridded and nested regional domains and define projection graphically on a world map. It also writes namelist.wps and namelist.input as defined by the user and provides facility to run the processes of WPS. Though it is a component of WRF Portal, It can downloaded and run as a standalone application. (Smith, McCaslin, 2008)

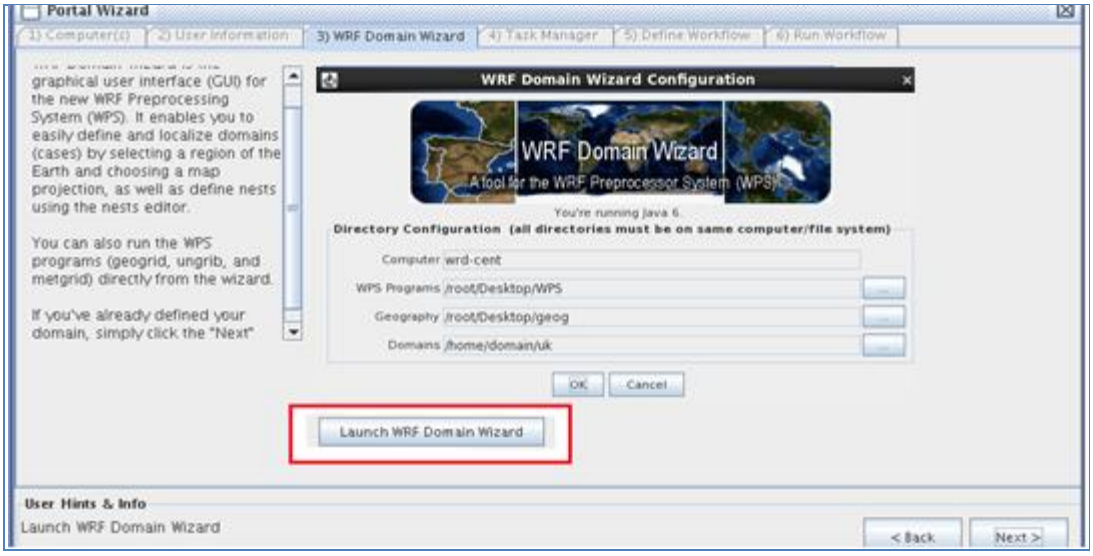

Figure 3.4 *WRF Domain Wizard startup*

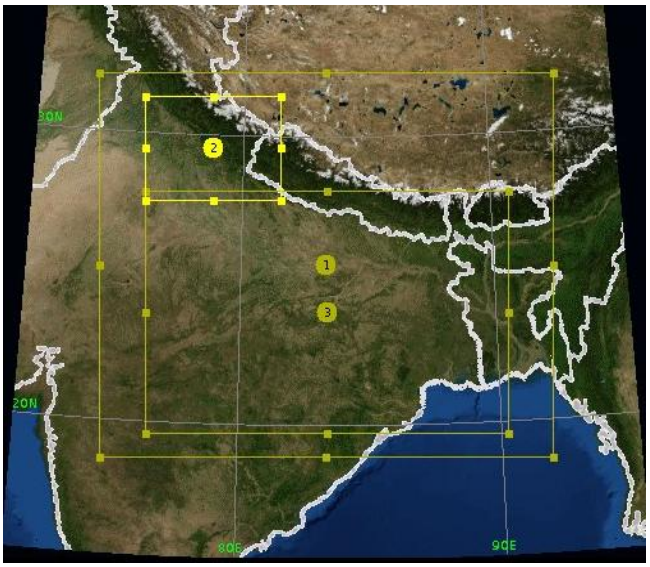

Figure 3.5 *Defining domain and creating nests in WRF Domain Wizard*

3.3 Variable infiltration capacity (VIC) model

Variable infiltration capacity model is a grid-based macroscale hydrological model designed to represent surface energy and hydrological fluxes for large river basins. The VIC model was developed for incorporation in GCMs, aiming to improve the representation of horizontal resolution and subgrid vegetation heterogeneity in a simple way employing the infiltration and surface runoff scheme in Xianjiang model (Zhao, 1980). A full suite of hydrologic variables is constructed from limited observed driving data (precipitation, maximum and minimum air temperature, and wind speed) (Nijssen *et al*., 2001). The sub grid heterogenous VIC model represents vegetation heterogeneity, multiple soil layers with variable infiltration, and non-linear base flow (*http://www.hydro.washington.edu/Lettenmaier/Models/VIC*).

3.3.1 VIC Model Components

The overall VIC model framework has been described in detail in literature (Liang *et al*., 1994, Liang *et al*., 1996, and Nijssen *et al*., 1997). VIC computes the vertical energy and moisture flux in grid cell based on specification at each grid cell considering soil properties and mosaic of vegetation classes in each grid. The resulted runoff and base flow is routed via a separate channel routing module to produce stream flow at selected point within the domain.
(http://www.hydro.washington.edu/Lettenmaier/Models/VIC)

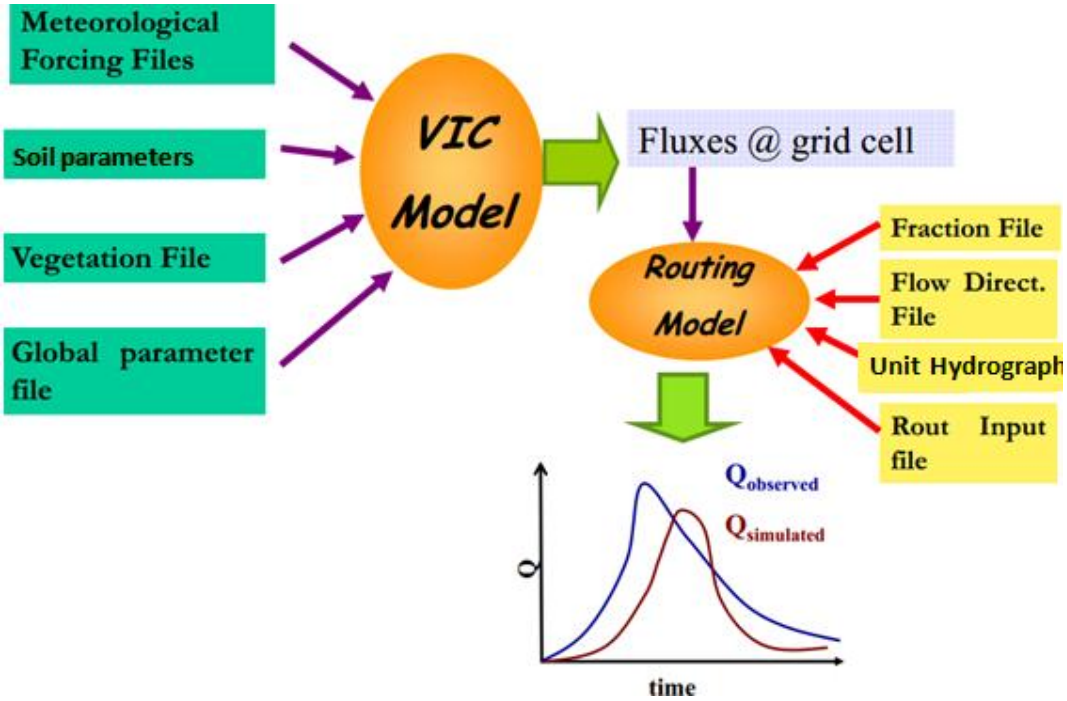

Figure 3.6 *Schematic flow of VIC Model processes (image courtesy: E. D. Maria)*

3.3.2 Vegetation cover

The surface of each grid cell is described by *N+1* land cover tiles, where n = 1, 2, … , N represents *N* different tiles of vegetation, and *n = N+1* represents bare soil. For each vegetation tile, the vegetation characteristics, such as LAI, albedo, minimum stomatal resistance, architectural resistance, roughness length, relative fraction of roots in each soil layer, and displacement length (in the case of LAI) are assigned. In the model, soil moisture distribution, infiltration, drainage between soil layers, surface runoff, and subsurface runoff are all calculated for each land cover tile at each time step. Then for each grid cell, the total heat fluxes (latent heat, sensible heat, and ground heat), effective surface temperature, and the total surface and subsurface runoff are obtained by summing over all the land cover tiles weighted by fractional coverage. *(http://www.hydro.washington.edu/Lettenmaier/Models/VIC)*

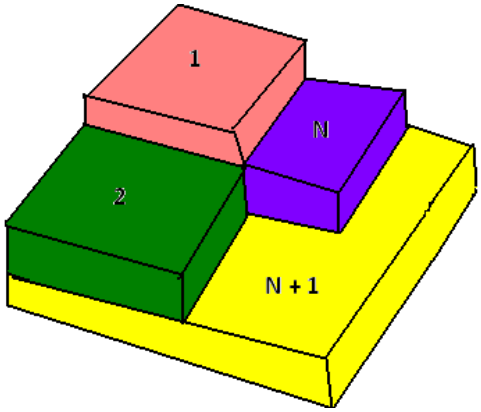

Figure3.7 *Grid cell vegetation coverage*

3.3.3 Soil layers

The parameters required by three layer soil layer model VIC-3L (Liang *et al*., 1996):

- Infiltration parameter
- Evaporation parameter
- Base flow recession coefficient
- Spatially varying vegetation within each grid cell
- Soil moisture in every layer

Soil parameters for each grid and soil layer is specified in user defined soil parameter file.

3.3.4 Rainfall

VIC model considers the sub-grid variability of precipitation which is distributed throughout all or a portion of grid cell as a function of rainfall intensity. Precipitation distribution can be expressed as follows,

$$\mu = (1-e^{-aI}) \quad (3.7)$$

- I = Precipitation intensity
- a = coefficient describing effect of grid cell size and geography

3.3.5 Evapotranspiration

Evapotranspiration is calculated according to the Penman-Monteith equation. The VIC model considers three types of evaporation (Liang *et al*., 1994):

- E_c = evaporation from the canopy layer of each vegetation tile
- E_t = transpiration from each of the vegetation tiles
- E_1 = evaporation from the bare soil

(All units in mm)
Total evapotranspiration over a grid cell is formulated as:

$$E = \sum_{n=1}^{N} C_n \cdot (E_{c,n} + E_{t,n}) + C_{N+1} \cdot E_1 \quad (3.8)$$

- C_n = vegetation fractional coverage for the nth vegetation tile
- C_{N+1} = bare soil fraction, and $\sum_{n=1}^{N+1} C_n = 1$

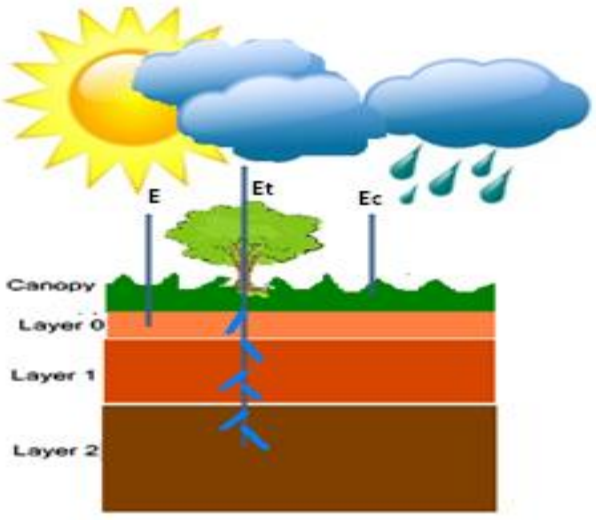

Figure 3.8 *Cell energy components and soil layers*

3.3.6 Infiltration

This model assumes that infiltration capacity of the soil is not uniform. Hence runoff generation and evaporation vary within an area owing to variations in topography, soil and vegetation. It also considers that infiltration capacity is storage and not a rate. Sub-grid variability scheme in

infiltration is used to account Variable Infiltration capacity. VIC uses infiltration formula used in Xinanjang model which assumes that precipitation in excess of the available infiltration capacity forms surface runoff.

$$i = i_m [1-(1-A)^{1/b_i}] \quad (3.9)$$

- i = Infiltration capacity upto which the soil is filled
- i_m = Maximum infiltration capacity
- A = represents the saturated fraction of the grid cell ($0 \leq A \leq 1$)
- b_i = shape parameter

Maximum soil moisture of soil layer W_{c1} is related to i_m and b_i as,

$$W_{C1} = \frac{i_m}{1+b_i} \quad (3.10)$$

Also VIC model assumes that runoff is generated by areas where precipitation added to soil moisture storage at the end of the previous time step exceeds the storage capacity of the soil. The direct runoff Q_d from the fraction of saturated area is given by,

$$Q_d = P-W_{c1}+ W_1^- \qquad i_0 + P \geq i_m \quad (3.11)$$

$$Q_d = P-W_{c1}+ W_1^- + W_{c1}\left(1- \frac{i_0 \quad p}{i_m}\right) \qquad i_0 + P \leq i_m \quad (3.12)$$

- W_1^- = soil moisture content in layer 1 at beginning of the time step
- i_0 = infiltration capacity of the saturated area.

For bare soil, water balance layer is described by,

$$W_1^+ = W_1^- + P - Q_d - Q_{12} - E \quad (3.13)$$

- W_1^+ = Soil moisture content in layers at the end of each time step
- Q_{12} = drainage from layer 1 to layer 2

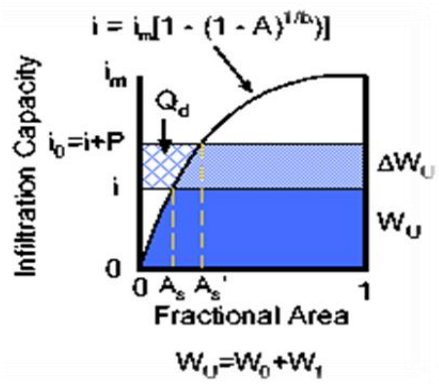

Figure 3.9 *Infiltration Capacity Curve*

3.3.7 Base flow

Drainage between soil layers is gravity derived as well as unsaturated hydraulic conductivity is a function of the degree of saturation of the soil. Base flow is derived as the function of soil moisture in the lowest soil layer using Arno-non linear formula.

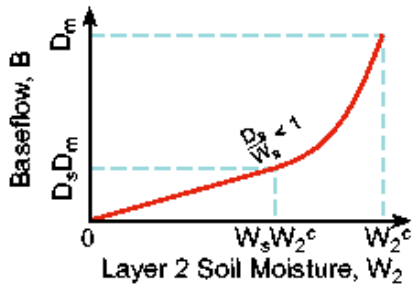

Figure 3.10 *Base flow curve*

- Dm = Maximum base flow parameter
- D_s = Fraction of Maximum base flow
- W_s = Fraction of maximum soil moisture
- W_{c2} = Maximum soil moisture in layer 2
- W_2^- = soil moisture at the beginning of time step in layer 2

3.3.8 Routing

To simulate streamflow, VIC results are typically post-processed with a separate routing model (Lohmann, *et al*., 1996; 1998a; b) based on a linear transfer function to simulate the streamflow.

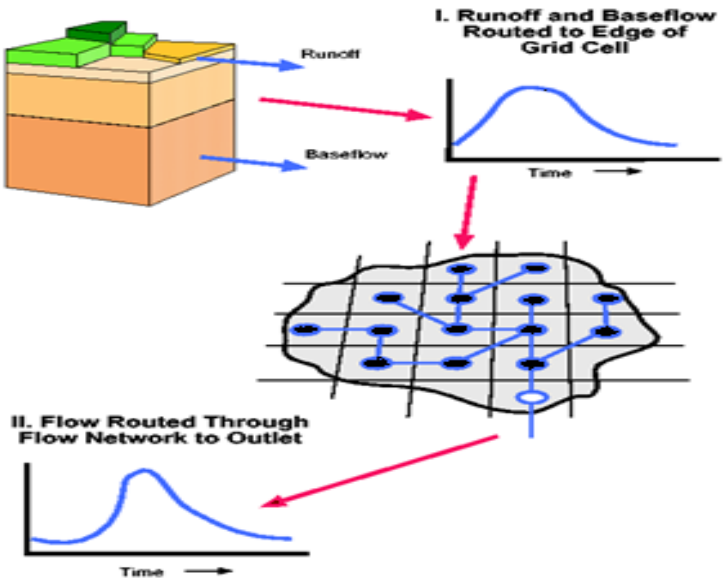

Figure 3.11 *Schematic of VIC network routing model*

It is assumed that most horizontal flow within the grid cell reaches the channel network within the grid cell before it crosses the border into a neighboring grid cell. Flow can exit each grid cell in eight possible directions but all flow must exit in the same direction. The flow from each grid cell is weighted by the fraction of the grid cell that lies within the basin. Once water flows into the channel, it does not flow back out of the channel and therefore it is removed from the hydrological cycle of the grid cells. The daily surface runoff and baseflow in VIC is calculated as given:

$$R_1 = \sum_{j=1}^{i<j} Q_j \tag{3.14}$$

- R_1 = Runoff routed internally at the grid outlet
- Qj = Runoff outflow
- I = Unit hydrograph time step
- j = Runoff time series time step
- i = Total number of time steps in runoff time series
- H = Ordinates of unit hydrograph

3.3.9 Water Balance Mode

The VIC model can be run in either a water balance mode or a water-and-energy balance mode. The water balance mode does not solve the surface energy balance. Instead, it assumes that the soil surface temperature is equal to the air temperature for the current time step. By eliminating

the ground heat flux solution and the iterative processes required to close the surface energy balance, the water balance mode requires significantly less computational time than other model modes (Andreadis *et al*., 2009; Bowling *et al*., 2004; Cherkauer and Lettenmaier 1999; Storck *et al*., 1998). The continuous equation used for water balance in VIC model for each time-step:

$$\frac{\partial S}{\partial T} = P - E - R \tag{3.15}$$

- $\frac{\partial S}{\partial T}$ = change of water storage for the time-step (mm)
- P = precipitation (mm)
- E = evapotranspiration (mm)
- R = runoff (mm)

Over vegetated areas, the water balance equation in the canopy layer is:

$$\frac{\partial W_i}{\partial t} = P - E_c - P_t \tag{3.16}$$

- W_i = canopy intercepted water (mm)
- E_c = evaporation from canopy layer (mm)
- P_t = througfall (mm)

3.3.10 Meteorological Forcing

The VIC model is forced with observed surface meteorological data which include:

- precipitation (mm)
- temperature (^oC)
- wind (m/s)
- vapor pressure
- incoming longwave radiation
- incoming shortwave radiation
- air pressure

3.3.11 Highlights of the VIC Model

In comparison to other land surface models, VIC's distinguishing hydrologic features are:

- VIC explicitly represents effects of multiple vegetation covers on water and energy budgets and simultaneously solves full surface energy and water balances giving multiple outputs.
- It represents of subgrid variability in soil moisture storage capacity as a spatial probability distribution, to which surface runoff is related (Zhao *et al*., 1980).
- It incorporates the representation of subgrid spatial variability of precipitation with the representation of spatial variability of infiltration to simulate energy and water budgets (e.g., energy fluxes, runoff, and soil moisture).

- It includes both the saturation and infiltration excess runoff processes in a model grid cell with a consideration of the subgrid-scale soil heterogeneity (Liang and Xie, 2001) and the frozen soil processes for cold climate conditions (Cherkauer and Lettenmaier, 1999).
- It belongs to the category of surface vegetation atmospheric transfer scheme (SVATS) and has ability to couple with Global Circulation Models (GCM) and other Climate models.

3.4 VIC Tool

Graphical User interface for VIC Hydrological model

The tool is specially designed to enable the VICModel user to execute the processes of the model in an efficient manner without going through the trouble of switching between Windows OS and linux OS. The primary functions performed by the tool is categorised as follows:

a. Data preparation
b. Soil parameter preparation
c. Vegetation parameter preparation
d. Forcing preparation
e. Model execution
f. Water balance mode
g. Global parameter preparation
h. Model run
i. Result analysis
j. Tabular analysis

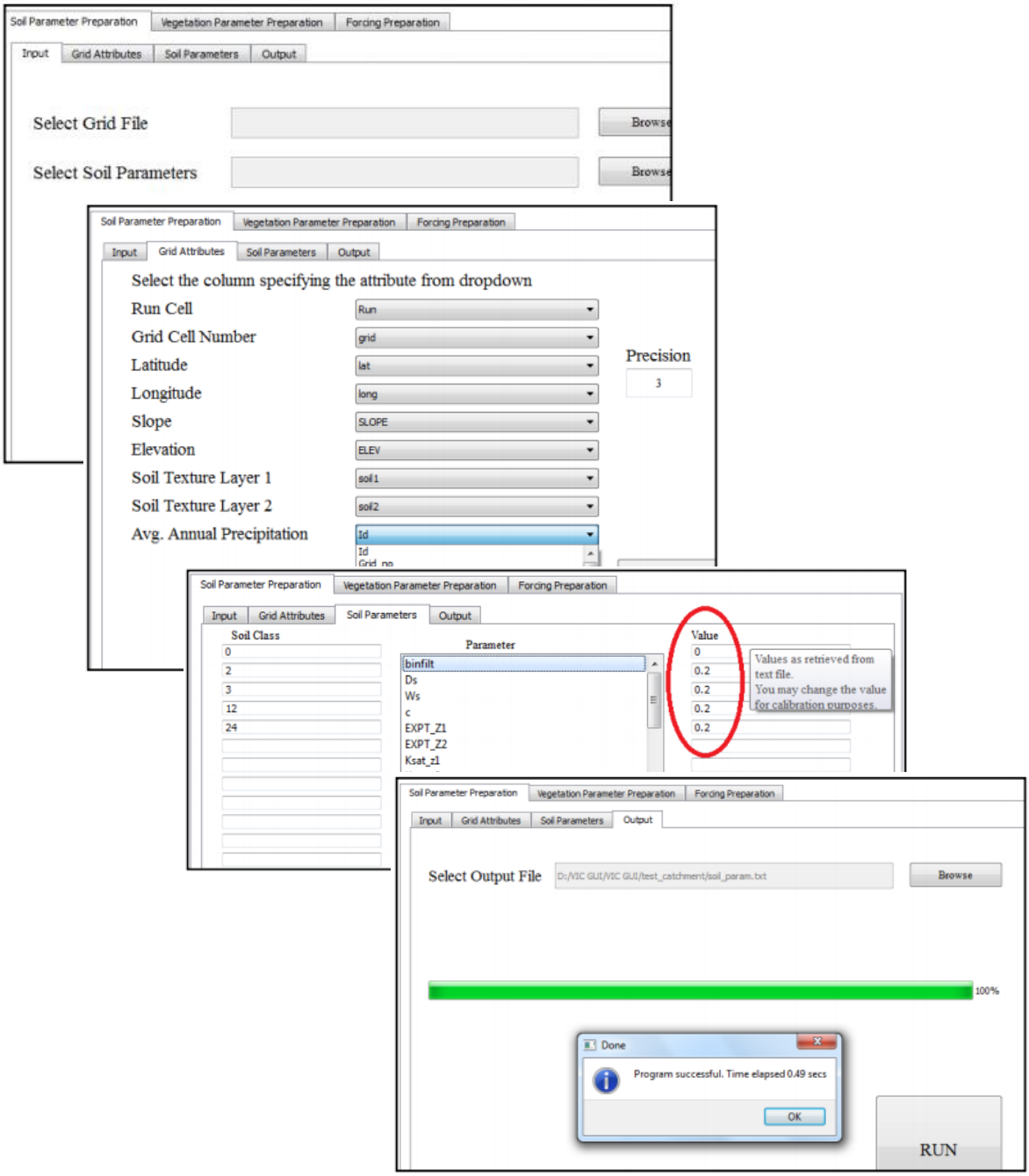

Figure 3.12 *Sample steps of execution of VIC tool. The tool was developed as part of ISRO-GBP project on LULC dynamics and impact of human dimensions in Indian River basins, IIRS Dehradun.*

4. STUDY AREA

The Ganga Basin

India's major part of fresh water resources come from more than 20 river systems along with several of their tributaries. The largest river basin among all the basins in India is the Ganga basin occupying nearly one-third of India's geographical. It is also one of the world's largest river systems endowed with remarkable diversity in topography, climate, soil type, land cover, flora & fauna, social and cultural life.
The Ganga River is a sacred river of India with several religious pilgrimages built along the river's course. The orgin of mythology of river Ganga goes as far in history as the foundation of civilization itself. The socio-economic, religious and cultural importance of river Ganga is legendary. The first Prime Minister of India, Jawaharlal Nehru, described Ganga as, "*She has been a symbol of India's age-long culture and civilization, ever changing, ever flowing, and yet ever the same Ganga*." (Jain *et al.*, 2007)

4.1. Location and Extent of Ganga Basin

The Ganges river system originates in the Central Himalayas, and extends into the alluvial Gangetic Plains and drains into the Indian Ocean at the Bay of Bengal. The Ganga basin principally covers major parts of India, and practically whole of Nepal and Bangladesh including parts of Tibet (China). The river flows through 11 states along with its tributaries namely Uttarakhand, Uttar Pradesh., Delhi, Madhya Pradesh., Rajasthan, Haryana, Himachal Pradesh, Chhattisgarh, Jharkhand, Bihar and West Bengal.

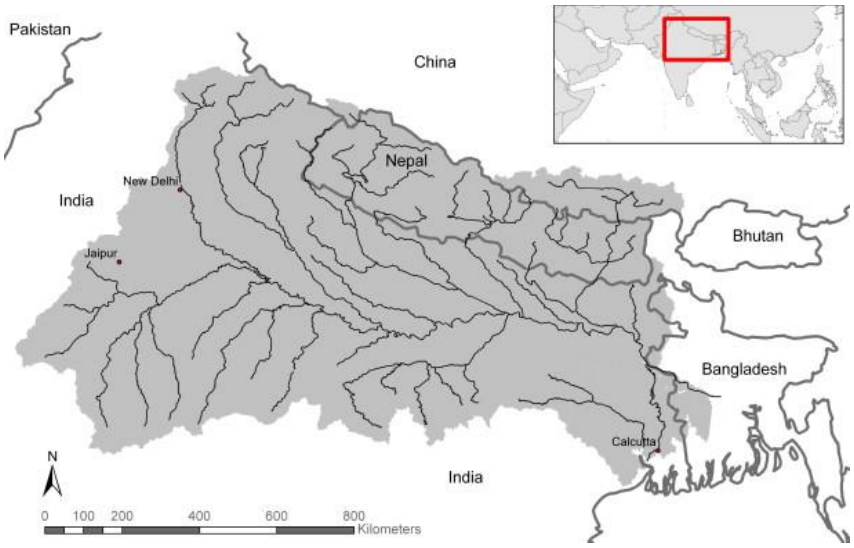

Figure 4.1 *Ganga Basin (Moors et. al., 2011)*

This project studies the Gangetic Plain comprising of areas from India as well as Nepal extending over an area of 9,23,821 sq. km. It lies between 73°38' E to 88°9' E longitudes and

22^{o} 45' N to 31^{o}45' N latitudes. The Farakka barrage is taken as the outlet point of the study basin situated at 87.9333° E longitude and 24.8047° N latitude. It was constructed in 1975 near Chapai Nawabganj District in West Bengal lying roughly 150 km downstream Kolkata.

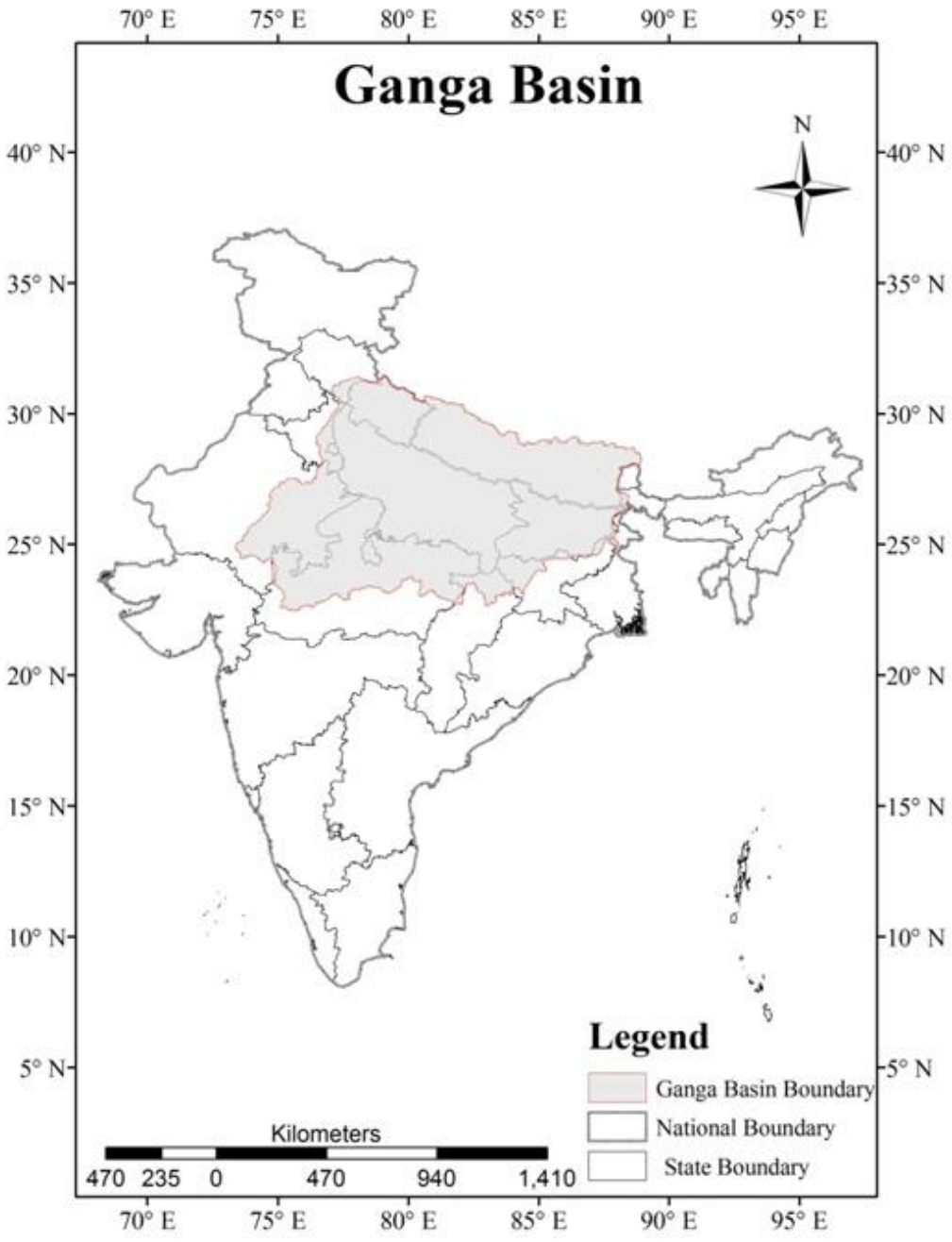

Figure 4.2 *Map Layout of Ganga Basin*

4.2 Course of the river

The Bhagirathi is said to be the source stream of the Ganga. It emanates from the Gangotri Glacier at Gaumukh at an elevation of 7,010 m in Uttarakhand, India (Jain *et al*., 2007). Numerous tributaries and small streams from India and Nepal comprise the headwaters of the Ganga and contribute towards the increased water flow of the river. It traverses a course of about 2525 km before flowing into Bay of Bengal. Some of the principal tributaries joining the Ganga River through its course are Tons, Yamuna, Kosi, Ramganga, Ghaghra, Gandak, Mahananda and Sone. Before draining into the vast ocean ganga is joined by another large river, Brahamaputra (Jain *et al*., 2007).
The river forks into two streams after Farakka barrage which was commissioned by India in 1975 (18km upstream from the Bangladesh border) to control the flow of river downstream.

Table 4.1 *State-wise Distribution of the Drainage Area of Ganga River in India (Source: Status paper on river Ganga, NRCD, MoEF, 2009))*

S. No.	State	Total Area (sq km)	Per Cent of Total Geographical Area
1	Uttar Pradesh & Uttarakhand	294364	34.2
2	Madhya Pradesh	198962	23.1
3	Bihar and Jharkhand	143961	16.7
4	Rajasthan	112490	13.1
5	West Bengal	71485	8.3
6	Haryana	34341	4.0
7	Himachal pradesh	4317	0.5
8	Delhi	1484	0.2
	Total	861404	100.0

Figure 4.3 *Gangotri: point of origin of Ganga*

4.3. Physiographic and Soil Characteristics of Ganga Basin

The Ganga basin can be largely segmented into several distinct physiographic divisions:
The Northern Mountains embracing the Himalayan range are endowed with numerous peaks with elevation upto7500 m. Some mountain peaks in the headwater reaches are permanently covered with snow.
The Gangetic plains encompass the most populous regions of India, Nepal and virtually all of Bangladesh with elevation below 300 m and less than 100 m in the lower plains. The Great Plains are gifted with extremely fertile plains that make the area best suited for large scale intensive cultivation.
The Central highlands lying to the south of the Great Plains consists of mountains, hills and plateaus intersected by valleys and river plains. They are largely covered by forests. Aravalli uplands, Bundelkhand upland, Malwa plateau, Vindhyan ranges and Narmada valley lie in this region.
The Basin exhibits a vast variety of types of soils with majority of sand, loam, clay and their combinations, such as sandy loam, loam, silt clay loam and loamy sand soils. The mountains of Northern Himalayas are susceptible to soil erosion due to steep slope while the lower plains are highly fertile due to accumulation of large amount of sediments brought down by the stream (Jain *et al.*, 2007).

Table 4.2 *Stream Characteristics along Different Sections of the Ganga (Source: Central water Commission)*

S.No.	Stretch	Section	Length (Km)	Average Slope of Land
1	Source to Rishikesh	Mountainous	250	1 in 67
2	Rishikesh to Allahabad	Upper plain	770	1 in 4,100
3	Allahabad to Farakka	Middle plain	1005	1 in 13,800

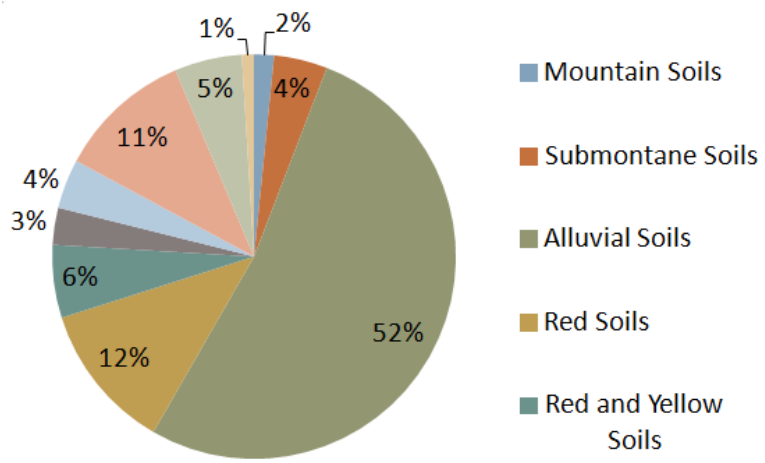

Figure 4.4 *Soil types in Ganga Basin*

4.5. Climate and Hydrology of Ganga Basin

The spatial distribution of precipitation in the basin exhibits largely varying pattern. Annual average rainfall in the Ganga Basin is in the range of 550-2500mm along its course . A major part of the rains is due to the south-western monsoon from July to October (Jayakody P. et al., 2011). The regions of Uttarakhand and upper Uttar Pradesh receive moderate rainfall averaging about 30–40 inches. The Middle Ganges Plain of Bihar receives rainfall from 40 to 60 inches. The delta regions of West Bengal witness highest rainfall, ranging in an average of 60 to 100 inches and also experience strong cyclonic storms both before the arrival and at the end of the monsoon season.

The temperature in Northern Himalayas is relatively lower to the rest of the basin while lower plains experience moderate temperatures. The temperature varies in the basin from 3°C to 4°C in January making it on average the coolest month of the year to 43°C to 45°C in May or June being the warmest.

Table 4.3 *Rainfall and Temperature Details at Selected Stations in the Ganga Basin (Source: Monthly mean data of important cities, India Meteorological Department)*

S.No.	Station and Year	Mean Annual Rainfall (mm)	Water Surplus in Wet Months: Jul-Sep (mm)	Jul-Sep Rainfall Expressed as Percentage of Annual Rainfall	Mean Temperature in ^{0}C	
1	Dehra Dun (1901-2000)	2209.0	1697.4	76.8	27.8	15.4
2	Delhi (Safdarjang) (1901-2000)	716.2	535.2	74.7	31.3	19.0
3	Hissar (1901-2000)	490.8	336.3	68.5	32.6	17.7
4	Agra (1901-2000)	724.8	576.2	79.5	32.5	18.9
5	Allahabad (1901-2000)	962.7	762.0	79.1	32.5	19.6
6	Gaya (1901-2000)	1130.4	847.3	75.0	32.1	20.1
7	Calcutta (Alipore) (1901-2000)	1651.2	950.2	57.5	31.4	22.0
8	Bareilly (1901-2000)	1040.0	784.1	75.4	31.2	18.7
9	Patna (1951-1980)	1003.4	807.1	80.4	31.9	20.8
10	Kota (1951-1980)	843.4	687.4	81.5	32.9	20.5

Considering the hydrology of river Ganga based upon statistics from WM Directorate, Central Water Commission, average annual flow of Ganga is 525023.00 MCM as published in Integrated Hydrological Data Book, 2012. The mean annual runoff at Farakka is 410 mm (Mirza, 1997).

Table 4.4 *Mean Annual Rate of Flow along Different Sections of the Ganga (Source: Central water Commission)*

S. No.	Stretch	Mean Annual Rate of Flow (cu m / second)
1	Source to Rishikesh	850
2	Rishikesh to Allahabad	850 - 1,700
3	Allahabad to Farakka	4,000 -10,200

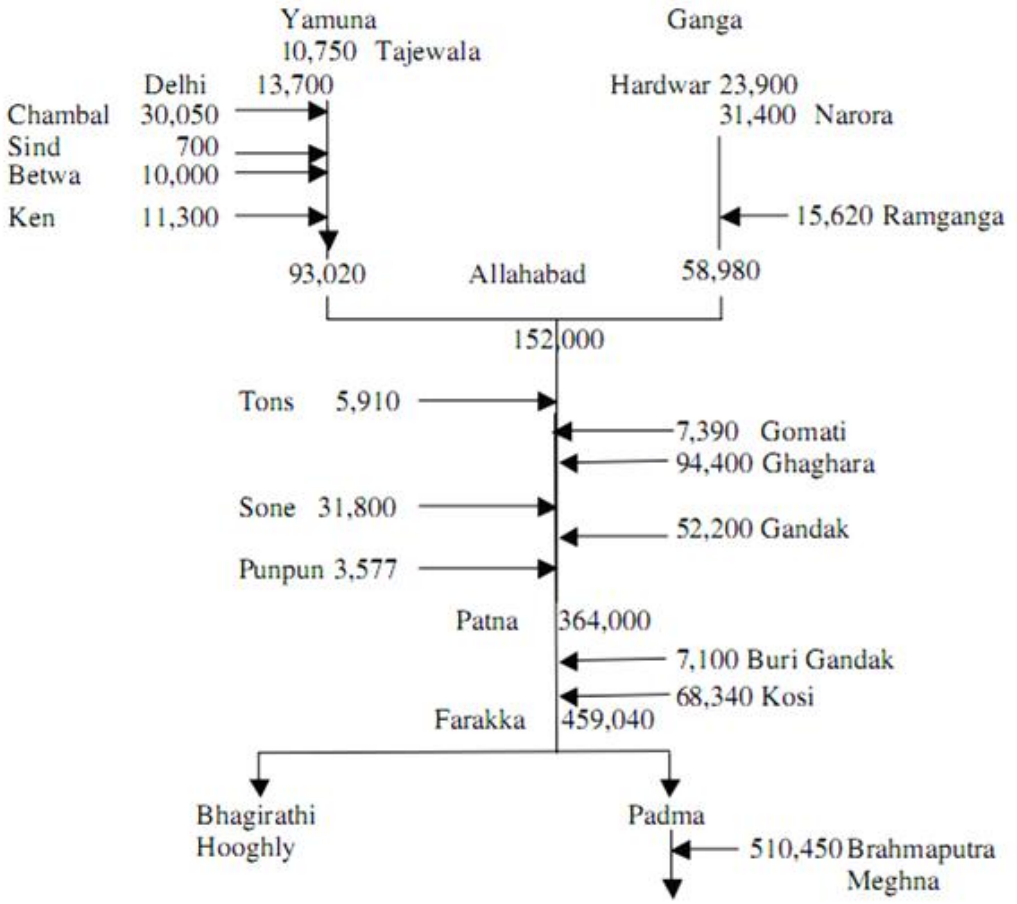

Figure 4.5 *Line diagram of Ganga and its major tributaries with average annual flows (MCM) (Jain S.K. et al, 2007)*

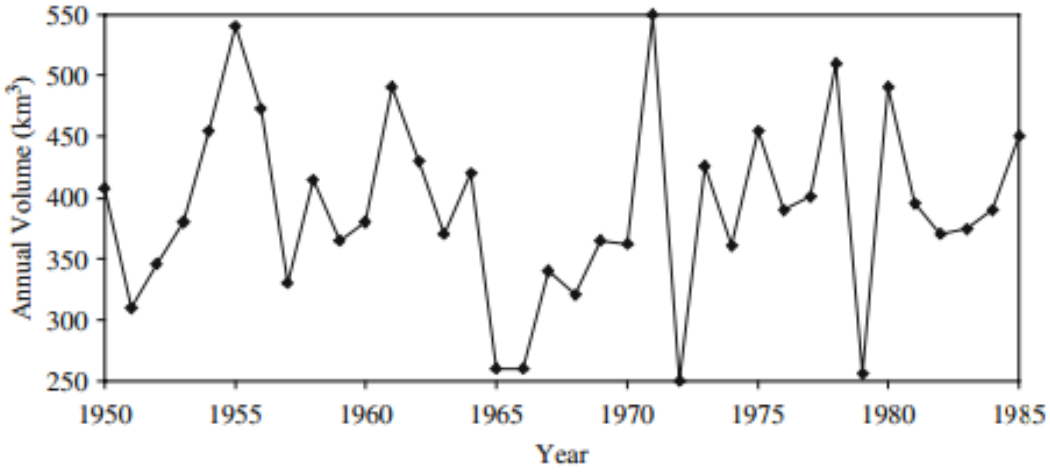

Figure 4.6 *Annual discharge of river Ganga at Farakka (Jain et al., 2007)*

The hydrograph in the Figure 4.6 shows that the discharges in Ganga basin from 1950 to 1985does not follow any particular trend. The annual fluctuation is extremely high, but there is no obvious change over the recorded time period. (Jain *et al.*, 2007)

4.6. Environmental, Demographic and Socio-economic aspects

The basin is home to large variety of flora and fauna. The diversified land cover includes evergreen and deciduous forests, shrubs, grasslands but to meet the needs of ever increasing population in the basin major part of the natural land cover has been transformed into cultivation area with intensive irrigation. The wild animals which were once found in abundance in the basin have now started to disappear.

The basin area covers the states of Uttarakhand, Uttar Pradesh., Delhi, Madhya Pradesh, Rajasthan, Haryana, Himachal Pradesh, Chhattisgarh, Jharkhand, Bihar and West Bengal, supporting the total population of 356.8 million with average density of 414 persons per sq.km. as per 1991 census.

Table 4.5 *Distribution of Population by States of India as per 2001 census*

	Uttarakhand	Uttar Pradesh	Bihar	Jharkhand	West Bengal	India
Total Population	8,489,349	166,197,921	82,998,509	26,945,829	80,176,197	1,028,610,328

Table 4.6 *Industrial cities with population exceeding 10 million (2001 census)*

State	Population (in millions)
Kolkata	13.2
Delhi	12.8
Kanpur	2.69
Lucknow	2.26
Patna	1.71
Agra	1.32
Meerut	1.17
Varanasi	1.21
Allahabad	1.05

The large population exerts huge pressure for large demand of water resources for fresh water supply. Also, the rapid growth rate of population is resulting in industrial development of the region at even faster rate. Besides these, a number of medium sized towns have emerged throughout the main stream of the Ganga. The untreated urban discharge of wastewater and agricultural chemicals from these oddly scattered areas has resulted in large-scale downstream pollution. In addition, there are 68 gross polluting industrial units along the course of the river and its tributaries which discharge untreated industrial effluents.

The primary occupation of major population in Ganga basin is farming. The cultivable area of Ganga sub-basin is about 57.96 M.ha which is 29.5% of the total cultivable area of the country.

The cultivated area of the Ganges basin experience huge advantage of a network of irrigation canals that has increased the production of such cash crops as sugarcane, cotton, and oilseeds. The older canals are mainly in the Ganges-Yamuna Doab (*doab* meaning "land between two rivers"). The Upper Ganga Canal and its branches have a combined length of 5,950 miles (9,575 km); it begins at Hardiwar. The Lower Ganga Canal, extending 5,120 miles (8,240 km) with its branches, begins at Naraura. The Sardar Canal irrigates land near Ayodhya, in Uttar Pradesh. Higher lands at the northern edge of the plain are difficult to irrigate by canal, and groundwater must be pumped to the surface (Pletcher, 2010). Other sources of economy include fishing in delta regions.

4.7. Issues of concern in the Basin

- Large variation in climate is experienced from semi-arid to sub-humid/sub-tropical regions
- Variation in soil texture and land-use on a large scale
- Spatial and temporal variation in meteorological parameters
- The basic problem in utilizing water resources in the Ganga basin is that in relation to the relatively large annual flow in the basin, the storage capacity of existing and foreseeable reservoirs in India is not large enough to permit conservation of flows during high flow season
- The flooding problem in the middle and terminal reaches is majorly due to drainage congestion, bank erosion, spillage of rivers as well as tidal effects. The Ganga Flood Control Commission was set up by the Government of India for flood management in the Ganga Basin.
- The dense population of the Ganga Basin, coupled with high growth rate is expected to generate huge demand for additional water in Ganga basin. Further, rapidly growing industries in the region will create substantial additional water demand as well as problems of water quality. Similar situations may be faced by the countries in the Ganga basin
- The conflict of sharing of water resources of river Ganga between Bangladesh and India has been evaded with the construction of Farkka barrage and has provided a long term solution
- To avoid the situation of conflict over utilizing the water flow of Ganga between Nepal, India, and Bangladesh there is a need to establish a well-coordinated water resources developing and sharing agreement.
- The countries sharing the Ganga water should resolve the existing problems at the earliest so that with mutual understanding the objective of the overall sustainable development of the region can be achieved.

  (http://nih.ernet.in/rbis/basin%20maps/ganga_about.htm)

5. MATERIALS/DATA USED

5.1 Remote Sensing data

5.1.1 Land Use land Cover map

5.1.1a ISRO GBP land use land cover map

ISRO GBP LULC, 2005 developed by Indian Institute of Remote sensing, Dehradun was used for mapping land cover in the region. Originally the map was prepared for 33 classes at a scale of 1:2, 50, 000 but as the extent was limited to Indian region only, the map was reclassified and recoded to 14 classes as present in Global land use land cover map by University of Maryland so that it can be merged with it and facilitate information for Ganga basin extending beyond Indian boundary.

5.1.1b Global land use land cover map by University of Maryland

The global land use land cover map produced at 1 km spatial resolution using Advanced Very High Resolution Radiometer (AVHRR) data for 1992–1993 by University of Maryland is also used in this study. The map is prepared on the basis of classification tree approach. The approach taken involved a hierarchy of pair-wise class trees where logic based on vegetation form was applied until all classes were depicted. Multitemporal AVHRR metrics were used to predict class memberships. Minimum annual red reflectance, peak annual Normalized Difference Vegetation Index (NDVI), and minimum channel three brightness temperature were among the most used metrics. The land use map has 14 classes.

5.1.2 Digital Elevation Model

5.1.2a GTOPO 30

GTOPO30 is a global digital elevation model (DEM) with a horizontal grid spacing of 30 arc seconds (approximately 1 kilometer). GTOPO30 was derived from several raster and vector sources of topographic information. GTOPO30, completed in late 1996, was developed over a three year period through a collaborative effort led by staff at the U.S. Geological Survey's Center for Earth Resources Observation and Science (EROS). The data was acquired from the URL: (http://edc.usgs.gov/products/elevation/gtopo30/gtopo30.html) for providing static geographic in downscaling model.

5.1.2b SRTM 90

The Shuttle Radar Topography Mission (SRTM) is a joint project between the National Geospatial-Intelligence Agency (NGA) and the National Aeronautics and Space Administration (NASA). The objective of this project is to produce digital topographic data for 80% of the Earth's land surface (all land areas between 60° north and 56° south latitude), with data points located every 3-arc second (approximately 30 meters) on a latitude/longitude grid. The absolute vertical accuracy of the elevation data will be 16 meters (at 90% confidence).
This radar system will gather data that will result in the most accurate and complete topographic map of the Earth's surface that has ever been assembled. The dataset is used for obtaining basin elevation and drainage.
SRTM made use of a technique called radar interferometry in which two radar images are taken from slightly different locations. Differences between these images allow for the calculation of surface elevation, or change.

5.2 Global Climate Model Data

5.2.1 NCEP FNL Operational Global Analysis

National Center for Environmental Prediction (NCEP)'s Global Forecast System (GFS), FNL (Final) Operational Global Analysis data are on 1.0x1.0 degree grids prepared operationally every six hours. This product is from the Global Data Assimilation System (GDAS), which continuously collects observational data from the Global Telecommunications System (GTS), and other sources. The analyses are available on the surface, at 26 mandatory (and other pressure) levels from 1000mb to 10mb with 40 atmospheric variables. The dataset is used for historical reanalysis. URL: (http://dss.ucar.edu/datasets/ds083.2)

5.2.2 Global driving data

Hadley Centre Coupled Model, version 3 is a fully coupled atmosphere-ocean general circulation model (AOGCM) developed at the Hadley Centre in the United Kingdom (Gordon, 2000 and Pope, 2000). It was one of the major models used in the IPCC Third Assessment Report in 2001. HadCM3 with A2 emission scenario global six hourly forcing data using simulations for 360-day calendar, where each month is 30 days, is a grid point model and has a horizontal resolution of 3.75 × 2.5 degrees in longitude × latitude. This gives 96 × 73 grid points with resolution of approximately 300 km. There are 19 levels in the vertical. The ocean model has a resolution of 1.25 × 1.25 degrees with 20 vertical levels. Model does not require any flux adjustments which implies that the model climate remains stable and does not significantly drift. Its good simulation of current climate without using flux adjustments was a major advance at the time it was developed and it still ranks highly compared to other models in this respect (Reichler and Kim, 2008). It also has the capability to capture the time-dependent

fingerprint of historical climate change in response to natural and anthropogenic forcing (Stott et al. 2000).

5.3 Observed Discharge data

Observed hydrological and meteorological data were collected for model calibration and validation of the results. These include the discharge data from Global Runoff Data Centre (GRDC) for six stations along the course of river Ganga. GRDC station catalogue and station metadata is made available at http://www.bafg.de/GRDC/EN/01_GRDC/grdc_node.html.

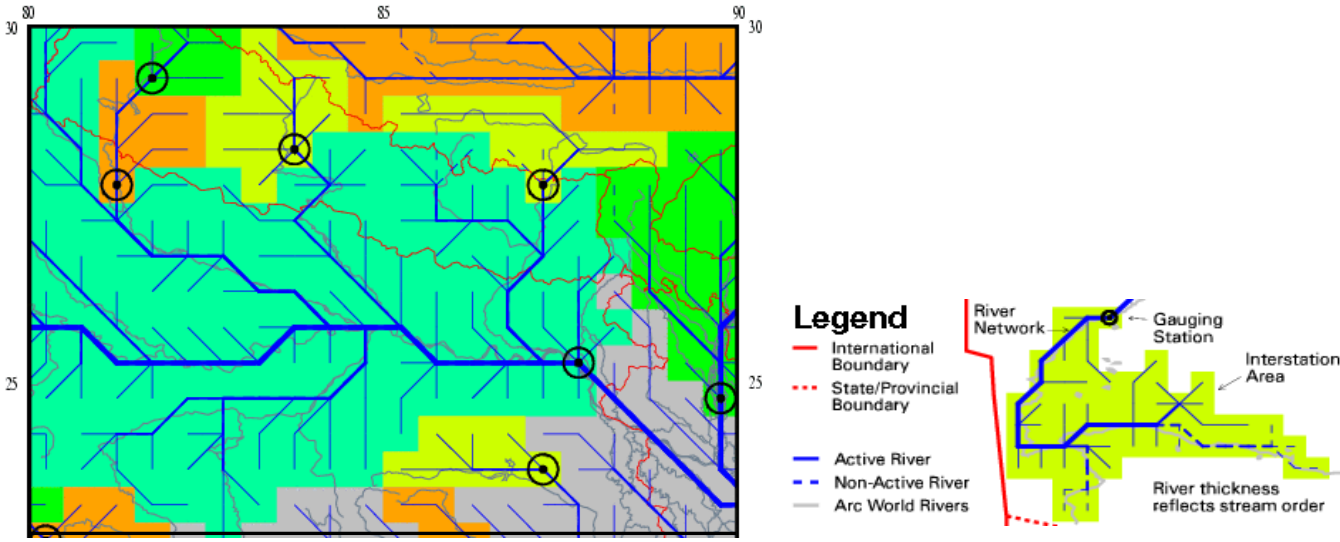

Figure 5.1 *GRDC guaging sites in Ganga Basin (UNH, GRDC)*

Table 5.1 *Availability of data at different gauging sites*
(GRDC: Global Runoff Data Centre, A: Available, N.A: Not Available)

Sl. No.	Station Name	Gauge Incharge	Discharge Data	Monthly Discharge	Mean monthly discharge	Time Period
1	Benighat	GRDC	A	N.A	A	1963-1993
2	Chisapani	GRDC	A	N.A	A	1962-1993
3	Devghat	GRDC	A	N.A	A	1963-1993
4	Farakka	GRDC	A	A	A	1949-1973
5	Turkeghat	GRDC	A	N.A	A	1976-1986

5.4 Ancillary data

5.4.1 NBSSLUP soil map

Digitized soil maps of Ganga basin lying in India were obtained at 1:50,000 scale. Soil mapping for Indian region has been done by NBSSLUP (National Bureau of soil survey and Landuse planning), Nagpur. Some of the associated soil properties were also derived from it. As the information provided by this dataset is limited to Indian region only, so, another soil dataset was required for the basin area extending beyond Indian boundary.

5.4.2 FAO soil map

To determine soil properties outside India FAO global soil map of world at scale 1:5, 00, 000 has been used. The subset of the area outside India within Ganga basin has been done. The subsetted map is merged with NBSSLUP soil map to produce soil map of Ganga Basin.

5.4.3 USGS 30s 24-category land use land cover data

The existing 24-category United States Geological Survey (USGS) land cover classification (Anderson *et al*., 1976) has been used to provide static geographical input in downscaling model. For more information on types of classes refer to Table 6.2.

5.4.4 Rainfall and temperature

Precipitation input was prepared using data set generated using monthly precipitation (P) from the University of Delaware (UDel) Willmott and Matsura (2007) gridded observation. Gauge Precipitation adjusted for gauge undercatch as described by Adam and Lettenmaier (2003) and for orographic effects as described by Adam et al. (2006). Monthly gridded minimum and maximum temperatures were obtained from the Climate Research Unit (CRU) of the University of Eastern Anglia (Mitchell et al., 2004). The daily variability of NCEP/NCAR was used to create daily P and temperatures data using monthly CRU (for temperatures) and Udel (for P) data as a control. The comlete compilation is available at a spatial resolution of 0.5O and at a daily temporal scale.
(http://www.hydro.washington.edu/SurfaceWaterGroup/Data/met_global_0.5deg.html)

5.4.5 Others

LDAS 8th database and MM5 Terrain dataset for extraction of physical parameters of the vegetation was used. LDAS contains pre- processed global soil data (http://ldas.gsfc.nasa.gov/LDAS8th/MAPPED.VEG/web.veg.monthly.table.htnl)

5.5 Computer Efficiency

Computational resources deployed for preparing, processing, storing, visualizing, analyzing and managing the data are listed under subsequent sections.

5.5.1 Server and Processors

Fujitsu server with 40 core processor and 2.0GHz/24MB Cache

5.5.2 Operating System

CentOS 6.3 32 bit, CentOS 6.4 64 bit, WindowsXP , Windows 7

5.5.3 Softwares

ERDAS Imagine 9.1, ArcGIS 10, ENVI 4.3, Cygwin, Microsoft office 2007

5.5.4 Languages

C, Fortran, Python 2.6, 2.7, GRADS, IDL

6. METHODOLOGY

The progress flow of the project was divided into two broad categories that were simultaneously processed:
a. Dynamic Downscaling of GCM using WRF (ARW core) model
b. Hydrological Modelling using VIC model

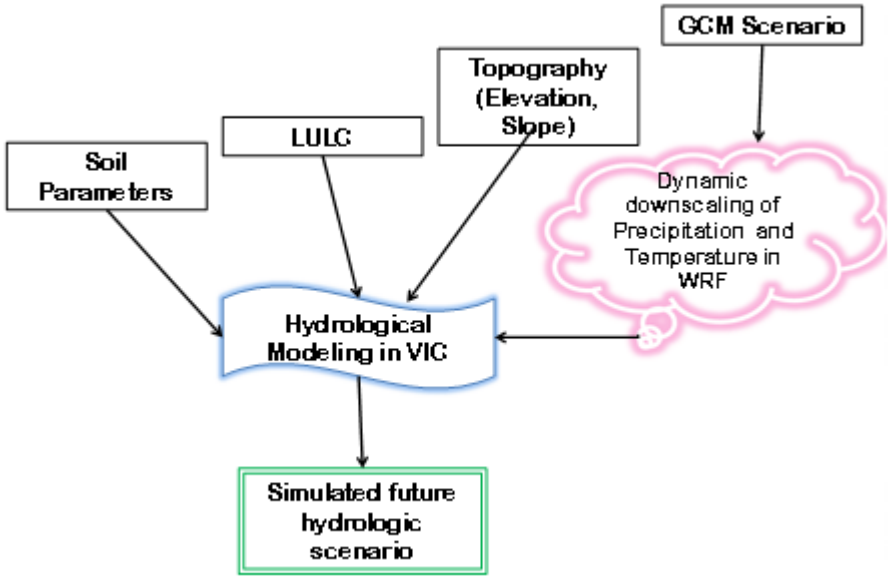

Figure 6.1 *Overall framework*

6.1 WRF Model Integration

This section focuses on configuring and compiling the WRF model along with WPS and WRF Domain Wizard and subsequently exercising dynamic downscaling of future climate scenario using model core.

6.1.1 WRF Model Attributes and Requirements

The WRF build relies on Perl version 5 or later and a number of UNIX/LINUX utilities. WRF code itself is standard Fortran (commonly referred to as Fortran90). WRF model was compiled on different systems with varying configurations and different numbers of processors to analyze the computational cost in terms of time and efficiency.

Table 6.1 *System configuration and installed libraries*

System Specifications	
Linux OS	CentOS release 6.4
Architecture	x86_64
Command shell	Bash
Compiler	gfortran with gcc
Library Requirements	
Distributed-memory processing	MPICH2
i/o format support	NetCDF4.0
GRIB2 support	JasPer, png, zlib
Visualization	NCL_NCARG, GRADS

6.1.3 WRF Model compilation

The successful compilation of the model on LINUX machine using appropriate environment settings and Fortran and C flags created two executables:

- ***real_nmm.exe***: WRF-NMM initialization
- ***wrf.exe***: WRF-NMM model integration

6.1.4 WPS compilation

After successful configuration and compilation of WRF core, next was to configure and compile WPS. Successful installation of WPS program creates three executables:

- ***geogrid.exe*** Define a model coarse domain and any nested domains
- ***ungrib.exe*** Extract meteorological fields from GRIB data sets for the simulation period
- ***metgrid.exe*** Horizontally interpolate meteorological fields to the model domains

6.1.5 Preparing input for real data simulation

Running of WPS is required for preparing the inputs for real data simulation. But before doing so several preparations had to be done to convert the external data into WPS intermediate format.

6.1.5.1 WPS Input Data

Static geographical data and meteorological fields ingested into WPS included:

- **geog** global land use and terrestrial data
- **SRTM 90 m DEM** domain specific elevation data
- **ISRO GBP LULC** domain specific land cover data
- **UKMO HadCM3 GCM** meteorological fields

6.1.5.2 Processing SRTM 90 m DEM for input into WPS

Step 1. Extracted the DEM according to domain size. Larger area slowed down the process to a great extent and flashed an out of memory error**.**

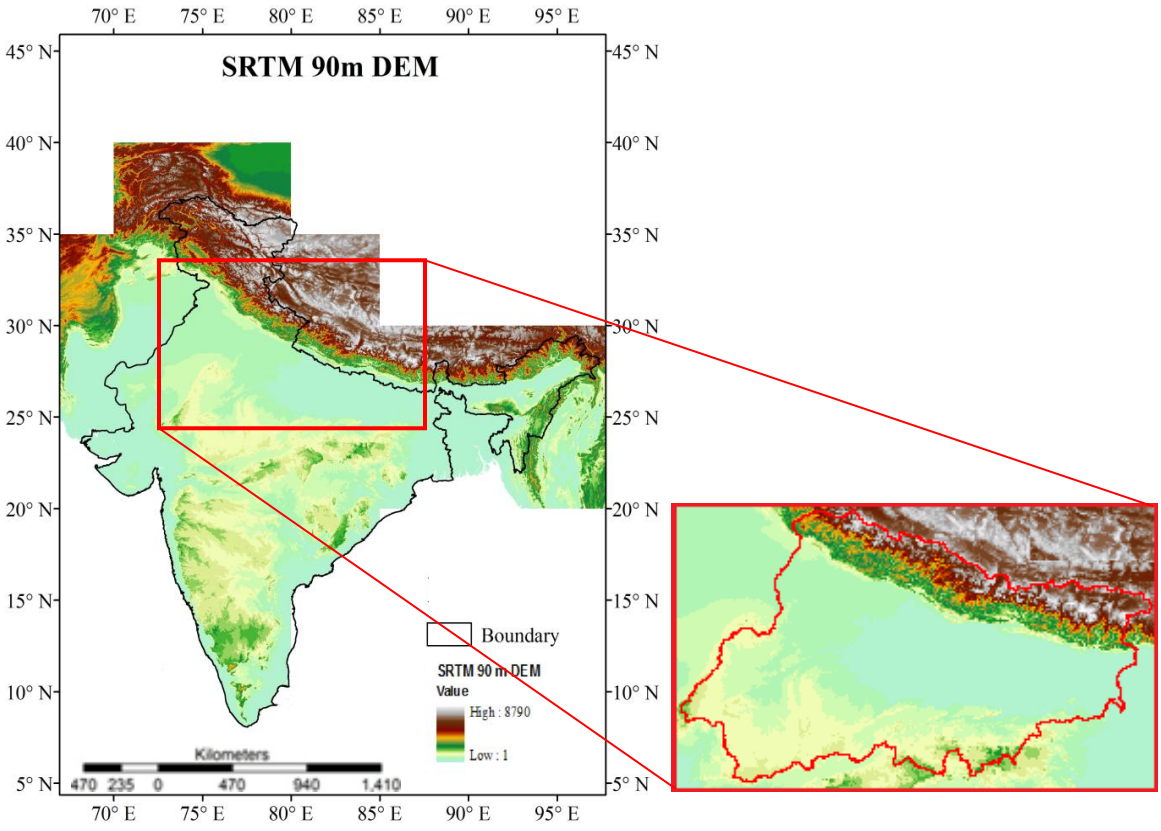

Figure 6.2 *Map Layout of extent of SRTM 90 m DEM extracted*

Step 2. Convert raster into ASCII using Conversion tool available in ArcGIS 10. It was to be taken into consideration that number of rows and columns were to be chosen wisely as to ensure that data do not go over bound.

```
ncols         19200
nrows         12000
xllcorner     73
yllcorner     22
cellsize      0.00083333333333333
NODATA_value  -9999
189 190 189 189 190 191 190 189 190 190 190 191 190 191 190 190 192
188 190 190 190 191 191 190 191 191 189 189 191 189 190 189 188 189
190 191 190 192 191 189 188 188 189 189 189 191 190 192 192 191 192
190 190 190 189 190 192 191 190 190 191 193 193 193 192 191 189 191
189 191 192 191 194 194 194 193 192 192 191 189 190 191 189 189 189
192 193 192 193 193 191 191 192 191 192 192 190 188 187 189 189 191
190 190 187 186 188 189 190 190 189 194 192 191 190 192 192 191 191
193 194 192 191 191 192 192 193 193 192 194 191 192 194 190 193 192
192 191 193 193 191 193 191 189 192 193 192 190 192 193 192 191 189
193 192 194 192 194 195 195 194 193 193 193 195 194 194 193 192 194
194 194 195 194 194 194 196 196 196 195 195 195 194 193 193 193 193
194 194 195 194 197 195 195 195 196 195 195 195 193 194 195 195 197
196 197 197 196 195 193 194 193 193 194 195 196 194 192 193 195 194
193 194 194 196 194 195 195 196 196 195 196 196 196 199 199 197 198
197 201 201 200 201 202 200 201 201 200 202 201 198 199 201 203 199
```

Figure 6.3 *SRTM 90 m DEM in ASCII format with the extent of Ganga Basin.*

Step 3. Converted ASCII to binary format that can be used by WPS. To serve the purpose a Fortran code was developed that takes as input ASCII file and converts it into Binary format. The code calls a module write_geogrid.c from WPS that stores the static data as regular 2-d arrays. The topography data set is written in binary array of dimension 12000 × 19200, containing a $10^{o} \times 15^{o}$ piece of data; whose south-west corner is located at (22N, 73E) is named 00001-19200.00001-12000

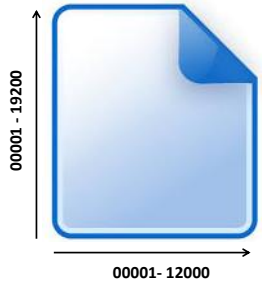

Figure 6.4 *Arrangement of binary file format*

Step 4. Created Index File. It is a metadata file that contains all the essential information geogrid looks for when processing a data set. It was saved in same folder as the binary files.

```
type = continuous
signed = yes
projection = regular_ll
missing_value = 0
dx = 0.000833333
dy = 0.000833333
known_x = 1.0
known_y = 1.0
known_lat = 22.0
known_lon = 73.0
wordsize = 2
tile_x = 19200
tile_y = 12000
tile_z = 1
tile_bdr=0
row_order = bottom_top
units="meters MSL"
description="Topography height"
```

Figure 6.5 *Index file for elevation data set*

Step 5. Modified GEOGRID.TBL in HGT_M and HGT_V sections that defines parameters of each of the data sets to be interpolated by geogrid.

```
name = HGT_M
priority = 1
dest_type = continuous
interp_option = SRTM : average_gcell(4.0)+four_pt+average_4pt
interp_option = 30s:average_gcell(4.0)+four_pt+average_4pt
interp_option = default:four_pt
smooth_option = smth-desmth; smooth_passes=1
fill_missing = 0.
rel_path =     SRTM:topo_SRTM/
rel_path =     30s:topo_30s/
rel_path = default:topo_30s/
```

6.1.5.3 Processing ISRO GBP LULC for input into WPS

The 33 class LULC data from ISRO GBP was reclassified into 24 classes of USGS, thus, evading changes in VEGPARM.TBL. After that same steps from 1 to 5 were followed as for processing the elevation data with corresponding changes in index file and GEOGRID.TBL.

Table 6.2 *USGS 24-category Land Use Categories*
(http://www.mmm.ucar.edu/wrf/users/docs/user_guide_V3/users_guide_chap3.html)

Land Use Category	Land Use Description
1	Urban and Built-up Land
2	Dryland Cropland and Pasture
3	Irrigated Cropland and Pasture
4	Mixed Dryland/Irrigated Cropland and Pasture
5	Cropland/Grassland Mosaic
6	Cropland/Woodland Mosaic
7	Grassland
8	Shrubland
9	Mixed Shrubland/Grassland
10	Savanna
11	Deciduous Broadleaf Forest
12	Deciduous Needleleaf Forest
13	Evergreen Broadleaf
14	Evergreen Needleleaf
15	Mixed Forest
16	Water Bodies
17	Herbaceous Wetland
18	Wooden Wetland
19	Barren or Sparsely Vegetated
20	Herbaceous Tundra
21	Wooded Tundra
22	Mixed Tundra
23	Bare Ground Tundra
24	Snow or Ice

6.1.5.4 Domain Configuration

A nested domain for Ganga Basin was created using WRF Domain Wizard. The specifications of parent domain and child nest are denoted in namelist.wps (Figure 6.7). The outer domain is the parent domain of low resolution with grid size of 75 km covering major part of Indian subcontinent. The nested inner domain is the child domain with grid size of 25 km covering the study area. This higher resolution child domain was configured such that it sparred an area a little larger than the specified study area so that the model could get sufficient boundary grids for model initialization and integration.

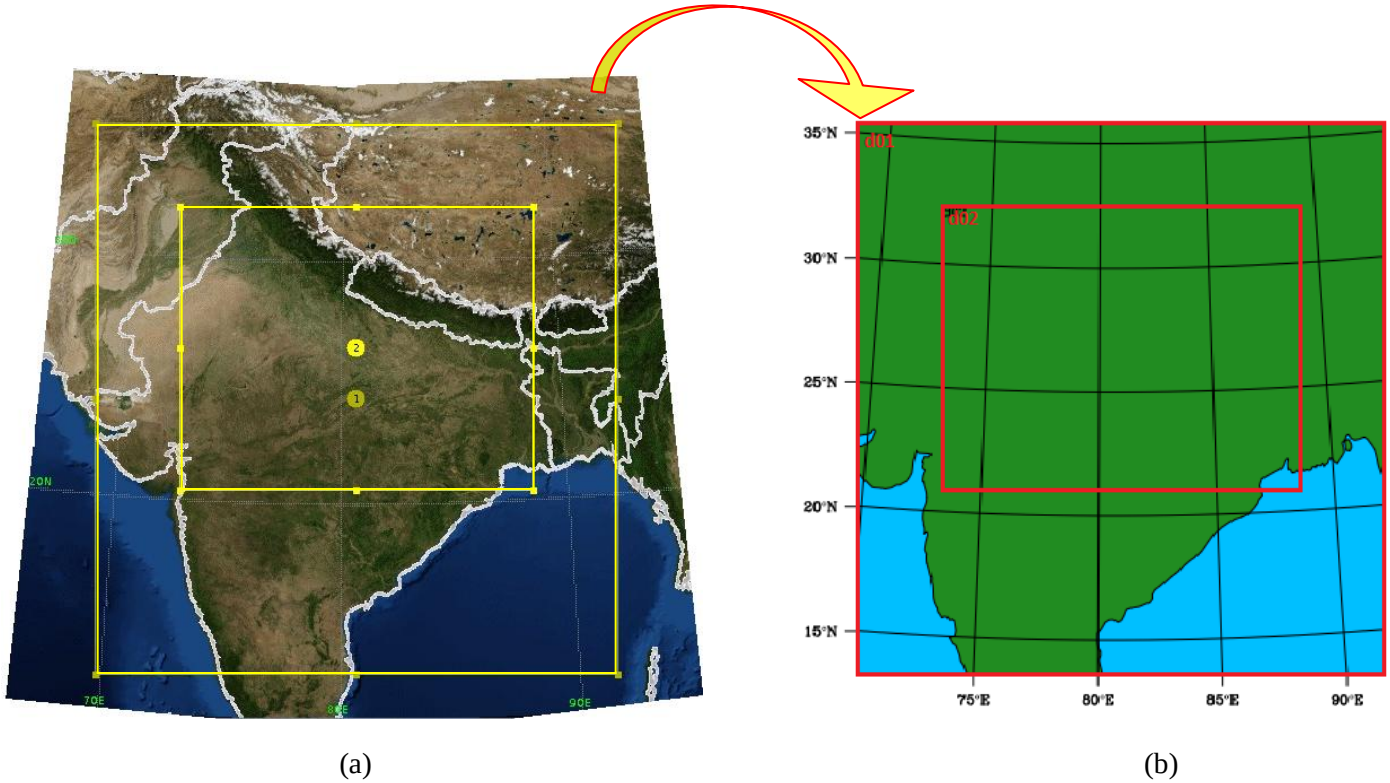

(a) (b)

Figure 6.6 *Domain Configuration with: (a) WRF Domain Wizard, (b) WPS*

6.1.5.5 Converting NetCDF met files into WPS intermediate format

The UKMO HadCM3 meteorological data was procured for sub daily time steps (6 hourly) for the 2020 year in NetCDF. Generally, GCM annual data is available for 360 days only (i.e. 30 days per month). To overcome this limitation and to convert these files into WPS intermediate format and extract meteorological fields at various pressure levels a Fortran code was employed. In other words, instead of being dependant on ungrib script, a Fortran program was used that proved to be subservient.

6.1.5.6 Running WPS

It includes modifying a common Namelist.wps file that contains the variable-specific information that is to be read by WPS for interpolating static and time variant fields to model domain. Each section of this namelist file has separate namelist records for each of the programs and a shared namelist record, which defines parameters that are used by more than one WPS program (Chapter3, WRF ARW v3 user guide)

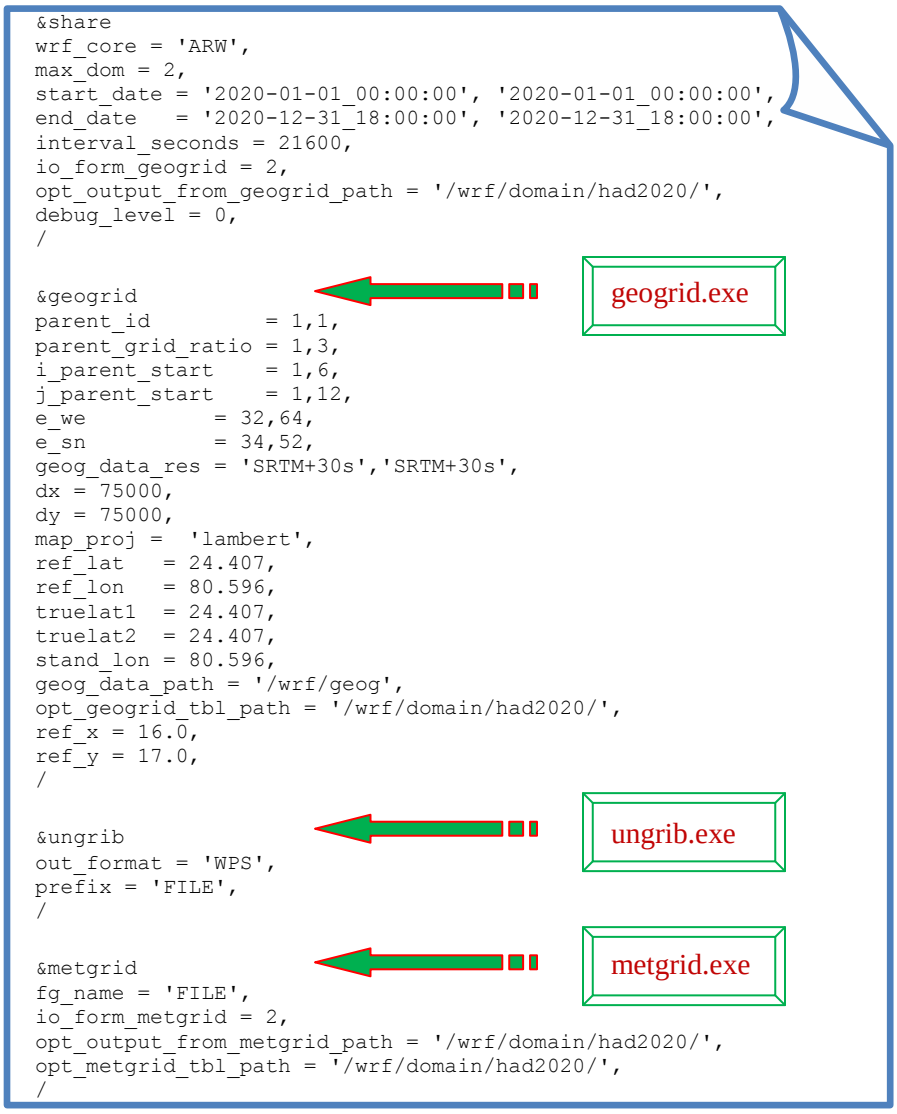

Figure 6.7 *Parameters defined in namelist records of Namelist.wps*

Further, executing the WPS script geogrid.exe created two static files of the type geo_em.d01.nc and geo_em.d02.nc for the two configured model domains containing information of horizontally interpolated static geographic data to the model domain. The ratio between two domains was taken as 1:3. The grid size of outer domain or the parent domain was 75 km so according to the grid ratio the child domain had a grid size of 25 km. The configuration of the two domains is shown in Figure 6.5.

Similarly, running metgrid.exe script created met_em.d0* files separately for both the coarser domain (d01) and the other nested higher resolution domain (d02) covering the entire Ganga basin. The met_em files for d01 had horizontally interpolated met fields to the lower resolution domain at time step of six hours. The met_em files for finer resolution, d02 were created for

every 3 hour. This enabled in obtaining a better temporal resolution along with refined spatial resolution.

6.1.5.7 Dynamic downscaling of GCM Data

Dynamic downscaling of the GCM fields to the model domain at specified time step involves processing of two scripts of the ARW core of WRF model:

1. **real.exe** real data initialization module; interpolates meteorological data to vertical model levels and generates initial and boundary data, required as input to the ***wrf.exe*** model. Two files were created: ***wrfbdy_d01,*** to provide boundary conditions and ***wrfinput_d01***, for providing initial conditions.
2. **wrf.exe** model integration; Numerically approximate the solutions to the model equations to produce a forecast

Input files required to run real and wrf scripts constitutes of:

- **met_em.d0*.data.nc** files produced from metgrid script run earlier
- **namelist.input** which serves as common file for real and wrf containing the all the necessary parameters divided into following basic sections:

```
&time_control
run_days                            = 30,
run_hours                           = 18,
run_minutes                         = 0,
run_seconds                         = 0,
start_year                          = 2020, 2020,
start_month                         = 05,   05,
start_day                           = 01,   01,
start_hour                          = 00,   00,
start_minute                        = 00,   00,
start_second                        = 00,   00,
end_year                            = 2020, 2020,
end_month                           = 05,   05,
end_day                             = 31,   31,
end_hour                            = 18,   18,
end_minute                          = 00,   00,
end_second                          = 00,   00,
interval_seconds                    = 21600
input_from_file                     = .true.,.true.
history_interval                    = 360,  180,
frames_per_outfile                  = 1, 1, 1000,
restart                             = .false.,
restart_interval                    = 432000,
io_form_history                     = 2
io_form_restart                     = 2
io_form_input                       = 2
io_form_boundary                    = 2
debug_level                         = 0
io_form_auxinput2                   = 1
/
```

(a) time_control

```
&domains
time_step                           = 225,
time_step_fract_num                 = 0,
time_step_fract_den                 = 1,
max_dom                             = 2,
e_we                                = 32,    64,
e_sn                                = 34,    52,
e_vert                              = 28,    28,
p_top_requested                     = 5000,
num_metgrid_levels                  = 43,
num_metgrid_soil_levels             = 0,
dx                                  = 75000, 25000,
dy                                  = 75000, 25000,
grid_id                             = 1,     2,
parent_id                           = 0,     1,
i_parent_start                      = 1,     6,
j_parent_start                      = 1,     12,
parent_grid_ratio                   = 1,     3,
parent_time_step_ratio              = 1,     3,
feedback                            = 1,
smooth_option                       = 0
/
```

(b) domains

```
 &physics
 mp_physics                          = 6,     6,
 ra_lw_physics                       = 1,     1,
 ra_sw_physics                       = 1,     1,
 radt                                = 10,    10,
 sf_sfclay_physics                   = 1,     1,
 sf_surface_physics                  = 1,     1,
 bl_pbl_physics                      = 1,     1,
 bldt                                = 0,     0,
 cu_physics                          = 1,     1,
 cudt                                = 5,     5,
 isfflx                              = 1,
 ifsnow                              = 0,
 icloud                              = 1,
 surface_input_source                = 1,
 num_soil_layers                     = 0,
 sf_urban_physics                    = 0,     0,
 /
```

(c) physics

```
&dynamics
w_damping                           = 0,
diff_opt                            = 1,
km_opt                              = 4,
diff_6th_opt                        = 0,       0,
diff_6th_factor                     = 0.12,    0.12,
base_temp                           = 290.
damp_opt                            = 0,
zdamp                               = 5000.,   5000.,
dampcoef                            = 0.2,     0.2,
khdif                               = 0,       0,
kvdif                               = 0,       0,
non_hydrostatic                     = .true.,  .true.,
moist_adv_opt                       = 1,       1,
scalar_adv_opt                      = 1,       1,
/
```

(d) dynamics

```
&bdy_control
spec_bdy_width                      = 5,
spec_zone                           = 1,
relax_zone                          = 4,
specified                           = .true., .false.,
nested                              = .false., .true.,
/
```

(e) bdy_control

Figure 6.8 *(a-e) Snippets of Namelist.input showing important parameterization*

On DM (distributed memory) parallel systems, mpirun command was needed to utilize the computation resources on high-end Linux server. The command to run MPI code using several processors looks like:

mpirun -np <*no. of processors*> ***./real.exe***
mpirun -np <*no. of processors*> ***./wrf.exe***

The following 6 hourly WRF output files for outer domain (coarse resolution) and 6 hourly WRF output files for inner domain (finer resolution) were created:

wrfout_d01_2020-01-01_00:00:00
wrfout_d02_2020-01-01_00:00:00
wrfout_d02_2020-01-01_03:00:00
wrfout_d01_2020-01-01_06:00:00
wrfout_d02_2020-01-01_06:00:00
wrfout_d01_2020-01-01_09:00:00
.
.
wrfout_d01_2020-12-31_18:00:00
wrfout_d02_2020-12-31_18:00:00

6.1.5.8 Global Forcing

Meteorological forcing parameters for hydrological model included daily precipitation and minimum and maximum temperature written into VIC acceptable intermediate format. Hence, there was a need to extract these variables from WRF outputs in NetCDF and convert them to VIC intermediate format. To accomplish the above said tasks python scripts were developed which proved to be instrumental. With the aid of python codes following operations were performed:

1. Converted wrfoutd02*.nc files (3-hourly) to .tif files of raster format extracting three different variables with 366 bands of time dimension namely,
   RAINC convective rainfall (mm)
   RAINNC non convective rainfall (mm)
   T2 Temperature at 2 m (K)
2. Extracted daily maximum and minimum temperature data from T2*.tif files
3. Extracted daily average rainfall from sum of RAINC and RAINNC .tif files
4. Put values from 366 bands of .tif files to workbook in .xlsx files according to the central latitude and longitude location of the grid (generated during VIC model integration)
5. Convert .xlsx files into VIC input ready intermediate format.

6.2 VIC model Implementation

In the present study, hydrological simulation of Ganga basin was carried out for which a semi distributed hydrological modelling approach was adopted. VIC is a semi distributed macroscale hydrological model that calculates statistically the water budget of the basin within each grid. Hence, to establish the VIC model it is essential to generate a grid map over Ganga basin and prepare database for input parameters.

6.2.1 Generation of Grid over study region

Entire study region was divided into of square grids of area 25 x 25 km constituting a shapefile using QGIS and then was imported into ArcGIS 10 software. The basic parameters of the grid files were:

1. latitudinal extent 22.208^{O}N to 31.458^{O}N
2. longitudinal extent 73.383^{O}E to 89.133^{O}E
3. Grid_ID 0-2331
4. RunGrid_ID 1383 run grids (grids covering area >= 25% of part of basin)
5. latitude and longitude of centre of grids
6. mean elevation (masl) of each grid computed from SRTM 90m DEM using mean zonal statistics tool in ArcGIS 10
7. mean slope gradient of each grid
8. average annual rainfall per grid (1976-2006 rainfall from VIC global 0.5^{O} meteorological data)
9. majority soil type per grid for two layers (NBSS&LUP + FAO soil maps)

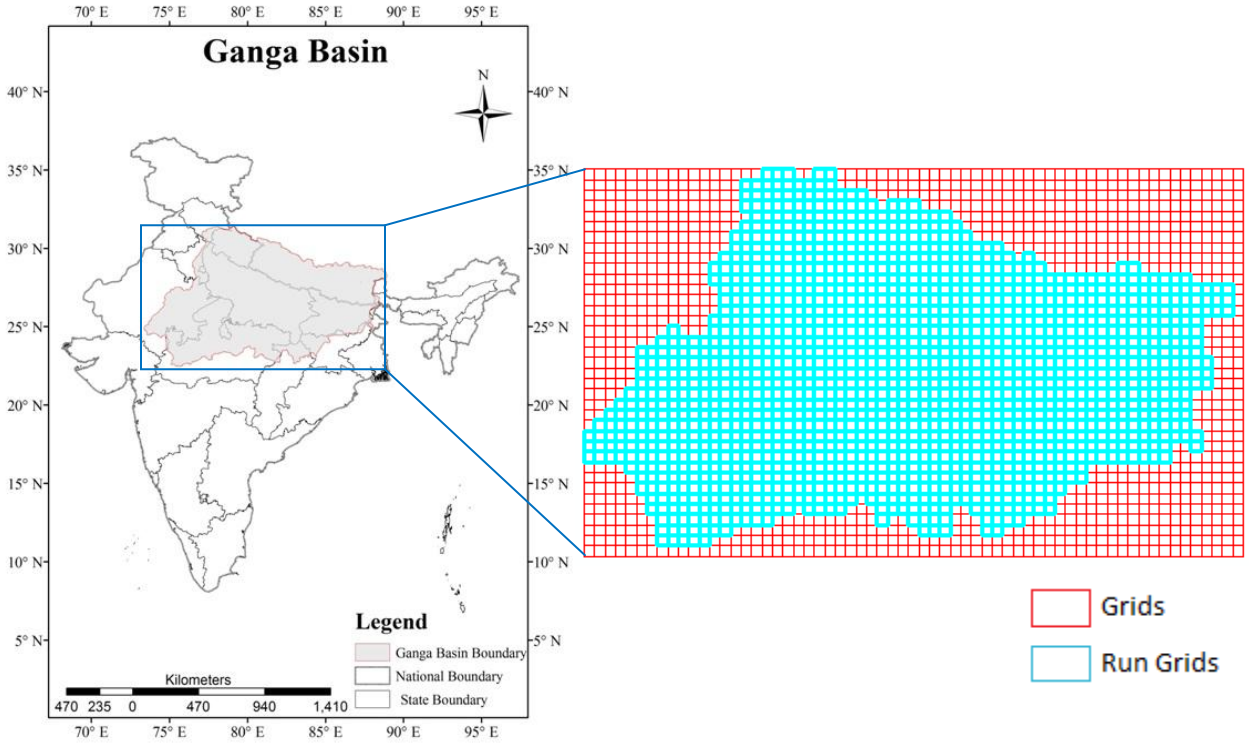

Figure 6.9 *Grid generation (25 X 25 km) over the study region*

6.2.2 Constructing Soil Parameter file

The primary data source to prepare this input was digital soil texture map prepared from NBSS & LUP. The second soil layer was taken as FAO global soil map of the world. Soil texture map was rasterised and overlaid with the grid map to extract dominant soil type in each grid. The two soil maps were merged to get soil information for the Study region. For translating the soil texture to their respective hydraulic properties a sample index file was consulted (Schaake, J., 2000). The soil parameter file was prepared for run grids only using VIC tool in a way that each column represented one parameter and every row represented a grid.

Table 6.3 *Sample index of soil hydraulic properties (http://www.hydro.washington.edu/Lettenmair/Models/VIC/Documentation/Info/soiltext.html)*

USDA Class	Soil Type	% Sand	% Clay	Bulk Density g/cm3	Field Capacity cm3/cm3	Wilting Point cm3/cm3	Porosity fraction	Saturated Hydraulic Conductivity cm/hr	Slope of Retention Curve (in log space) b
1	s	94.83	2.27	1.49	0.08	0.03	0.43	38.41	4.1
2	ls	85.23	6.53	1.52	0.15	0.06	0.42	10.87	3.99
3	sl	69.28	12.48	1.57	0.21	0.09	0.4	5.24	4.84
4	sil	19.28	17.11	1.42	0.32	0.12	0.46	3.96	3.79
5	si	4.5	8.3	1.28	0.28	0.08	0.52	8.59	3.05
6	l	41	20.69	1.49	0.29	0.14	0.43	1.97	5.3
7	scl	60.97	26.33	1.6	0.27	0.17	0.39	2.4	8.66
8	sicl	9.04	33.05	1.38	0.36	0.21	0.48	4.57	7.48
9	cl	30.08	33.46	1.43	0.34	0.21	0.46	1.77	8.02
10	sc	50.32	39.3	1.57	0.31	0.23	0.41	1.19	13
11	sic	8.18	44.58	1.35	0.37	0.25	0.49	2.95	9.76
12	c	24.71	52.46	1.39	0.36	0.27	0.47	3.18	12.28

Table 6.4 *List of soil hydrologic and thermal parameters needed to create soil parameter file (http://www.hydro.washington.edu/Lettenmaier/Models/VIC/Documentation/SoilParam.shtml)*

Sl.No	Variable Name	Units	Values	Description
1	RUN	N/A	1	1 = Run Grid Cell, 0 = Do Not Run
2	Gridcel	N/A	1	Grid cell number
3	Lat	degrees	1	Latitude of grid cell
4	Lon	degrees	1	Longitude of grid cell
5	Infilt	N/A	1	Variable infiltration curve parameter (b_{infilt})
6	Ds	fraction	1	Fraction of Ds_{max} where non-linear baseflow begins
7	Dsmax	mm/day	1	Maximum velocity of baseflow
8	Ws	fraction	1	Fraction of maximum soil moisture where non-linear baseflow occurs
9	C	N/A	1	Exponent used in infiltration curve, normally set to 2
10	Expt	N/A	Nlayer	Parameter describing the variation of Ksat with soil moisture
11	Ksat	mm/day	Nlayer	Saturated hydrologic conductivity
12	Phi_s	mm/mm	Nlayer	Soil moisture diffusion parameter
13	Int_moist	mm	Nlayer	Initial layer moisture content
14	elev	m	1	Average elevation of grid cell
15	depth	m	Nlayer	Thickness of each soil moisture layer
16	bulk_density	kg/m^3	Nlayer	Bulk density of soil layer
17	soil_density	kg/m^3	Nlayer	Soil particle density, normally 2685 kg/m^3
18	off_gmt	hours	1	Time zone offset from GMT
19	Wrc_fract	fraction	Nlayer	Fractional soil moisture content at the critical point (~70% of field capacity) (fraction of maximum moisture)
20	wpwp_fract	fraction	Nlayer	Fractional soil moisture content at the wilting point (fraction of maximum moisture)
21	rough	m	1	Surface roughness of bare soil
22	annual_prec	mm	1	Average annual precipitation.
23	resid_moist	fraction	Nlayer	Soil moisture layer residual moisture.
24	fs_active	1 or 0	1	Set to 1, frozen soil algorithm is activated for the grid cell. 0 indicates that frozen soils are not computed even if soil temperatures fall below 0°C.

6.2.3 Vegetation Parameter file

The land cover in VIC model was described using two files:

1. Vegetation library file: describing hydrologically important characteristics of different land cover types
2. Vegetation parameter file: contains the spatial variability of land cover and describes the vegetative composition of each grid cell, and uses the same grid cell numbering as the soil file

The final LULC map was derived from merging of two different land cover projects, ISRO-GBP and University of Maryland. The final LULC map was overlaid on the grid map to determine the number and fractions of LULC classes present in each grid.

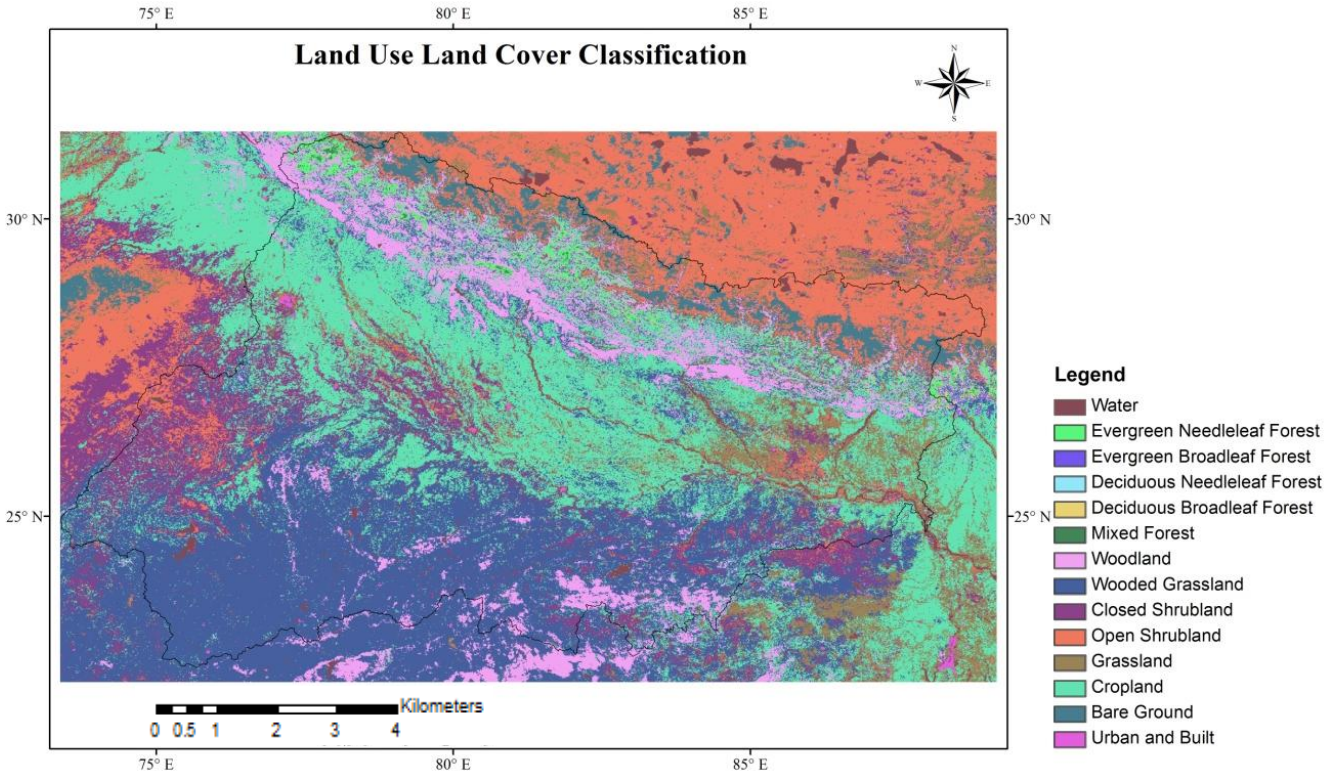

Figure 6.10 *Land Use Land Cover Classification over entire Grid*

Table 6.5 *Veg library file format used for all VIC model grid cells (http://www.hydro.washington.edu)*

Sl. No	Variable Name	Units	Description
1	Gridcel	N/A	Grid cell number
2	Vegetation_type_no	N/A	Number of vegetation types in a grid cell
3	Veg_class	N/A	Vegetation class identification number
4	Cv	fraction	Fraction of grid cell covered by vegetation type
5	Root_depth	m	Root zone thickness (sum of depths is total depth of root penetration)
6	Root_fraction	fraction	Fraction of root in the current root zone

Table 6.6 *Description of the variables required to be specified in the Vegetation parameter file (http://www.hydro.washington.edu)*

Sl. No	Variable Name	Units	Number of Values	Description
1	veg_class	N/A	1	Vegetation class identification number (reference index for library table)
2	overstory	N/A	1	Flag to indicate whether or not the current vegetation type has an overstory (TRUE for overstory present, FALSE for overstory not)
3	rarc	s/m	1	Architectural resistance of vegetation type (~2 s/m)
4	rmin	s/m	1	Minimum stomatal resistance of vegetation type (~100 s/m)
5	LAI		12	Leaf-area index of vegetation type
6	albedo	Fraction	12	Shortwave albedo for vegetation type
7	rough	m	12	Vegetation roughness length (typically 0.123 * vegetation height)
8	displacement	m	12	Vegetation displacement height (typically 0.67 * vegetation height)
9	wind_h	m	1	Height at which wind speed is measured.
10	RGL	W/m^2	1	Minimum incoming shortwave radiation at which there will be transpiration. For trees this is about 30 W/m^2, for crops about 100 W/m^2.
11	rad_atten	fraction	1	Radiation attenuation factor. Normally set to 0.5, though may need to be adjusted for high latitudes.
12	wind_atten	fraction	1	Wind speed attenuation through the overstory. The default value has been 0.5.

13	trunk_ratio	fraction	1	Ratio of total tree height that is trunk (no branches). The default value has been 0.2.
14	comment	N/A	1	Comment block for vegetation type. Model skips end of line so spaces are valid entries.

Other variables like roughness length, displacement height, overstory, architectural resistance, minimum stomatal resistance were derived from LDAS 8th database (http://ldas.gsfc.nasa.gov/LDAS8th/MAPPED.VEG/web.veg.monthly.table.html) and MM5 terrain dataset. As with vegetation data, LDAS contains pre-processed global soil data.

6.2.4 Meteorological forcing file

Each grid cell has its own met data file. File names were of format *data_<lat>_<lon>*. As for the present study this file contained following meteorological variables required to force the VIC model:

1. Tmax Daily maximum temperature (°C)
2. Tmin Daily minimum temperature (°C)
3. Precp Daily precipitation (mm)

Input forcing file for each grid having 365 rows (366 in case of leap year) and 3 columns in ASCII format was provided to drive VIC model. Precipitation input was prepared using data set generated using monthly precipitation (P) from the University of Delaware (UDel) Willmott and Matsura (2007) gridded observation. Gauge Precipitation adjusted for gauge undercatch as described by Adam and Lettenmaier (2003) and for orographic effects as described by Adam et al. (2006). Monthly gridded minimum and maximum temperatures were obtained from the Climate Research Unit (CRU) of the University of Eastern Anglia (Mitchell et al., 2004). The daily variability of NCEP/NCAR was used to create daily P and temperatures data using monthly CRU (for temperatures) and Udel (for P) data as a control. The complete compilation is available at a spatial resolution of 0.5^{O} and at a daily temporal scale. (http://www.hydro.washington.edu/SurfaceWaterGroup/Data/met_global_0.5deg.html, Accessed date: 03.04.2013)
For future year simulation downscaled outputs of WRF model were used to force VIC model.

6.2.5 Preparation of global control file

A Global control file where the necessary information to specify various user preferences and parameters are was prepared. It contains information like N-layers, Time step, start time, end time, Wind_H, snow temp, rain temp., Location of the input output files, modes which are to be activated etc.

6.2.6 VIC model Run

VIC 4.0.5 source code was downloaded from the site and the code was unzipped and untared into local source code directory. Then VIC was compiled using gcc complier on Linux operating system. The code was compiled using the make file included in the archive, by typing 'make'. The compiled code creates an executable entitled 'vicNl'. To begin running the model, ‘vicNl -g (global control file name)' was written at the command prompt of cygwin emulator. Global control parameters were modified according to the input characteristics and to activate the ware balance. In addition to that input and output path were specified.

6.2.7 VIC model run and routing the surface flow

VIC source code was executed in the LINUX environment to generate the flux files for each basin grid. These flux files contain fluxes of surface runoff, evapotranspiration, baseflow, soil moisture etc. produced at that location. In order to simulate streamflow at an outlet, routing of runoff component was done using a routing model developed by Lohmann et. al (1998a, b). Primary input files fed to the routing model were:

- Flow direction file (compulsory)
- Fraction file
- Station location file (compulsory)
- Unit hydrograph file (compulsory)

Above stated input files were prepared using SRTM 90 m DEM as the primary input. A control file defining user preferences and location of input files was used to call the routing code in LINUX environment. Routing was done for 5 stations namely Benighat, Chisapani, Devghat, Farakka and Turkeghat. Daily, monthly and yaerly streamflows in mm and cfs (cubic feet per second) for each outlet location were obtained as the output.

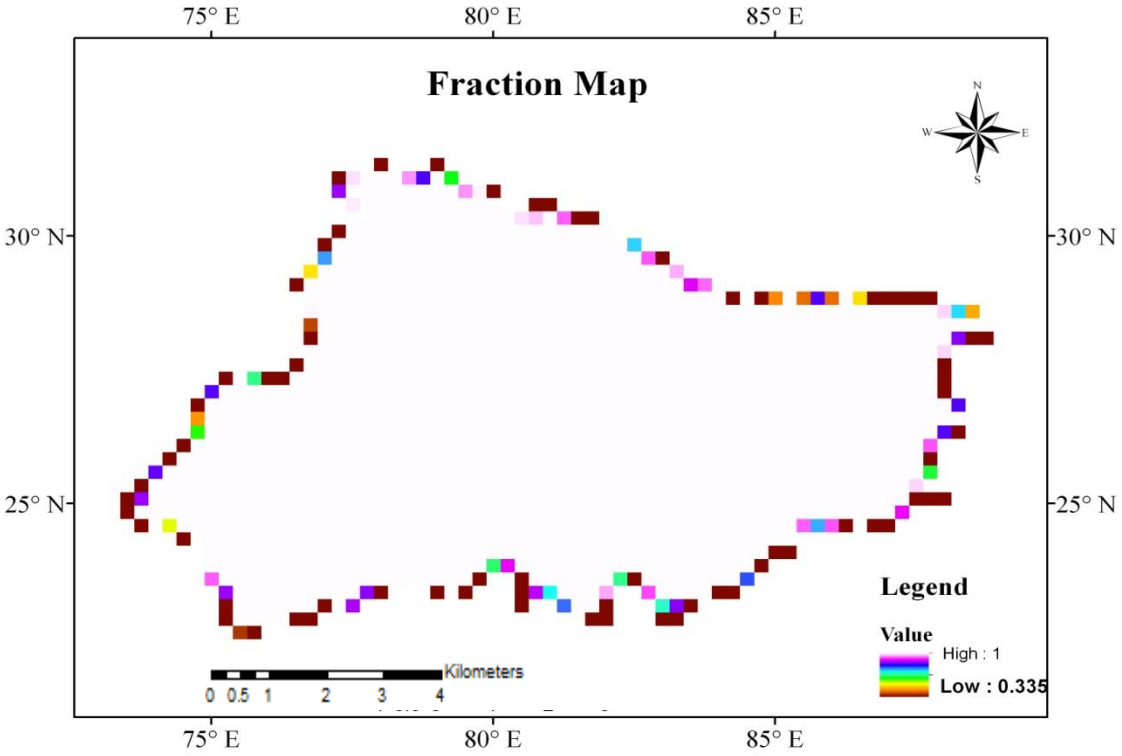

Figure 6.11 *Fraction Map of the study region*

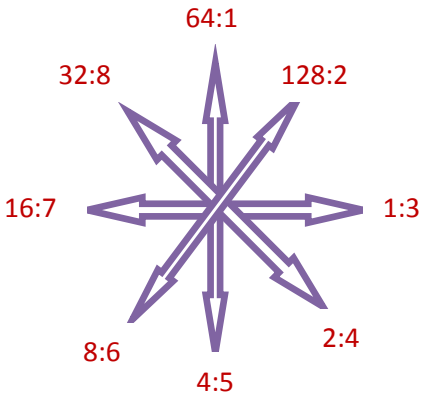

Figure 6.12 *Conversion scheme for flow directions (ArcGIS:VIC)*

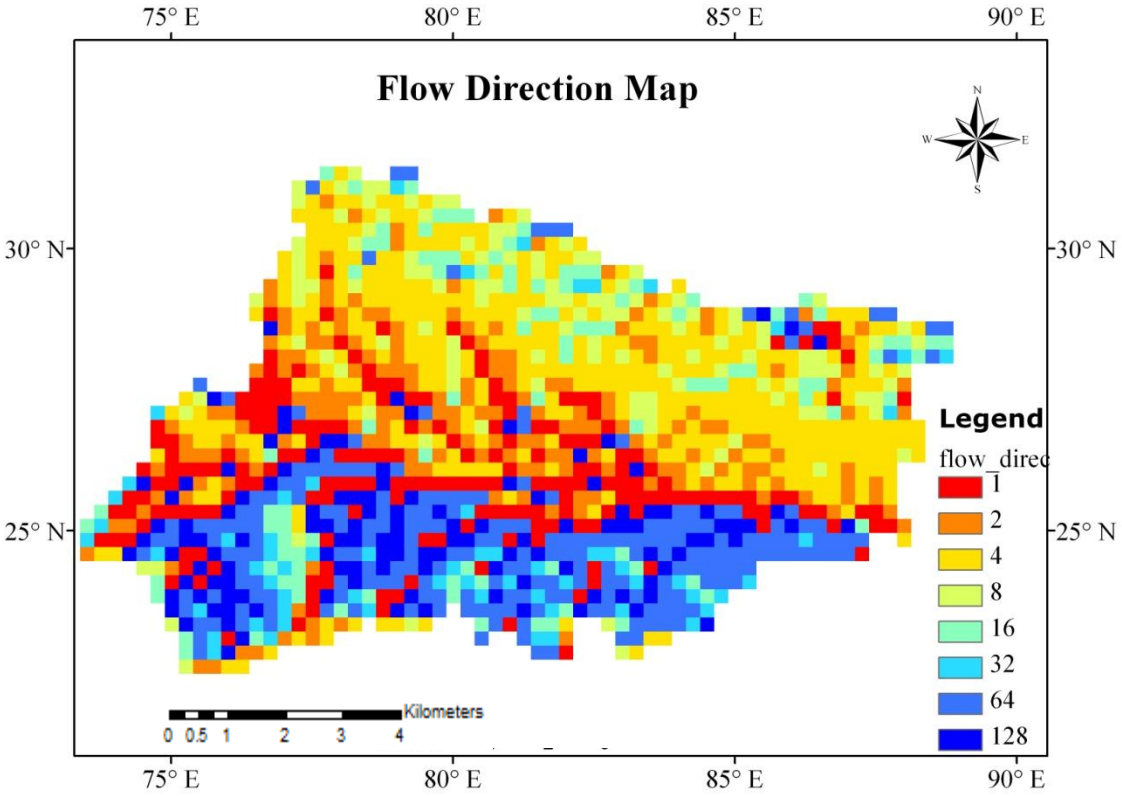

Figure 6.14 *Flow Direction Map of the study region*

6.2.8 VIC Model calibration and validation

Soil parameters that were adjusted during calibration

1. Infiltration parameter (bi)
2. Baseflow parameters:
   – The fraction of maximum baseflow (Ds),
   –The fraction of maximum soil moisture content of the third layer (Ws) at which a nonlinear baseflow response is initiated.

7. RESULTS AND DISCUSSION

7.1 Dynamic Downscaling

To assess the future hydrological scenario future climate projection from a GCM model was downscaled using WRF model. WRF model is a physical based model that means the simulations should be more representative of detailed processes than any other statistical method. Downscaling is mainly categorized as statistical and dynamical. The differences between the two approaches are discussed in detail in chapter 2, section 2.8. In the present study, dynamical downscaling was adopted and applied over Ganga basin. WRF model was configured for ARW core and proceedings of dynamic downscaling of HadCM3 future projections for the year 2020 involved two processes:

- Spatial Downscaling
- Temporal Downscaling

7.1.1 Spatial Downscaling

GCM forcing at a resolution of 2.5^{O} X 3.75^{O} was input into WRF model. The coarse resolution GCM data was downscaled at a grid size of 25 km over the study area. The results showed that the regional details that were poorly simulated by GCM were now adequately distinguishable after downscaling to higher spatial resolution.

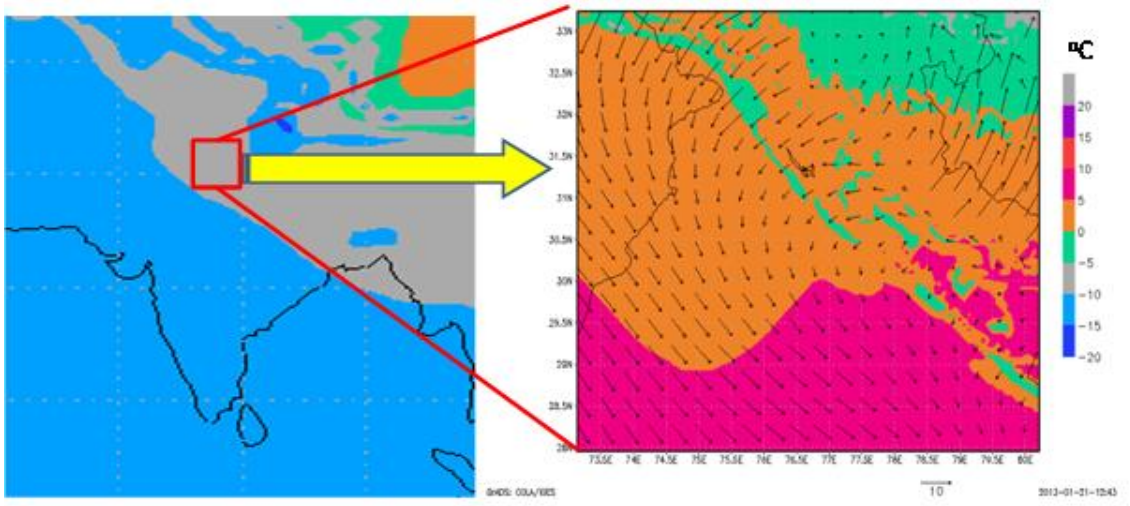

Figure 7.1 *Downscaled temperature of the test area with increased spatial resolution*

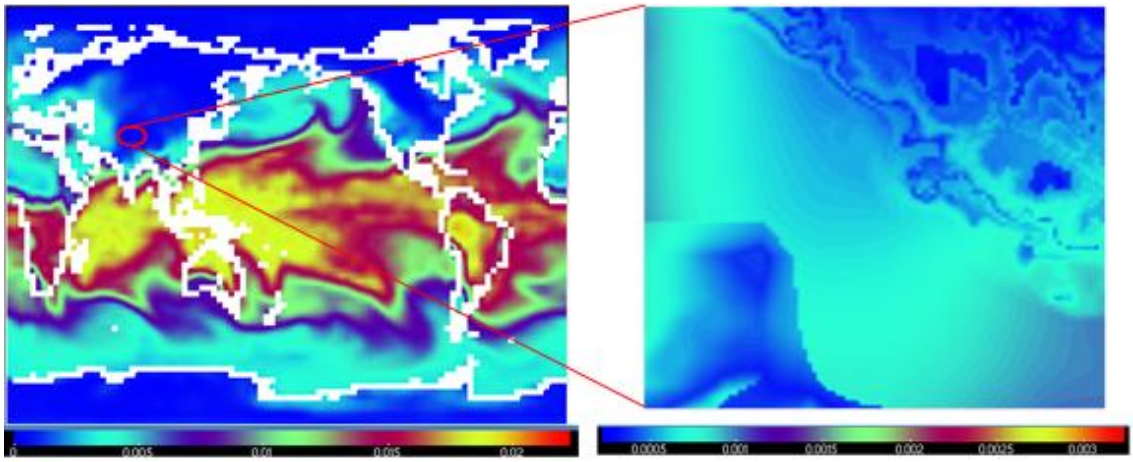

Figure 7.2 *Downscaled specific humidity (kg/kg) of a test area with increased spatial resolution*

However, the more the resolution of study domain, the higher the computational cost of the processing. Increasing the spatial resolution makes the subsequent procedures computationally demanding. So, there is a tradeoff between grid size of computational domain and computational efficiency. Table 7.1 shows the computational time observed for running WRF model for different domain size. Observations are based on 3 days forecast of same dataset over equal area.

Table 7.1 *Observed computational time for running WRF model at different spatial resolutions*

Grid size (km)	Computational Time
25	3 hrs
9	8 hrs
3	1 day 9 hrs

Note: The computational time may vary with different system configurations.

The effect of downscaling on topography was observed with varying resolutions of parent and nested domains where for d01, dx = 75km and for d02, dx = 25km. With increasing resolution of the domain topography over the study region was better resolved. Thus, it can be stated that WRF was successful in resolving the topography by interpolating the DEM values to a finer scale useful in simulating the hydrology of the basin which requires elevation data at higher resolution.

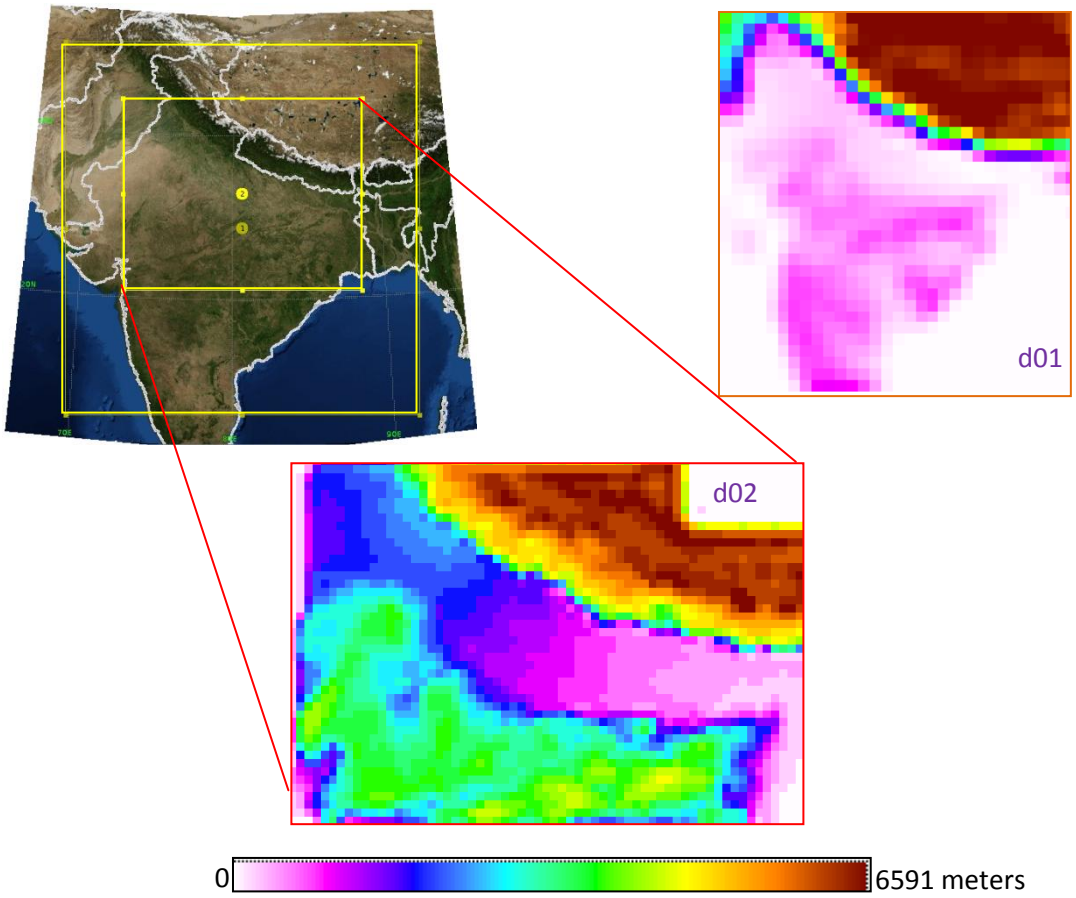

Figure 7.3 *Effect of spatial downscaling on topography in nested domains*

In the areas where terrain is reasonably flat GCM was able to simulate the topography adequately but in the mountains or areas with lot of variation in topography GCM could prove inadequate and hence, may not be able to simulate regional phenomena accurately. While, from Figure 7.1 it is apparent that the topography is well interpolated over the grids of higher resolution domain, and hence, is suitable for simulating phenomena occurring at finer spatial scale.

Similarly, the effect of spatial downscaling with increasing resolution was observed over the study region in terms of change in the resolution of land use land cover classes. In coarser domain where the difference between various land use land cover classes was barely visible, in higher resolution domain the different classes became sufficiently distinguishable.

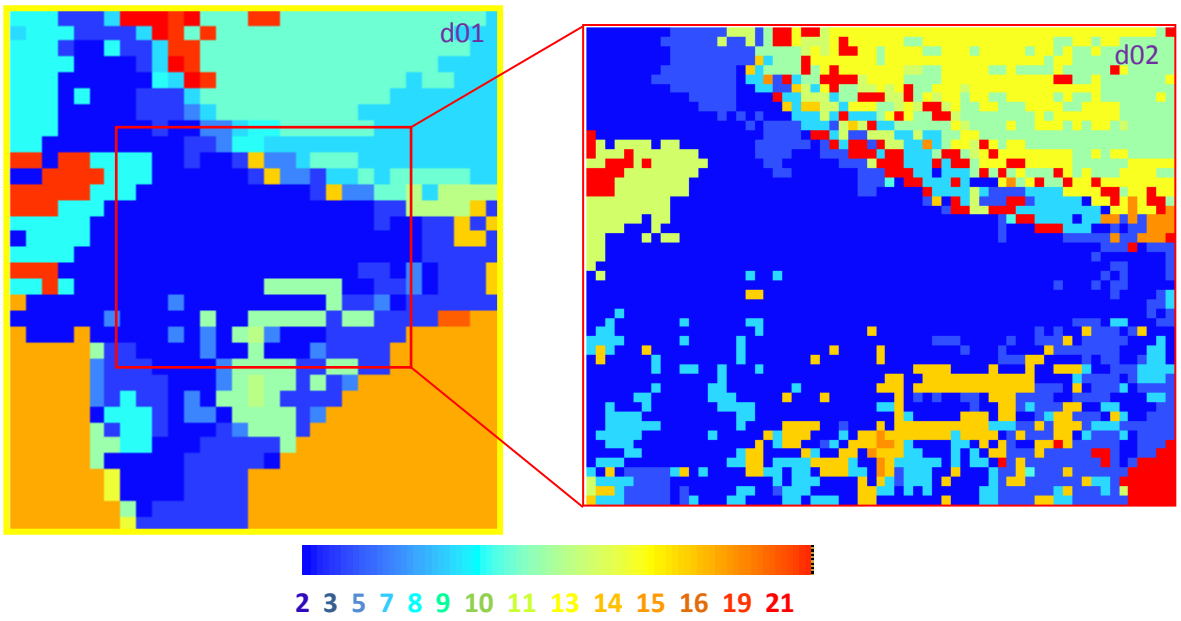

Figure 7.4 *Effect of spatial downscaling on land use land cover classification in nested domains (refer to Table 6.2 for LULC classification)*

7.1.2 Temporal downscaling

GCM forcing for every six hours for the year 2020 was provided for driving the downscaling in WRF model. The Results of WRF downscaling provided eight 3 hourly outputs for each day for the year 2020. It was observed that the temporal resolution of the input forcing files was increased by providing desired values to the history_interval parameter in the common namelist file. But the limitation was imposed due to computational efficiency. Higher the temporal resolution, larger the time required for model running. Time taken for model to run for different temporal resolutions was analyzed and it was concluded that to decrease computational cost there had to be a tradeoff between the desired temporal resolution and available computation resources. Choosing history_interval equal to 180 minutes (3 hours) was a favorable decision for the present study as concluded from the analysis based on observations in Table 7.2 for entire year.

Table 7.2 *Observed computational time for running full year WRF model at different temporal resolutions*

Temporal Resolution (hours)	Computational Time	Status
6	7 days	completed
3	More than 12 days	completed
1	More than 20 days	Aborted after 22 days

7.2 Normal and projected rainfall

Climate is driven by emission scenario and landuse land cover. But in the present study, the VIC hydrological model for Ganga basin was run for LULC dataset of the year 2005 only. That is why a long run future simulation is not feasible with a past land use land cover scenario. The VIC run results were analyzed only for the years adjacent to the year 2005 and then compared with near future simulation of the year 2020.

Table 7.3 *Datasets used for VIC modeling with different resolution and count of run grids*

Dataset	Resolution	Count
Average Annual Rainfall	0.5	1383
IMD 2004 Annual	0.5	286
2006 Annual	0.5	1383
2020 annual	0.25	1383

The annual average rainfall for the past years from 1977 to 2006 was compiled for the study basin. The minimum average rainfall was found to be about 211 mm and maximum rainfall was 4725 mm. The mean rainfall of the basin was found to be 1221.47 mm. The mean rainfall for the years 2004 and 2006 were, 958.06 mm and 1052.8 mm respectively over the study basin which makes about 21% and 13% decrease respectively from average rainfall received over Ganga basin.

As per the study by Moors *et al.* (2011), rainfall in subsequent years over the basin does not follow any particular trend but the results of the present study showed that mean annual rainfall was increasing with progressing years. The projected future rainfall over the study basin is found to be in compliance with the annual average rainfall over Ganga basin. Results suggest that in the year 2020, Ganga basin will experience minimum rainfall of around 240mm and maximum of about 4606 mm rainfall. The results showed an overall decrease of 4% in the mean rainfall for the year 2020 from that of average annual rainfall. But these statistics were still not sufficient to predict the rainfall variability concerning future climate change scenario. Classified maps showing rainfall distribution of different datasets (as discussed above in Table 7.3) over Ganga basin (masked by run grids) are plotted and displayed in Figure 7.5 below. It is also noted from the maps that the downscaled product is better able to simulate the orographic rainfall. The statistical analysis of the same is shown in a graphical form in Figure 7.6.

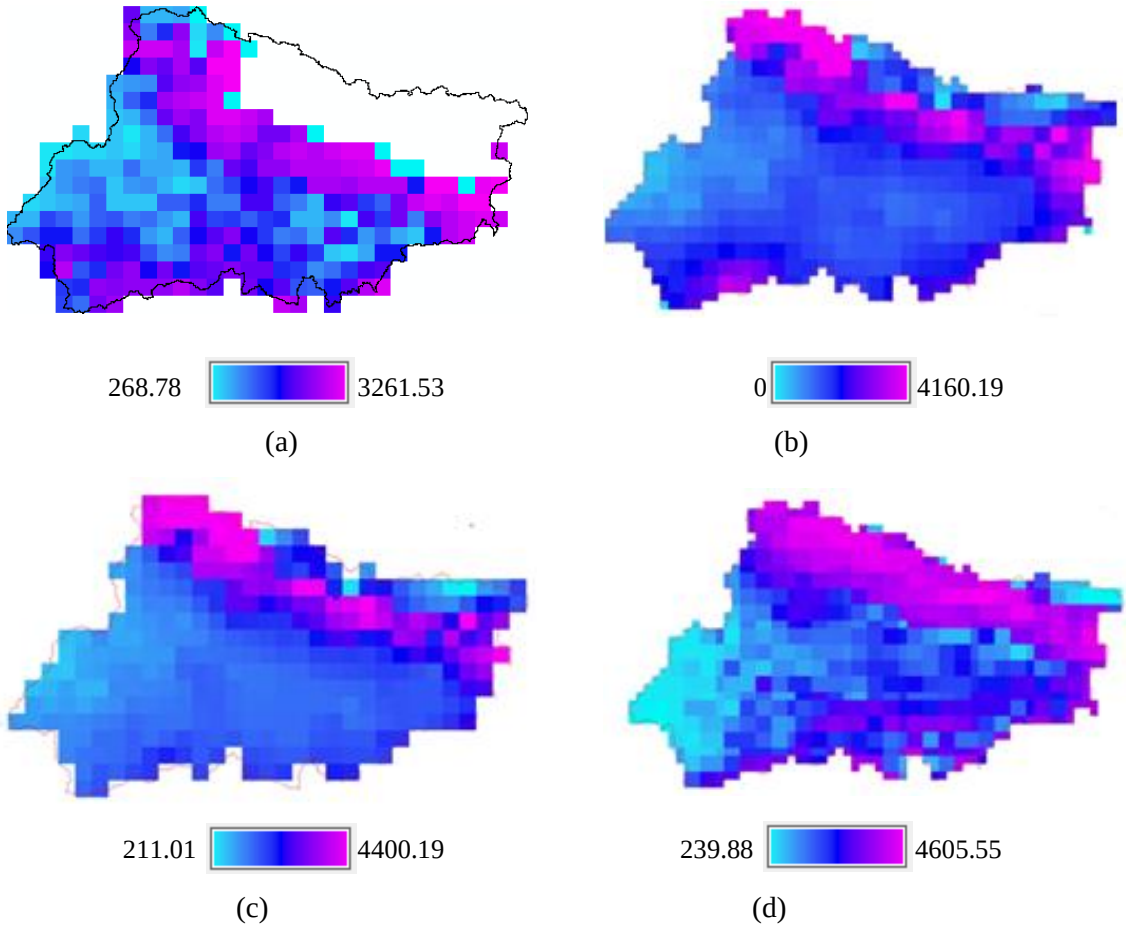

Figure 7.5 *Average rainfall maps over Ganga Basin for the years*
(a) 2004 IMD
(b) 2006 (Adam and Lettenmaier (2003); Adam et al (2006))
(c) 1977-2006 (Adam and Lettenmaier (2003); Adam et al (2006))
(d) 2020 WRF downscaled HadCM3

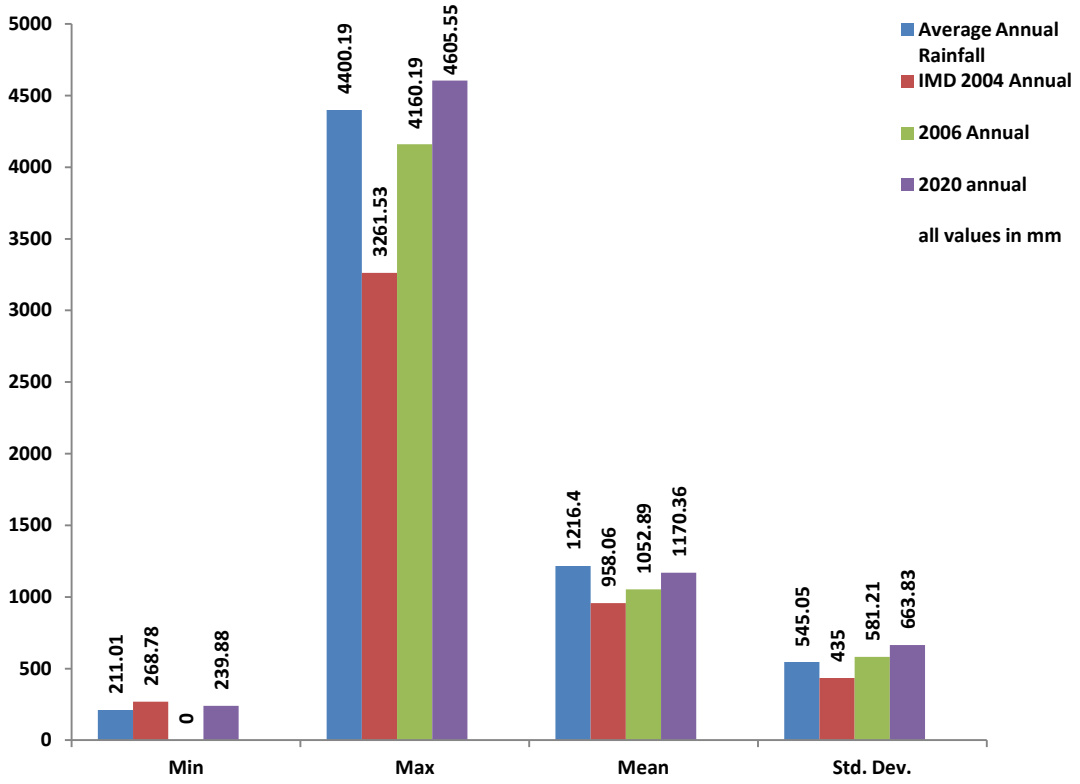

Figure 7.6 *Comparative plot of variability in rainfall pattern over the study basin*

It is apparent from Figure 7.6 that the minimum rainfall of 2020 is lesser than the past years while maximum rainfall of the year 2020 peaks over the past years. Increase in overall rainfall will be there as per the results shown in Figure 7.6. High values of standard deviation for the year 2020 suggest occurrence of extreme events. The results are in agreement with the study by Turner and Slingo (2009), according to which rainfall simulations of future years experience intensification of extreme rainfall events.

Time series plot of average rainfall in the year 2006 and 2020 shown in Figure 7.7 indicate occurrence of continuous rainfall in the monsoon season, i.e. June to September with high precipitation events in the month of January, March and December in 2020. But the rest of the months experience near dry conditions. Overall rainfall has increased considerably in 2020 in comparison to 2006. The results shown in Figure 7.7 represent the values averaged over the entire Ganga basin (for run grids only).

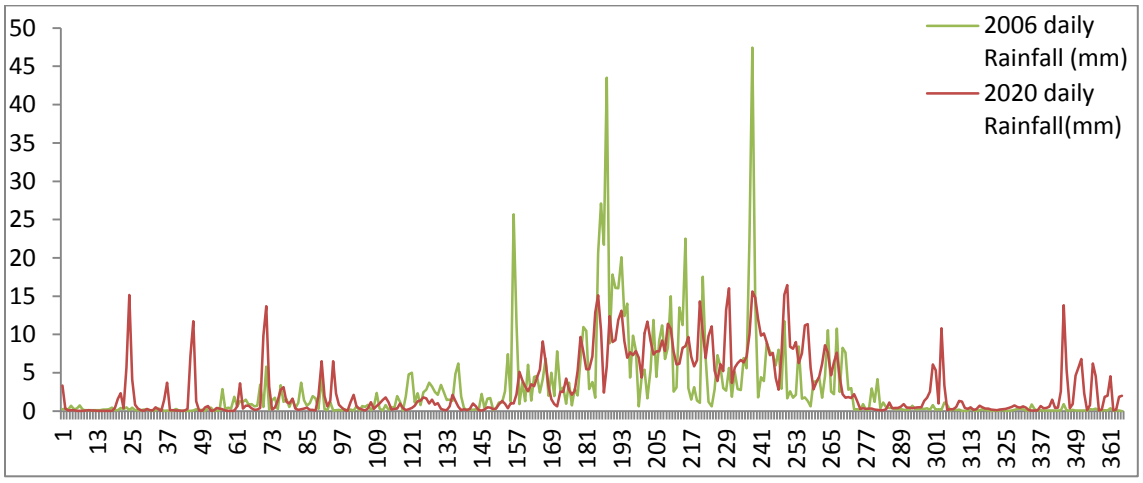

***Figure** 7.7 Time series plot of daily rainfall in the years 2006 and 2020 averaged over basin*

7.3. Normal and projected Hydrological components

VIC model was set up over Ganga basin with grid size of 25 X 25 km to find the grid wise hydrological components for years 2006, 2008 and 2020 as shown in Table 7.4

***Table 7.4** Observed annual values of hydrologic components averaged over basin*

	Rainfall (mm)	Runoff (mm)	Base flow (mm)	Evaporation (mm)
2006	1029.358	357.3012	58.5315	552.8146
2020	1144.365	257.5894	142.5385	545.5383

The results in above Table 7.4 indicate that though the total rainfall is high for the year 2020, yet the total runoff in the Ganga basin in the same year is lesser than in the year 2006 which is receiving lesser rainfall. Annual baseflow averaged over the basin has increased considerably in the year 2020. The evaporation of the two years does not show large variations.

Figure 7.8 show comparative daily runoff of the years 2006 and 2020 averaged over the basin. Although, rainfall is high in 2020, yet, runoff is low for the same year. As per Figures 7.7 the 2020 scenario shows increase in rainfall in winter season rather than in monsoon season while in 2006 rainfall is more in monsoon. In 2006, higher rainfall in monsoon season has caused higher runoff in monsoons. In 2020, the rainfall is lesser in monsoon season, due to which total runoff in 2020 is less than in 2006, but as increase in rainfall is mainly in winter season, therefore, baseflow in 2020 is higher than 2006 (Table 7.4).

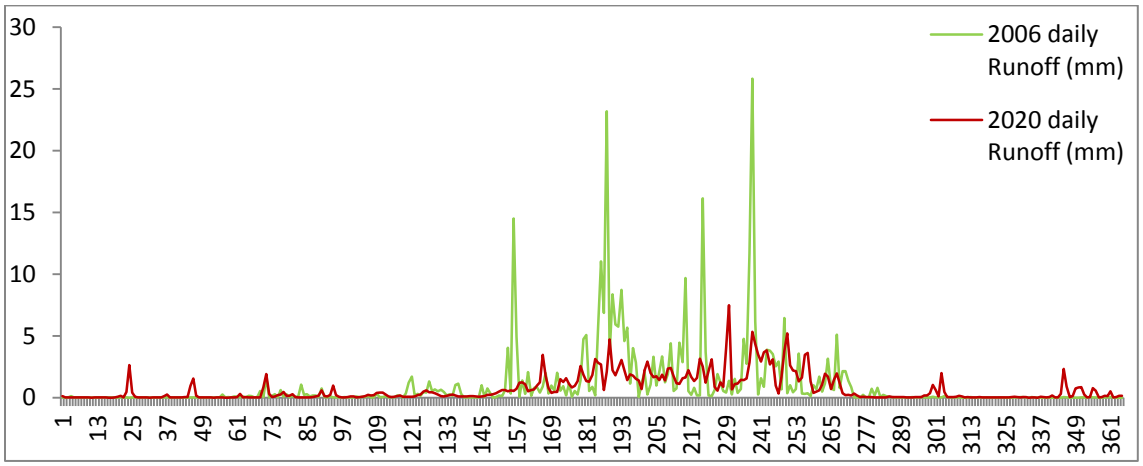

Figure 7.8 *Time series plot of daily runoff in the years 2006 and 2020averaged over basin*

Considering the results of VIC simulation at a single grid provides detailed insight of variations in hydrological components at a grid level. Figure 7.9 shows comparison between runoff at Farakka (grid center: 25.084^{O}N, 88.008^{O}E) for the years 2006 and 2020 against rainfall. The rainfall at Farakka in the year 2020 has increased to 1469.53 mm from about 1453 mm in 2006. The results also indicate increase in runoff at Farakka in the year 2020 to 589.5 mm from around 500 mm in 2006.

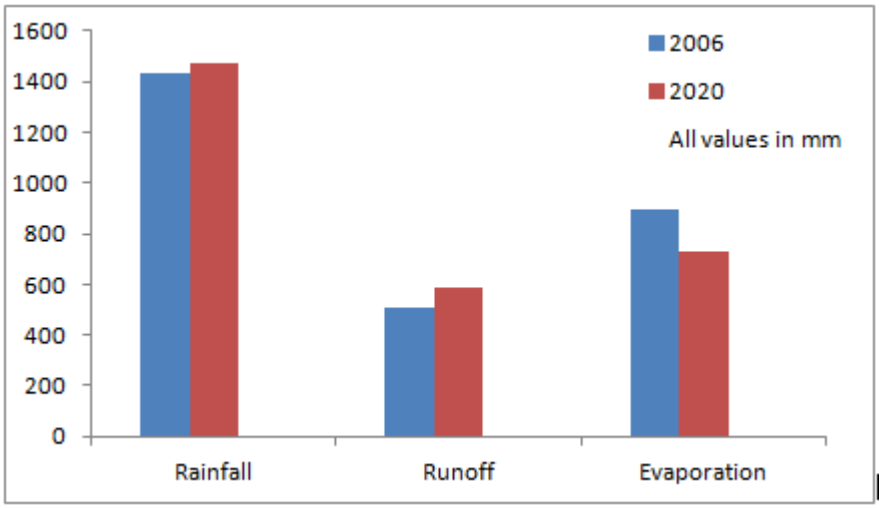

Figure 7.9 *Plot of estimated evaporation and runoff against rainfall for the years 2006 and 2020 at Farakka*

From the graphical interpretation of the amount of rainfall and runoff experienced at Farakka in the months of Indian summer monsoon for the years 2006 and 2020 as shown in Figure 7.10, it is inferred that the year 2020 experiences an early onset of monsoon season and receives heavy rainfall in the month of June. In general June is the starting of the monsoon season and receives lesser rainfall than consecutive months of July and August as in 2006. For the year 2006 rainfall and runoff distribution in the monsoon months follows a general trend. But in the year 2020 rainfall and runoff are more in the month of June and decrease considerably with successive months. June, 2020 experiences more than 700 mm rainfall and more than 450 mm runoff which suggests increased frequency of rainfall at the expense of moderate seasonal rainfall.
Figure 7.10 indicates decrease in number of rainy days in the months of monsoon in 2020.

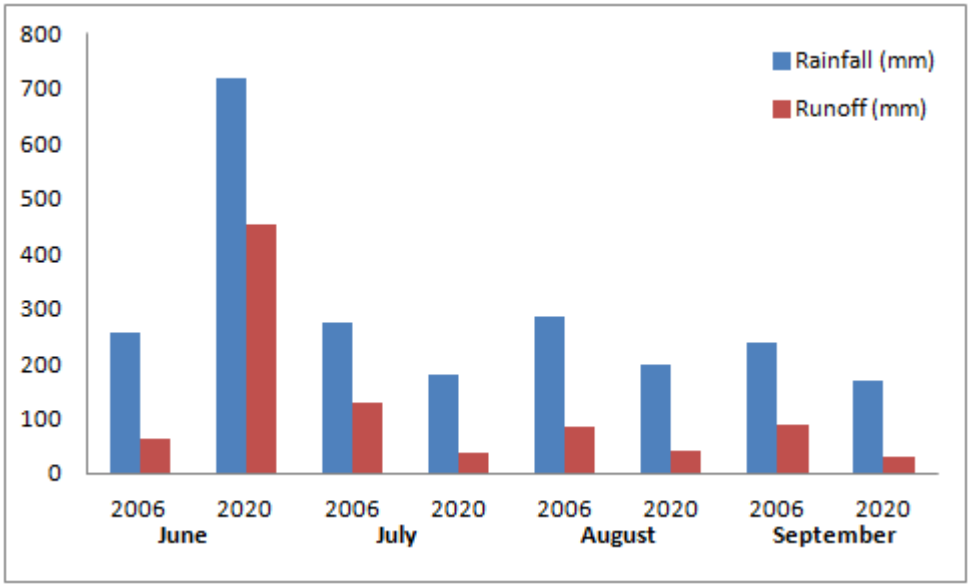

Figure 7.10 *Comparative plot of runoff against rainfall for monsoon season*

To study the variations in rainfall and runoff intensity in a month at Farakka, daily distributions of rainfall and runoff in the month of June for the year 2006 and 2020 are plotted as shown in Figure 7.11 and 7.12 respectively.
Number of rainy days in June, 2006 is more than that in June, 2020 but the maximum rainfall and runoff intensity per day is higher in 2020 than in 2006 as inferred from Figure 7.11 and Figure 7.12.
Analyzing the above results show that the number of rainy days in a month decreases and per day intensity of rainfall increases in the year 2020. Subsequently, the runoff intensity per day increases with an overall decrease in total runoff in the year 2020.

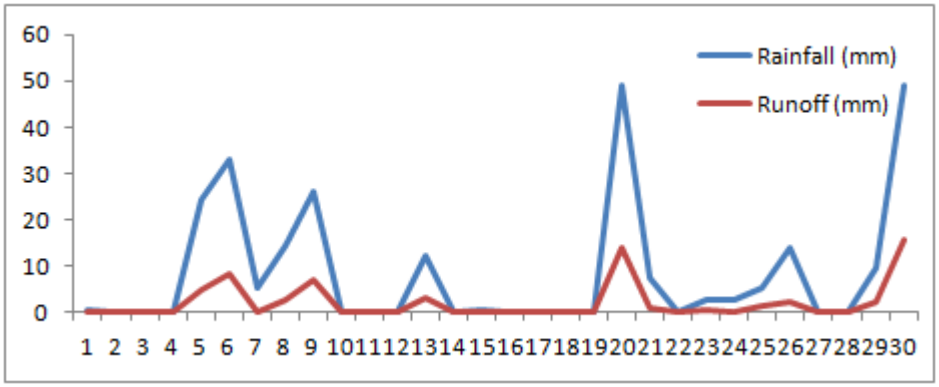

Figure 7.11 *Time series plot of estimated runoff against rainfall in June, 2006*

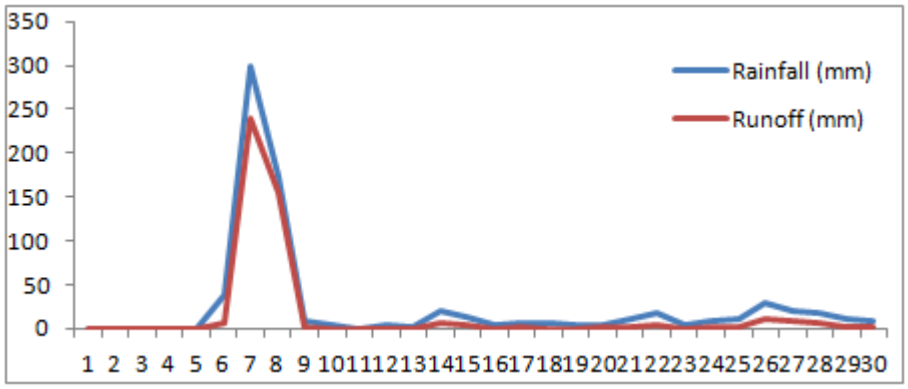

Figure 7.12 *Time series plot of estimated runoff against rainfall in June, 2020*

7.4 Results of Model Calibration and Validation

Calibration of a hydrological model is an iterative process which involves changing the values of sensitive model parameters to obtain best possible match between the observed and simulated values. For details on parameters refer section 6.2.8. The adjusted values assigned to the soil parameters during calibration were:

1. bi: 0.3
2. Ds: 0.01
3. Ws: 0.08

The variation in values of routed runoff at various stations found after calibration is shown in Table 7.5 with an overall R^2 of 0.8216.

Table 7.5 *Model calibration and validation results*

S. No.	GRDC Station	*Mean Annual Runoff as per GRDC*	*Mean annual Runoff before calibration*	*Mean annual Runoff after calibration*
1	*Farakka*	*400*	*315*	*500*
2	*Chisapani*	*950*	*292*	*560*
3	*Benighat*	*909*	*286*	*855*
4	*Devghat*	*1582*	*198*	*1475*

8. CONCLUSIONS AND RECOMMENDATIONS

8.1 Conclusions

The main objective of the present study was to downscale the future climate scenario and hydrological simulation. The Ganga basin has been recently facing the adverse climatic conditions such as floods, droughts etc. repetitively. Frequency of these events indicates a shift in the hydrological response of the basin attributed to future climate change scenario. Changes in future meteorological parameters affect the hydological components of a basin.
The present study attempts to use high temporal and spatial resolution of forcing data (precipitation and temperature) for simulation of hydrological components in Ganga basin. The specific conclusions derived from the present study are enumerated below:

- WRF model for dynamical downscaling of 6 hourly meteorological data from GCM at 2.5° X 3.75° grids to generate 3 hourly model outputs at 25 X 25 km grids for Ganga basin has been successfully set up producing efficient results.
- The choice of the domain, in terms of spatial extent and resolution, is one the vital factors affecting the realism of the phenomenon of downscaling.
- The downscaled precipitation and temperature parameters were successfully used to force the VIC hydrological model for hydrological simulation over Ganga basin.
- The simulated average rainfall for 2020 is in compliance with the average annual rainfall over Ganga basin with an overall decrease of 4%.
- The estimated runoff of 257mm for the year 2020 is found to be lesser than that of 2006 while baseflow of 142mm in 2020 is higher than that of 2006
- Clear tendency is found for increased intensity of rainfall per day at the expense of moderate number of rainy days.
- Errors in estimated runoff over the study basin are due to the reason that VIC model does not run for bare ground.

8.2 Recommendations

- For future improvements the downscaled results from WRF model may be compared with other downscaling models along with their statistical verification.
- Downscaling to be carried out in a continuous mode for more number of years starting from current time.
- VIC model simulation considering the snow melt in mountainous regions should be attempted to better represent fluxes in these areas.
- Simulation to be performed for a period greater than the actual simulation period for better analysis of initial hydrological conditions and that in future.

- Incorporation of future land use land cover change scenario for long run future simulation could lead to significant improvement in model performance since hydrological components are also sensitive to the land use land cover**.**
- Incorporating data assimilation techniques to improve the simulation accuracy of hydrological and weather research forecasting models.
- Using observed discharge data from more number of stations for model calibration and validation.

REFERENCES

- Arnell, N.W., Reynard, N.S., 1996. The effects of climate change due to global warming on river flows in Great Britain. Journal of Hydrology, 183, 397–424.
- Arnell, N. W., 2003. Relative effects of multi-decadal climatic variability and changes in the mean and variability of climate due to global warming: future streamflow in Britain. Journal of Hydrology 270, 195–213.
- Anderson, J. R., Hardy, E. E., Roach, J. T., Witmer, R.E. 1976. A land use and land cover classification system for use with remote sensor data. U.S. Government Printing Office, Washington, D.C.
- Asrar, G., Dozier, J., 1994. EOS, Science Strategy for the Earth Observing System, AIP Press, 1, pp. 128.
- Bader, D.C., Covey, C., Gutkowski, W.J., Jr., Held, I.M., Kunkel, K.E., Miller, R.L, Tokmakian, R.T., Zhang, M.H., 2008. Climate models: An assessment of strengths and limitations. *A Report by the U.S. Climate Change Science Program and the Subcommittee on Global Change Research*, Synthesis and Assessment Product 4.3, Department of Energy, Office of Biological and Environmental Research, Washington, D.C.
- Barnett, T.P., Adam, J.C., Lettenmaier, D.P., 2005. Potential impacts of a warming climate on water availability in snow-dominated regions. Nature 438(17), 303–309.
- Bergstrom, S., Carlsson, B., Gardelin, M., Lindstrom, G., Pettersson, A., Rummukainen, M., 2001. Climate change impacts on runoff in Sweden: An assessment by global climate models, dynamic downscaling and hydro-logical model. Climate Research, 16, 101–112.
- Bharati L., Jayakody, P, 2010. Hydrology of the upper Ganga River (No. H043412). International Water Management Institute.
- Bras, R. A., 1990. Hydrology, an Introduction to Hydrologic Science. pp. 643, Addison-Wesley.
- Castro, C.L., Dominguez F., Chang H.I., Rivera E., Carrillo C., Luong T., January 2011. Creating dynamically downscaled seasonal climate forecast and climate projection information for the North American Monsoon region suitable for decision making purposes. Department of Atmospheric Sciences, University of Arizona, Tucson, Arizona, USA, 91st American Meteorological Society Meeting, 23rd Conference on Climate Change and Variability Seattle, Washington.
- Christensen, N., Wood, A., Voisin, N., Lettenmaier, D., Palmer. R., 2004. Effects of climate change on the hydrology and water resources of the Colorado River Basin. Climatic Change, 62, 337-363.
- Climate Change, 2007. The AR4 Synthesis Report. Geneva (Suisse): IPCC.

- Dadhwal, V.K., Aggarwal, S.P., Mishra, N., July, 2010. Hydrological simulation of Mahanadi river basin and impact of land use/land cover change on surface runoff using a macro scale hydrological model. ISPRS TC VII Symposium–100 Years ISPRS, Vienna, Austria, Vol. 38, 165-170.
- **Dümenil, L., Todini, E., 1992.** A rainfall-runoff scheme for use in the Hamburg climate model, Advances in Theoretical Hydrology. In: A Tribute to James Dooge (Ed. O'Kane, J.P.), European Geophysical Society Series on Hydrological Sciences, 1, Elsevier Press Amsterdam, 29-157.
- Entekhabi D., Asrar G., Betts A., Beven K.J., Bras R.L., Duffy C.J., 1999. An agenda for land surface hydrology research and a call for the second International Hydrological Decade. Bulletin of the American Meteorological Society, 2043-2058.
- Fiorentino, M., 1996. Geographical information systems in hydrology. Kluwer Academic Publishers.
- Francini, M., Pacciani, M., 1991. Comparative analysis of several conceptual rainfall-runoff models. Journal of Hydrology, 122, 161-219.
- Gao, S., Wang, J., Xiong, L., Yin, A., Li, D., 2002. A macro-scale and semi-distributed monthly water balance model to predict climate change impacts in China. Journal of Hydrology, 268, 1-15.
- Gordon, C., Cooper, C., Senior, C.A., Banks, H., Gregory, J.M., Johns, T.C., Mitchell, J.F.B., Wood, R.A., 2000. The simulation of SST, sea ice extents and ocean heat transports in a version of the Hadley Centre coupled model without flux adjustments. Climate Dynamics, 16, 147–168.
- Groisman, P.Y. Knight, R.W., Easterling, D.R., Karl, T.R., Hegerl, G.C., Razuvaev, V.N., 2005. Trends in intense precipitation in the climate record. Journal of Climate, 18:1326–1350.
- Gupta P.K., Panigrahy S. and Parihar J.S., September, 2011. Impact of climate change on runoff of the major river basins of India using global circulation model (Hadcm3) projected data. Journal of the Indian Society of Remote Sensing, Volume 39, Issue 3, 337-344.
- Harding, B.L., Wood, A. W., Prairie, J. R., 2012. The implications of climate change scenario selection for future stream flow projection in the Upper Colorado River Basin. Hydrology Earth System Science, 9, 847-894.
- Hewitson B.C., Crane, R.G., 1996. Climate downscaling: techniques and application. CR Vol. 07, No. 2.
- Huntington, T.G., 2006. Evidence for intensification of the global water cycle: Review and synthesis. Journal of Hydrology, 319(1), pp 83-95.
- Jain, S.K., and Aggarwal, P.K., 2007. Hydrology and water resources of India. Vol. 57, Water Science and Technology library, Springer.
- Kattsov, V. M., February 8, 2010. Statistical downscaling approach and downscaling of AOGCM climate change projections. International Arctic Science Committee.

- Kim, J.W., Chang, J.T., Baker, N.L., Wilks, D.S., Gates, W.L., 1984. The statistical problem of climate inversion: Determination of the relationship between local and large-scale climate. Monthly Weather Review 112, 2069–2077.
- Kimball, J.S., Running, S.W., Nemani, R., 1997. An improved method for estimating surface humidity from daily minimum temperature. Agriculture, Forestry, Meteorolology, 85(1-2), 87-98.
- Kumar S., Sekhar, M., Bandyopadhyay S., 2009. Assimilation of remote sensing and hydrological data using adaptive filtering techniques for watershed modeling. Current Science, Special Section: Civil Engineering Research, Vol. 97, No. 8.
- Lenart, Melanie, September 14, 2008. Downscaling Techniques. The University of Arizona.
- Liang, X., Lettenmaie D.P., Wood E.F., Burge S.J., 1994. A simple hydrologically based model of land surface water and energy fluxes for general circulation model. Journal of Geophysical Research, Vol. 99, NO. 20 July, D7, 14,415-14,428.
- Liang, X., Lettenmaier, D.P., Wood, E.F., 1996. One-dimensional statistical dynamic representation of subgrid spatial variability of precipitation in the two -layer variable infiltration capacity model. Journal of Geophysical Research, 101(D16): 21,403-21,422.
- Liang, X., Wood, E.F., Lettenmaier, D.P., 1996a. Surface soil moisture parameterization of the VIC-2L model: Evaluation and modifications. Global and Planetary Change, 13: 195-206.
- Lohmann, D.E., Raschke, Nijssen, B., Lettenmaier, D.P., 1998. Regional scale hydrology: II, Application of the VIC -2L model to the Weser River, Germany. Hydrological Sciences, 43(1): 143 -158.
- Lutz, W. (ed.), 1996. The Future Population of the World: What can we assume today? 2nd Edition. Earthscan, London.
- Maidment, D.R., 1992. Handbook of hydrology, McGraw-Hill Inc.
- Manabe, S., Stouffer, R.J., 1988. Two stable equilibria of a coupled ocean-atmosphere model, Journal of Climate, 1(9), 841–866.
- Margulis, S.A., McLaughlin, D., Entekhabi, D., Dunne, S., 2002. Land data assimilation and estimation of soil moisture using measurements from the Southern Great Plains: 1997 field experiment. Water Resources Research, 2002, 38, 1299.
- Maurer, E.P., Hidalgo, H.G., 2007. Utility of daily vs. monthly large-scale climate data: An intercomparison of two statistical downscaling methods. Hydrology and Earth Systems Sciences Discussions, 12: 551-563.
- Menzel, L., Bürger, G., 2002. Climate change scenarios and runoff response in the Mulde catchment (Southern Elbe, Germany). Journal of Hydrology, 267, 53–64.
- Middelkoop, H., Daamen, K., Gellens, D., Grabs, W., Kwadijk, J.C.J., Lang, H., Parmet, B.W.A.H., Schädler, B., Schulla, J., Wilke, K., 2001. Impact of climate change on hydrological regimes and water resources management in the Rhine Basin. Climatic Change, 49, 105-128.
- Milly P.C.D., Dunne, K.A., Vecchia, A.V., 2005. Globalpattern of trends in stream flow and water availability in a changing climate. Nature 438, 347–350.

- Mirza, M.Q. 1997. Precipitation-discharge modeling for assessing future flood hazard in Bangladesh under climate change. A Draft: PhD Thesis, The Centre for Environmental and Resource Studies (CEARS), University of Waikato.
- Mishra N., March 2008. Macroscale hydrological modelling and impact of land cover change on stream flows of the Mahanadi River Basin. M. Tech. Thesis submitted to Andhra University.
- Moors, E.J., Groot, A., Biemans, H., van Scheltinga, C.T., Siderius, C., Stoffel, M., Huggel, C., Wiltshire, A., et. al., 2011. Adaptation to changing water resources in the Ganges basin, northern India, Environmental Science and Policy, Vol.14, Issue 7, 7 November, pp. 758–769.
- Moradkhani , H., 2008. Hydrologic remote sensing and land surface data assimilation. Sensors, 8, 2986-3004, DOI: 10.3390/s8052986.
- Muszik, I., 1996. Lumped modeling and GIS in flood prediction. Geographical information systems in hydrology, Kluwer Academic Publishers.
- Nakicenovic, N., Swart, R., (Eds.) 2000. Special report- emission scenarios. A special report of working group III of the Intergovernmental Panel on Climate Change. Cambridge University Press, UK, 570.
- Nijssen, B.N., Lettenmaier, D.P., Liang, X., Wetzel, S.W., Wood, E.F., 1997. Stream flow simulation for continental-scale river basins. Water Resources Research, 33(4), 711-724.
- Nijssen, B.N., Schnur, R., Lettenmaier, D.P., 2001. Global retrospective estimation of soil moisture using the variable infiltration capacity land surface model, 1980-93. Journal of Climate, 14(8), 1790-1808.
-
- Peters-Lidard C.D., McHenry, J.N., Coats, C.J., Trayanov, A., Fine S., Alapaty, K., Pan, F., 1999. Re-thinking the atmospheric LSP problem from a hydrological perspective. Preprint Volume, 14th Conference on Hydrology, American Meteorological Society, Dallas, TX, USA.
- Pilling, C.G., Jones, J.A.A., 2002. The impact of future climate change on seasonal discharge, hydrological processes and extreme flows in the Upper Wye experimental catchment, mid-Wales. Hydrological Processes, 16, 1201–1213.
- Pletcher, K., 2010. The geography of India: Sacred and historic places, understanding India. Rosen Publishing Group, Incorporated.
- Pope, V.D., Gallani, M.L, Rowntree, P.R., Stratton, P.R., 2000. The impact of new physical parameterizations in the Hadley Centre climate model: HadAM3. Climate Dynamics, 16, 123–146.
- Prashant, 2012. Atmosphere and ocean satellite observations for Regional Climate Model. Tropmet-2012, IMS, Dehradun Chapter.
- Randall, D.A., Wood, R.A., Bony, S., Colman, R., Fichefet, T., Fyfe, J., Kattsov, V., Pitman, A., Shukla, J., Srinivasan, J., Stouffer, R.J., Sumi, A., Taylor, K.E., 2007. Climate models and their evaluation, Climate Change 2007: The physical science basis, Contribution of working group I to the Fourth Assessment Report of the

Intergovernmental Panel on Climate Change [Solomon, S., Qin, D., Manning, M., Chen, Z., Marquis, M., Averyt, K.B., Tignor, M., Miller, H.L. (eds.)]. Cambridge University Press, Cambridge, United Kingdom and New York,

- Reichler, T., Kim, J., 2008. How well do coupled models simulate today's climate? Bulletin of American Meteorological Society, 89, 303-311.
- Rodell, M., Houser, P.R., 2004. Updating a land surface model with MODIS-derived snow cover. Journal of Hydrometorology, 5, 1064-1075.
- Salathé E.P., 2005. "Downscaling simulations of future global climate with application to hydrologic modeling". International Journal of Climatology, 25:419–436.
- Sausen, R., Barthel, K., Hasselmann, K., 1988. Coupled ocean-atmosphere models with flux correction. Climate Dynamics, 2, 145–163.
- Schaake J., February, 2000. A draft: Average hydraulic properties of ARS soil texture classes.
- Schulze, R.E., 2002. Hydrologic Modeling - Concepts and Practice. IHE Lecture Notes.
- Sheffield, J, Wood, E.F., 2008. Projected changes in drought occurrence under future global warming from multi-model, multi-scenario, IPCC AR4 simulations. Climate Dynamics, 31:1, 79-105.
- Shekhar, M.S., Ramakrishna, S.S.V.S., Bhutiyani, M.R., Ganju, A., 2012. Numerical simulation of cloud burst event on, over Leh using WRF mesoscale model. Natural Hazards, 62:1261–1271, DOI 10.1007/s11069-012-0145-1.
- Shelton, Estes, J.E., 1981. Remote sensing and geographic information system an unrealized potential. Geo-Processing, 385-420.
- Shenglian, G., Jing, G., Jun, Z., Hua, C., 2009. Coupling VIC with GCM models to predict climate change impact in the Hanjiang basin, China. IAHS Publication, 333, pp 176-182.
- Singh, V.P., 1996. Lumped modeling and GIS in flood prediction. Kluwer Academic Publishers.
- Smith, J., McCaslin, P., July 2008. WRF domain wizard: A tool for the WRF processing system.
- Stamm, J.F., Wood, E.F., Lettenmaier, D.P., 1994. Sensitivity of a GCM simulation of global climate to the representation of land surface hydrology, Journal of Climate, In press.
- Steele-Dunne, S., Lynch, P., McGrath, R., Semmler, T., Wang, S., Hannafin, J., Nolan, P., The impacts of climate change on hydrology in Ireland. Meteorology and Climate Centre, University College Dublin, Belfield, Dublin, Ireland.
- Stott, P.A., Tett, S.F.B., Jones, G.S., Allen, M.R., Mitchell, J.F.B., Jenkins, G.J., 2000. External control of 20th century temperature by natural and anthropogenic forcings, Science, 290, 2133-2137.
- Su Z., Wen J., Wagner W., 2010. Advances in land surface hydrological processes field observations, modelling and data assimilation. Hydrology and Earth System Sciences, 14, 365–367.
- Subramanya, K., 2008. "Engineering Hydrology". McGraw-Hill Book Company Inc.

- Thornton, P.E., Running, S.W., 1999. An improved algorithm for estimating incident daily solar radiation from measurements of temperature, humidity and precipitation. Agriculture and Forest Meteorology, 93(4), 211-228.
- Tomlinson, R.F., ed., 1972. Geographical data handling, commission on geographical data sensing and processing for the UNESCO/IGU. Second Symposium on Geographical Information Systems, Ottawa.
- Trenberth, K.E., Jones, P.D., Ambenje, P., Bojariu, R., Easterling, D., Klein Tank, A., Parker, D., Rahimzadeh, F., Renwick, J.A., Rusticucci, M., Soden, B., Zhai, P., 2007. Observations: Surface and atmospheric climate change. In: Climate change 2007: The physical science basis. Contribution of working group I to 4th assessment report Intergovernmental Panel on Climate Change [Solomon, S., Qin, D., Manning, M., Chen, Z., Marquis, M., Averyt, K.B., Tignor, M., Miller, H.L., (eds)]. Cambridge University Press, Cambridge, United Kingdom and New York, USA, pp. 235–336.
- Troch, P.A., Paniconi, C., McLaughlin, D., 2003. Catchment-scale hydrological modeling and data assimilation. Advances in Water Resources, 26: 131–135.
- Turner, A., Slingo, J., January 2009. Uncertainties in future projections of extreme precipitation in the Asian monsoon regions: A GCM perspective. UK-India workshop on downscaling and linking to applications, UEA.
- Verlinde, J., 2011. TRMM rainfall data downscaling in the Pangani Basin in Tanzania. M.Sc. Thesis, Delft University of Technology, August, 2011.
- Wolf-Schumann, U., Vallant, S., 1996. HydroGIS 96: Application of geographic information systems in hydrology and water resources management. Proceedings of the Vienna Conference, April 1996, IAHS Publication no.235, 1996. Germany.
- Wuebbles, D.J., Hayhoe, K., 2004. Climate change projections for the United States Midwest. Mitigation and adaption strategies for global change, 9 (4), 335–363.
- Zhao, R., Zuang Y., Fang L., Liu X., Zuang Q., 1980. The Xinanjiang model. Hydrological Forecasting Proceedings Oxford Symposium, IASH 129, 351-356.

WEB RESOURCES

- Hydrologic Cycle, Northwest River Forecast Center, NOAA, http://www.nwrfc.noaa.gov/info/water_cycle/hydrology.cgi . (Accessed 20 September, 2012)
- Landman W., Downscaling: An introduction. Retrieved from **www**.wmo.int/pages/prog/wcp/wcasp/clips/.../mod3_postprocessing.ppt . (Accessed 12 January, 2013).
- National Centers for Environmental Prediction, National Weather Service, NOAA, U.S. Department of Commerce, 2000, updated daily. NCEP FNL Operational Model Global Tropospheric Analyses, continuing from July 1999. Research Data Archive at the

National Center for Atmospheric Research, Computational and Information Systems Laboratory. http://rda.ucar.edu/datasets/ds083.2 . (Accessed 30 September, 2012).

- Pidwirny, M., 2006. "The Hydrologic Cycle". *Fundamentals of Physical Geography, 2nd Edition*. http://www.physicalgeography.net/fundamentals/8b.html . (Accessed 13 June, 2013).
- Southwest Climate Change network. http://www.southwestclimatechange.org/climate/modeling/downscaling . (Accessed 23 November, 2012)
- The Weather Research & Forecasting Model, http://www.wrf-model.org . (Accessed 15 June, 2012)
- Variable Infiltration Capacity (VIC) Macroscale Hydrologic Model, http://www.hydro.washington.edu/Lettenmaier/Models/VIC/ . (Accessed 1 September, 2012).
- Water budget, National Institute of Hydrology, http://nih.ernet.in/rbis/India_Information/Water Budget.htm . (Accessed 23 October, 2012).
- Weather Research and Forecasting (WRF) Model. NESL's Mesoscale and Microscale Meteorology Division, http://www.mmm.ucar.edu/wrf/ . (Accessed 23August, 2012).
- Zavisa, J., July 2011. The WRF NMM core, http://www.mmm.ucar.edu/wrf/users/tutorial/201107/NMM_Dynamics_jul2011_sent.ppt.pdf . (Accessed 08 February, 2013)

Appendix

Sample Fortran codes

1. Code for ASCII to Binary conversion

```
! #gfortran -o ascii_to_binary.exe ascii_to_binary.f90 write_geogrid.o
! #./ascii_to_binary.exe

program ascii_to_binary

 implicit none

 integer :: i,j
 integer :: isigned,endian,wordsize
 integer :: nx,ny,nz
 character*25 :: head12
 real :: scalefactor
 real*8 :: xllcorner, yllcorner, cellsize, missvalue

 real, allocatable :: rarray(:,:), iarray(:,:)

 isigned = 1
 endian = 0
 wordsize = 2
 scalefactor = 1.0
 nz = 1

 open (10, file = 'srtm.asc')

 read(10,*) head12, nx
 read(10,*) head12, ny
 read(10,*) head12, xllcorner
 read(10,*) head12, yllcorner
 read(10,*) head12, cellsize
 read(10,*) head12, missvalue

 allocate (rarray(nx,ny))
 allocate (iarray(nx,ny))
```

```
 do j= 1,ny
   read(10,*) iarray(:,j)
 end do

! reverse the data so that it begins at the lower left corner

 do j = 1,ny
   rarray(:,j) = iarray(:,ny-(j-1))
 end do

 call write_geogrid(rarray, nx, ny, nz, isigned, endian, scalefactor, wordsize)
! print*,'R',rarray(nx,ny)
 deallocate (rarray)

end program ascii_to_binary
```

Sample Python Codes

2. Convert .nc to .tif file format

```
import arcpy, glob

input_folder = 'F:\\wrfoutnc\\'
output_folder = 'F:\\wrfouttif\\'
arcpy.env.workspace = output_folder
arcpy.env.overwriteOutput = True
files = glob.glob(input_folder+"*00")

counter = 0
for eachfile in files:
   print("Endru Processing: " + eachfile)
   outfile1 = 'rainc'+ eachfile[-30:] + '.tif'
   outRaster1 = output_folder + "/" + outfile1
   outfile2 = 'rainnc'+ eachfile[-30:] + '.tif'
   outRaster2 = output_folder + "/" + outfile2
   outfile3 = 'T2'+ eachfile[-30:] + '.tif'
   outRaster3 = output_folder + "/" + outfile3
   print counter, outfile1
```

```
    print counter, outfile2
    print counter, outfile3
    counter += 1

    arcpy.MakeNetCDFRasterLayer_md(eachfile, "RAINC", "west_east", "south_north",
            outfile1, "", "", "BY_VALUE")
    arcpy.MakeNetCDFRasterLayer_md(eachfile, "RAINNC", "west_east",
            "south_north", outfile2, "", "", "BY_VALUE")
    arcpy.MakeNetCDFRasterLayer_md(eachfile, "T2", "west_east", "south_north",
            outfile3, "", "", "BY_VALUE")

    arcpy.CopyRaster_management(outfile1, outRaster1+ "", "", "", "", "NONE", "NONE",
            "")
    arcpy.CopyRaster_management(outfile2, outRaster2+ "", "", "", "", "NONE", "NONE",
            "")
    arcpy.CopyRaster_management(outfile3, outRaster3+ "", "", "", "", "NONE", "NONE",
            "")
    print "done"
    del outfile1
    del outfile2
    del outfile3
```

3. Extracting daily average rainfall

```
import numpy
import numpy as np
import gdal, osr
import sys, os, glob
from osgeo import gdal
from gdalconst import *

input_folder = r'F:\wrfouttif'
print 'Reading img files from input folder'
os.chdir(input_folder)

raincfiles = glob.glob('RAINC*.tif')
rainncfiles = glob.glob('RAINNC*.tif')
raincfiles.sort()
rainncfiles.sort()
```

```
image = len(raincfiles)
print "no of images are:"
print image

ref = raincfiles[0]
ds = gdal.Open(ref, GA_ReadOnly)
if ds is None:
   print 'Could not open ' + ref
   sys.exit(1)
driver = ds.GetDriver()
ds.GetGeoTransform()
ds.GetProjection()
cols = ds.RasterXSize
rows = ds.RasterYSize
op = numpy.zeros((rows,cols), numpy.float64)
op1 = numpy.zeros((rows,cols), numpy.float64)

c=0
for data1 in raincfiles:
   rainc = data1[-34:-10]
   rain = data1[-34:-13]
   print data1
   print "rainc"
   print rainc

   for data2 in rainncfiles:
      rainnc = data2[-34:-10]
      print "rainnc"
      print rainnc
      if rainc==rainnc:
         print "found"
         ds1 = gdal.Open(data1, GA_ReadOnly)
         if ds1 is None:
            print 'Could not open ' + data1
            sys.exit(1)
         driver = ds1.GetDriver()
         a1 = ds1.GetGeoTransform()
         b1 = ds1.GetProjection()
         cols1 = ds1.RasterXSize
```

```
rows1 = ds1.RasterYSize
driver=ds1.GetDriver()
arr1 = ds1.ReadAsArray()

ds2 = gdal.Open(data2, GA_ReadOnly)
if ds2 is None:
   print 'Could not open ' + data2
   sys.exit(1)
driver = ds2.GetDriver()
a2 = ds2.GetGeoTransform()
b2 = ds2.GetProjection()
cols2 = ds2.RasterXSize
rows2 = ds2.RasterYSize
driver=ds2.GetDriver()
arr2 = ds2.ReadAsArray()

op=op+arr1+arr2
print "added"
c += 1

if c%8==0:
   op1=op/8 # to get daily avg of 3 hr data
   print "averaged"
   print ('File no:'+rainc)

   outDs = driver.Create("F://wrfhad//prec_"+rain+".tif", cols1,
           rows1, 1 , GDT_Float32)
   if outDs is None:
      print 'Could not create downscaled data image'
      sys.exit(1)
   outBand = outDs.GetRasterBand(1)
   outData = numpy.zeros((rows1,cols1), numpy.float16)
   outDs.SetGeoTransform(ds1.GetGeoTransform())
   outDs.SetProjection(ds1.GetProjection())
   outBand.WriteArray(op1, 0, 0)
   outBand.FlushCache()
   outDs.FlushCache()
   outDs = None
   del outData
```

```
print "done"
print ('File no:'+rainc)

op = numpy.zeros((rows,cols), numpy.float64)
op1 = numpy.zeros((rows,cols), numpy.float64)
```

4. Extracting daily minimum and maximum temperature

```
 import numpy
import numpy as np
import gdal, osr
import sys, os, glob
from osgeo import gdal
from gdalconst import *
from numpy import matrix
from numpy import linalg as LA

input_folder = r'F:\wrfouttif'
print 'Reading img files from input folder'
os.chdir(input_folder)
temfiles = glob.glob('T2*.tif')
##rainncfiles = glob.glob('RAINNC*.tif')
##raincfiles.sort()
temfiles.sort()
image = len(temfiles)
print "no of images are:"
print image
ref = temfiles[0]
ds1 = gdal.Open(ref, GA_ReadOnly)
if ds1 is None:
   print 'Could not open ' + ref
   sys.exit(1)
driver = ds1.GetDriver()
ds1.GetGeoTransform()
ds1.GetProjection()
cols = ds1.RasterXSize
print cols
rows = ds1.RasterYSize
```

```
print rows

mindata = numpy.zeros((rows,cols), numpy.float64)
maxdata = numpy.zeros((rows,cols), numpy.float64)
counter=0
dailydata = numpy.zeros((8,rows,cols), numpy.float64)
##print dailydata
for eachfile in temfiles:
   print eachfile
   ds2 = gdal.Open(eachfile, GA_ReadOnly)
   if ds2 is None:
      print 'Could not open ' + eachfile
      sys.exit(1)
   driver = ds2.GetDriver()
   a1 = ds2.GetGeoTransform()
   b1 = ds2.GetProjection()
   cols1 = ds2.RasterXSize
   rows1 = ds2.RasterYSize
   driver=ds2.GetDriver()
   data = ds2.ReadAsArray()
   counter+=1
   dailydata[counter%8,:,:]=data
   print counter
   if counter%8==0:
      for i in range (rows):
         for j in range (cols):
            mindata[i,j]=dailydata[:,i,j].min()
            print mindata
            maxdata[i,j]=dailydata[:,i,j].max()
      outfile=eachfile[-34:-13]
      outDs1 = driver.Create("F://wrfhad//tmax_"+outfile+".tif", cols1,     rows1, 1 ,
GDT_Float32)
      if outDs1 is None:
         print 'Could not create downscaled data image'
         sys.exit(1)
      outBand1 = outDs1.GetRasterBand(1)
      outDs1.SetGeoTransform(ds1.GetGeoTransform())
      outDs1.SetProjection(ds1.GetProjection())
      outBand1.WriteArray(maxdata, 0, 0)
```

```
outBand1.FlushCache()
outDs1.FlushCache()
outDs1 = None

outDs2 = driver.Create("F://wrfhad//tmin_"+outfile+".tif", cols1,     rows1, 1 ,
    GDT_Float32)
if outDs2 is None:
   print 'Could not create downscaled data image'
   sys.exit(1)
outBand2 = outDs2.GetRasterBand(1)
outDs2.SetGeoTransform(ds1.GetGeoTransform())
outDs2.SetProjection(ds1.GetProjection())
outBand2.WriteArray(mindata, 0, 0)
outBand2.FlushCache()
outDs2.FlushCache()
outDs2 = None

print "done"
print ('File no:'+eachfile)

mindata = numpy.zeros((rows,cols), numpy.float64)
maxdata = numpy.zeros((rows,cols), numpy.float64)
```

5. Converting .xlsx files to VIC intermediate format

```
import osr
import sys, os, glob
import numpy
import csv
from openpyxl.workbook import Workbook
from openpyxl.reader.excel import load_workbook
from openpyxl.writer.excel import ExcelWriter
from openpyxl.cell import get_column_letter


input_folder = r'F:\wrfxl'
print 'Reading files from input folder'
os.chdir(input_folder)
```

```
files = glob.glob('*.xlsx')
files.sort()
no=len(files)
print "total no. of files are:"
print no

for eachfile in files:
   n=0
   wb_r = load_workbook(filename = eachfile)
   ws_r = wb_r.worksheets[0]
   print "reading the excel file" + eachfile+ "..."

   itr=ws_r.get_highest_row()
   c = numpy.zeros(itr-1, numpy.float)
   d = numpy.zeros(itr-1, numpy.float)
   e = numpy.zeros(itr-1, numpy.float)

   print "writing to text file..."

   text = open("F:\\forcing2020\\"+eachfile[:-5]+".", "w")

   for a in range(itr):
      c[a] = ws_r.cell('A'+str(a+2)).value
      d[a] = ws_r.cell('B'+str(a+2)).value
      e[a] = ws_r.cell('C'+str(a+2)).value

   with open('F:\\forcing2020\\'+eachfile[:-5]+'.', 'w') as f:
      for f1, f2, f3 in zip(c, d, e):
         print >> f, f1, f2, f3

   text.close()

   print "text file created for file"
   print eachfile
```

Field Trip to Tehri